Time-scale analysis of antepartum fetal heart rate variability

Time-scale analysis of antepartum fetal heart rate variability

Chris Peters

Time-scale analysis of antepartum fetal heart rate variability

Chris Peters

Cover design by Chris Peters, photograph by Melvin Mukrab.

Financial support for the publication of this thesis has been kindly provided by School of Medical Physics and Engineering Eindhoven and Wetenschapsfonds Jeroen Bosch Ziekenhuis. Additional financial support by Grafimedics, Maastricht Instruments, Mortara Instrument, Nemo Healthcare and Technomed Europe is gratefully acknowledged.

A catalogue record is available from the Eindhoven University of Technology Library
ISBN 978-90-386-2444-0 NUR 954

Time-scale analysis of antepartum fetal heart rate variability

PROEFSCHRIFT

ter verkrijging van de graad van doctor aan de
Technische Universiteit Eindhoven, op gezag van de
rector magnificus, prof.dr.ir. C.J. van Duijn, voor een
commissie aangewezen door het College voor
Promoties in het openbaar te verdedigen
op woensdag 30 maart 2011 om 16.00 uur

door

Christiaan Hendrik Leonard Peters

geboren te Sittard

Dit proefschrift is goedgekeurd door de promotoren:

prof.dr.ir. P.F.F. Wijn
en
prof.dr. S.G. Oei

Copromotor:
dr. P. Andriessen

voor de kleintjes

Summary

Reliable evaluation of fetal condition and early detection of fetal distress is one of the largest challenges in modern obstetrics. Safely protected within the maternal womb, the fetus is rather inaccessible for physiological measurements. One of few physiological phenomena that can be measured antenatal, is fetal heart activity. The heart plays an essential role in the transportation of oxygen to the tissues, but is only one of multiple factors that influence oxygen supply. Consequently, fetal heart activity provides direct, but rather limited information for the evaluation of fetal condition. Cardiotocography, the simultaneous recording of fetal heart rate and uterine activity, has been the standard in fetal monitoring for more than 30 years. Nevertheless, cardiotocography is insufficiently capable of predicting bad fetal outcome and therefore its value in clinical practice is limited. As a result, any additional information that can contribute to reliably evaluating fetal condition, is highly appreciated.

The beat-to-beat variability of the fetal heart rate is an expression of cardiovascular control by the autonomic part of the fetal central nervous system. As this cardiovascular control will respond to changes in fetal condition, fetal heart rate variability will indirectly reflect fetal condition. Fetal heart rate activity therefore contains potentially useful information that cardiotocography does not reveal. As modulation by different parts of the autonomic nervous system occurs on characteristic timescales, time-frequency analysis of fetal heart rate variability might provide additional information that can be used to more reliably assess fetal well-being. However, interpretation of this information is complicated by the complexity of the physiological mechanisms for cardiovascular control. Additionally, to obtain accurate spectral information, the beat-to-beat fetal heart rate is required, which can only be obtained in clinical practice by measuring the fetal electrocardiogram directly from the fetal scalp. This currently limits the application of the method to intrapartum measurements.

To further explore the potential of time-frequency analysis of fetal heart rate variability for monitoring fetal condition, application of the analysis technique to antepartum measurements is highly appreciated.

The first goal of this doctoral dissertation therefore is to:

1. *Obtain the beat-to-beat fetal heart rate throughout pregnancy*

Given the limited successes in literature, it is expected that the obtained fetal heart rate will contain considerably more artifacts than the fetal heart rate obtained from scalp ECG measurements during labor does. Standard techniques for time-frequency analysis, such as the fast Fourier transform, will then fail to provide accurate spectral information. The second goal of this dissertation therefore is to:

2. *Obtain accurate spectral information on antepartum fetal heart rate variability*

To measure fetal heart activity antepartum, a dedicated data-acquisition system has been developed for electrophysiological measurements on the abdomen of a pregnant woman (chapter 2). A novel method developed by a coworker was chosen to remove the dominating maternal electrocardiogram from the recorded signals. An online software implementation of this method has been realized to process the recorded signals real-time.

To achieve the first goal of the dissertation, chapter 3 presents an algorithm that uses a priori knowledge on the physiology of the fetal heart to enhance the fetal ECG components in multi-lead abdominal fetal ECG recordings, before QRS-detection. Evaluation of the method on generated fetal ECG recordings with controlled signal-to-noise ratios showed excellent results. However, for actual recordings, evaluation of the results by experts learned that fine-tuning of the algorithm is necessary.

In chapter 4, a more theoretical approach has been used to exploit the spatial correlation of multi-channel fetal ECG recordings for increasing the signal-to-noise ratio of the retrieved fetal electrocardiogram. A three-dimensional representation of the fetal vectorcardiogram is constructed by means of the inverse Dower matrix. An ellipse is fitted to the QRS loop of several overlayed heartbeats and the axes of the ellipse are calculated to determine the source signals of the fetal electrocardiogram. In future work, this technique could be used for calculating the linear combinations that are used in the algorithm of chapter 3, which will increase the accuracy of the heart rate detection.

The suitability of non-invasive fetal ECG recordings for fetal monitoring in clinical practice was evaluated by using the developed technology in a longitudinal patient study (chapter 5). Repeated measurements on pregnant patients learned that the performance of the method for removing the maternal electrocardiogram was good and remained more or less constant throughout pregnancy. Between 20 and 25 weeks of gestational age, the quality of the retrieved fetal ECG waveforms generally was very high, and the beat-to-beat fetal heart rate could be

accurately detected. For this stage of pregnancy, abdominal measurement of the fetal electrocardiogram offers an opportunity to obtain unique cardiac information on the fetus. However, to increase the performance of the technology throughout pregnancy, the noise in the electrophysiological recordings must be significantly reduced. Still, it remains uncertain whether this will be adequate when isolating sections of the vernix caseosa reduce the amplitude of the fetal electrocardiogram that is measured on the maternal abdomen.

For stages of pregnancy in which abdominal recording of the fetal electrocardiogram fails to provide the beat-to-beat heart rate, chapter 6 offers an alternative. By processing Doppler waveforms of ultrasound signals reflected at the fetal heart, the beat-to-beat fetal heart rate can be obtained. However, the measurement requires a skilled operator and is very sensitive to fetal movement.

The presence of artifacts in the beat-to-beat fetal heart rate obtained from either abdominal recordings of the fetal electrocardiogram or Doppler ultrasound recordings, is common and cannot be prevented. To obtain the second goal of the dissertation, a continuous wavelet based analysis method has been developed to reliably calculate the power within the scales of interest (chapter 7). This method provides accurate results when up to 20 % of the dataset is missing due to artifacts.

In chapter 8, the continuous wavelet based method has been applied for time-scale analysis of the recordings from chapter 5. The results of this analysis correspond with literature on the development of the fetal autonomic nervous system. In addition, the results suggest that functional development of the sympathetic nervous system takes place around 22 weeks of gestational age.

The final chapter reflects on the realization of the goals of this dissertation and provides specific directions for future work. Although additional clinical research might contribute to obtaining clinically relevant information from time-scale analysis of fetal heart rate variability, focus should be on solving the technical limitations of the used instrumentation for abdominal recording of the fetal electrocardiogram.

x

Contents

Chapter 1

Clinical background and outline of the thesis

1.1 Clinical problem

The early development of new life is truly one of nature's most fascinating processes. Perhaps almost just as fascinating is the wide variety in this process of development that, despite the presence of many similarities, exists between different species. In humans and many other mammals, the fetus is safely protected within the maternal womb. Under normal circumstances, the conditions in the womb are optimal for the development of the unborn child. However, these conditions fluctuate under the influence of multiple factors and might turn adverse for the development of the fetus. Such an unfavorable situation might seriously affect fetal development or otherwise harm the fetus and even lead to intra-uterine death. When the health of a fetus is at risk, medical interventions, such as a Caesarian section, will be considered. Decision making, however, is in these situations often very difficult, as medical intervention generally will not be without consequences. For example, a fetus in a preterm pregnancy that is at risk, will in case of a Caesarian section be forced to continue his development in an artificial environment under conditions that are not ideal. Risks and benefits will therefore be considered carefully and unnecessary interventions will be avoided as much as possible. To be able to decide what is in the best interest of the unborn child, it is essential that the condition of the fetus can be assessed reliably. However, due to his presence in the uterus, the fetus is not easily accessible, which makes it difficult to determine fetal condition. Reliable evaluation of fetal condition and early detection of fetal distress remains one of the largest challenges in obstetrics nowadays.

One of the largest risks for fetal health is a deficiency in the supply of oxygen to tissues, which can lead to acidemia and cause severe organ damage and in case of persistent asphyxia eventually lead to fetal death. Therefore, adequate monitoring of fetal condition would require monitoring the oxygen supply to organs,

and the oxygen supply to the brain in particular. However, direct intrauterine measurement of oxygen supply is technically impossible. One of very few fetal physiological phenomena that can be measured antenatal, is fetal heart activity. As the heart functions as a pump in the circulation of blood through the vascular system, the heart plays an essential role in the transportation of oxygen. However, the regulation of blood flow is complex and heart activity is only one of multiple factors that influence oxygen supply. Fetal heart activity therefore provides direct, but rather limited, information on the oxygen supply to organs. However, the heart itself is a muscle and deficiencies in the supply of oxygen will therefore also affect the functioning of the heart. As a results, changes in oxygen supply may be reflected in, often very subtle, changes in heart activity.

1.2 Fetal heart rate monitoring

1.2.1 History

By far the easiest way to obtain information on fetal heart activity, is by listening to the sounds that are produced when the fetal heart contracts. The first reports of auscultation of fetal heart tones date already from the 1820's [1]. Not much later, fetal heart decelerations were noted to be associated with fetal distress [2]. In 1895, Adolphe Pinard developed a wooden fetal stethoscope, which is still being used in clinical practice today [3], [4]. Although auscultation of the fetal heart can be reassuring in specific cases, generally it offers only limited information on fetal condition. In an attempt to improve this situation, fetal phonocardiography was introduced [5]. Phonocardiography uses a paper registration of heart sounds, which allows for a more objective evaluation. However, fetal phonocardiography never grew to success, as better alternatives became available quickly.

One of the largest breakthroughs in medicine was the first practical measurement of the electrocardiogram (ECG) by Willem Einthoven in 1903. During each contraction of the heart, the muscle cells in the myocardium depolarize in a synchronized manner. This synchronized depolarization results in large extracellular potential differences, which can be measured at the skin surface. Although the electrical activity of the heart had been measured before, Willem Einthoven realized a breakthrough by using a string galvanometer that he had developed, which was much more sensitive than the previously used electrometers. In 1906 Max Cremer reported the first recording of electrical activity of the fetal heart, using a string galvanometer [6]. As the fetal heart is much smaller than the heart of adults or adolescents, the amplitude of the fetal electrocardiogram is 10 to 100 times smaller than the amplitude of the adult electrocardiogram. Consequently, the recording by Max Cremer showed a pattern of very small peaks that could just be distinguished from the baseline of the much stronger maternal electro-

cardiogram that was present in the measurement. Improvements of electronics in the following decades did improve the quality of the measurements, but the largest improvement was achieved by applying an electrode directly to the fetus in 1953 [7]. By using electrodes directly applied to the fetus, the presence of maternal ECG components in the recordings was significantly reduced, eliminating the need for signal separating techniques. Further developments eventually led to the introduction of a disposable spiral scalp electrode by Edward Hon in 1972 [8]. Since then, measurement of the fetal scalp electrocardiogram has been the golden standard for measuring fetal heart activity during labor.

Although a satisfactory fetal electrocardiogram could be obtained during labor, antenatal measurement of the fetal ECG still suffered from difficulties that could not be solved properly. Electrical recordings on the maternal abdomen contain a mixture of signals and noise, and the fetal electrocardiogram is largely obscured by the much stronger maternal electrocardiogram. Although various methods have been developed to retrieve fetal heart activity from these recordings [9], [10], [11], some of which even became commercially available, none of these methods was really successful. In the second half of the 1960's the first instruments were introduced that use Doppler ultrasound to measure fetal heart activity [12]. These instruments transmit ultrasonic waves, typically in the range of 2 – 5 MHz, into the maternal abdomen in the direction of the fetus. These waves reflect, among other objects, on the fetal heart. As the heart is moving during systole, a Doppler shift occurs in the waves that are reflected on the wall and valves of the fetal heart. The Doppler shift that occurs in the reflected waves is in the audible range. A similar Doppler shift occurs in the waves that are reflected on fetal blood flow in either the heart or the umbilical cord. Consequently, this technique is perfectly capable of making fetal heart activity audible, and provides a better alternative for phonocardiography. Since the 1970's Doppler ultrasound has become the standard technique for antenatal measurement of fetal heart activity, and has more or less caused abdominal measurement of fetal ECG to disappear.

1.2.2 Cardiotocography

In the 1960's the first electronic fetal monitors were developed to be able to detect fetal distress more accurately [13], [14]. Next to fetal heart activity these monitors also measured maternal uterine activity, either by means of a tocodynamometer or by means of an intrauterine pressure catheter. This simultaneous registration of uterine activity and fetal heart activity, as illustrated in figure 1.1, is called cardiotocography and makes it possible to recognize specific patterns in fetal heart activity, particularly in response to uterine contractions. Visual evaluation of the cardiotocogram and recognition of these specific patterns has shown to provide valuable information on fetal wellbeing. Eventually this resulted in the worldwide

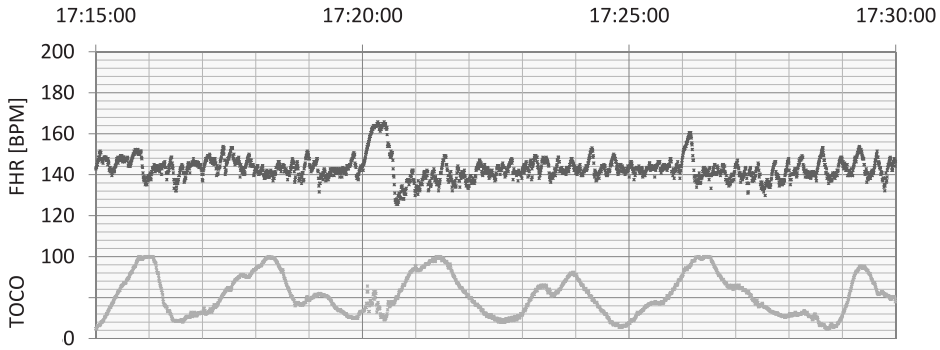

Figure 1.1: *Typical example of a cardiotocographic recording. The upper graph represents fetal heart activity expressed in beats per minute. The lower graph represents dimensionless uterine activity.*

use of cardiotocography, which has been the standard in fetal monitoring already for more than 30 years [15]. With technological developments, the accuracy of the measured data has improved over time, but the basic information that is displayed in the CTG has remained unchanged. In the last three decades insight in the interpretation of cardiotocographic recordings has continuously evolved, however, the CTG remains difficult to interpret. Interpretation of CTG requires the strict use of criteria for classification of the recorded signals. However, the definition of these criteria has been subject of discussion ever since the introduction of cardiotocography in clinical practice [16].

A reassuring CTG can be established fairly well by means of visual evaluation, in which case the fetus generally will be in good condition. At the other end, in case of severe hypoxia when the life of the fetus is seriously at risk, the CTG will display very specific, abnormal patterns such as late and variable decelerations without fetal heart rate variability or bradycardia, which generally will be recognized and diagnosed as fetal distress. Between these extremes, there is a wide range of cardiotocographic patterns that cannot be classified as normal, but neither are consistent with fetal distress. Unfortunately, these abnormal CTG recordings have a predictive value for bad fetal outcome that is as low as 50% [17]. The information that cardiotocography provides is therefore of limited value in clinical practice. This is illustrated by the rather contradictive character of literature on this subject. Publications in the 1970's reported drastic reductions in perinatal mortality rates in units where cardiotocography had been introduced [18], [19]. However, it is unlikely that this reduction can be ascribed to the use of cardiotocography alone. Nevertheless, this led to the opinion that it would be

immoral to withhold the available technology from patients, which initially made it rather difficult to perform controlled trials to study the effects of cardiotocography. The results from the randomized controlled trials that were performed in the second half of the 1970's and in the 1980's suggested that cardiotocography does not improve pregnancy outcome when compared with intermittent auscultation [20], [21]. In addition, the results of these trials showed that the use of cardiotocography resulted in increased rates of Caesarian sections, which in the US almost led to cardiotocography being banned from maternity wards. However, these randomized trials have been criticized, among others, for the size and unrepresentative nature of the patient population and differences in CTG interpretation [22]. The Dublin trial in 1985 did not show significant increases in Caesarian section rate. However, apart from a reduction in neonatal seizures, this trial also showed little benefits for normal risk labor [23].

Despite all its limitations, cardiotocography currently still is the only technique that is available for continuous monitoring of fetal condition. In clinical practice, users need to be educated on the limitations that exist and in particular be aware that CTG interpretation alone often cannot be used to reliably assess fetal condition. The greatest challenge clearly is in the group where a non-reassuring CTG is recorded, but additional information is required to assess fetal condition. A nowadays common method to acquire additional information for assessing fetal condition during labor is to determine the pH of a fetal blood sample. This sample is acquired from either the fetal scalp or the umbilical cord. The pH of the fetal blood has been shown to correlate with neonatal condition directly after birth, expressed by Apgar scores [24]. Although of great added value, disadvantages of fetal blood sampling are its invasiveness – the method can only be applied after rupture of the amniotic membrane – and the difficulty of the procedure. Additionally, fetal blood sampling only provides information on fetal condition at a specific moment. Therefore, any additional information that can contribute to a reliable evaluation of fetal condition and preferably is available on a continuous and non-invasive basis, would be highly appreciated.

1.2.3 Recent developments

Computerized CTG analysis

Visual evaluation of the CTG examines only general changes in fetal heart activity that occur on a timescale of multiple minutes. Smaller, beat-to-beat variations in fetal heart activity are not visible in cardiotocographic recordings, but can contain valuable clinical information. Fetal heart rate recordings therefore potentially contain more useful information than cardiotocography currently reveals. The variability of the fetal heart rate is an expression of cardiovascular control by the

autonomic part of the fetal central nervous system. As this cardiovascular control will respond to changes in fetal condition, fetal heart rate variability will indirectly reflect fetal condition. Currently, this information is not used for evaluating fetal condition, except in cases of fetal distress, where a lack of variability is also visible in the CTG. To be able to include information on heart rate variability in the evaluation of fetal condition, computerized analysis of digital cardiotocographic recordings can be used

A well-known example of computerized CTG analysis is the Sonicaid System 8000 that originates from the Oxford University in the UK and is based on the work of Christopher Redman and Geoffrey Dawes [25]. System 8000 includes the short-term variation (STV) into the computerized analysis of antepartum recordings of fetal heart activity, which has been demonstrated to increase the predictive value of cardiotocography. Another example of computerized CTG analysis, is the SisPorto system [26], developed at the University of Porto in Portugal that uses, among other parameters, short-term and long-term heart rate variability for automated classification of cardiotocographic recordings, both antepartum and during labour.

However, the heart rate variability parameters that both systems use, do not assess true beat-to-beat information. As a result, the systems rather contribute to a reproducible CTG interpretation by mathematically characterizing fetal heart patterns than exploit the potential of heart rate variability analysis for evaluating fetal condition. Partially, this is due to the lack of measurement techniques that allow for accurate and patient friendly acquisition of beat-to-beat fetal heart rate data throughout pregnancy.

P-R interval

In current clinical practice, the beat-to-beat fetal heart rate can only be obtained during labor, by recording the fetal electrocardiogram directly from the fetal scalp. In addition to providing the beat-to-beat fetal heart rate, measurement of the direct fetal electrocardiogram allows also for ECG waveform analysis. Within the limited possibilities to access the fetus, fetal ECG waveform analysis may provide valuable additional information to assess fetal well-being. An example of this additional information is the P-R interval, the time between the onset of atrial depolarization and the onset of ventricular depolarization. The Nottingham FECG system evaluates the ratio of the P-R and R-R interval, for which a change from a positive to a negative relationship has been suggested to correlate with umbilical cord pH [27] and to be a potential detector of fetal hypoxia during labor [28]. However, multi-center randomized trials showed no significant improvements in neonatal outcome nor a significant benefit in decreasing operative intervention [29] and demonstrated that changes from positive to negative P-R/R-R relationship

also occur in fetuses with normal cord acid-base status [30]. Further, umbilical cord occlusion experiments in fetal sheep showed that the change from positive to negative P-R/R-R relationship is not related to acidosis [31].

ST-analysis

Recently, ST-analysis of the fetal scalp electrocardiogram (STAN) was introduced to be used for fetal monitoring. The analysis technique, as developed by Neoventa Medical AB. in Sweden, evaluates the ST segment of averaged fetal ECG waveforms. The information that STAN provides is additional to cardiotocography and interpretation of the STAN information requires very strict CTG interpretation according to the guidelines supplied by Neoventa [32]. In the umbilical cord occlusion experiments in fetal sheep, on which the analysis method is based [33], the correlation between changes in the ST segment and the induced hypoxia was not evident. Nevertheless, in randomized clinical trials the use of cardiotocography in combination with ST-analysis has been shown to result in reduced operative delivery rates and improved neonatal outcome, compared to the use of cardiotocography alone [34], [35]. Recent multi-center trials in Finland and in the Netherlands, however, showed a reduced incidence of fetal blood sampling, but no reduction in operative deliveries or improvement in neonatal outcome [36], [37]. Also, it is unclear to what extent the observed reduction in fetal blood sampling can be ascribed to the use of ST-analysis, as the goal of the Dutch trial originally was to compare cardiotocography with ST-analysis to cardiotocography with fetal blood sampling, and the study protocol a priori restricted the use of fetal blood sampling in the ST-analysis group [38].

1.2.4 Current situation

In the past two decades, several methods for fetal monitoring have been introduced that provide information that is additional to cardiotocography. As the developed techniques build on existing measurements, the methods can be easily integrated in routine clinical practice. However, the clinical value of the additional information that is provided, has proven to be rather limited. Although the developments have contributed to a more reproducible (computerized analysis of CTG) and strict (STAN guidelines) interpretation of cardiotocography, the need for additional information to evaluate fetal condition has remained. The current widespread use of some of these methods is perhaps more illustrative for this need, than for the actual value of the additional information that is offered by the method.

1.3 Autonomic cardiovascular control

1.3.1 Introduction

The supply of oxygen to tissues depends, among others, on the perfusion of the tissues and on the amount of oxygenated blood that is circulated by the heart. Under normal circumstances, adequate perfusion of tissues is ensured by regulating blood pressure. The amount of blood that the heart pumps into the body, commonly referred to as cardiac output, is regulated by adapting stroke volume, which is the blood volume the heart ejects in one contraction, and heart rate, which is the number of cardiac contractions in one minute.

1.3.2 Blood pressure

For the regulation of blood pressure, short term and long term mechanisms exist. Short term regulation of blood pressure occurs by vasoconstriction and vasodilatation, the narrowing and widening of the blood vessels. Vasoconstriction and vasodilatation is regulated by the sympathetic nervous system, that innervates all blood vessels. The sympathetic nervous system operates by controlling the release of noradrenalin, which causes the vessel muscles to contract. Sympathetic innervations is largest in the small arteries and in the arterioles, which determine the peripheral vascular resistance. Long term regulation of blood pressure occurs by the kidneys, that control the total amount of fluid in the body.

1.3.3 Stroke volume

The stroke volume of a heart beat is determined by the contraction strength of the heart muscle. Similar to skeletal muscles, the contraction strength and the length of the muscle cells of the heart show a Frank-Starling relationship. This means that to a certain muscle length, the contraction strength increases with stretching of the muscle. If the muscle is overstretched, the contraction strength decreases again. The stretching of the muscle cells in the heart wall, and consequently also the contraction strength, depends on the amount of blood that is returned to the heart by the venous system. The stroke volume of a heart beat therefore strongly depends on the filling of the heart during the diastole of the preceding heart beat. Apart from this mechanisms on cell level, the sympathetic nervous system also plays an important role in the regulation of stroke volume. By controlling the release of noradrenaline through the nervi accelerantes, the contraction strength of the heart muscles is influenced by the sympathetic nervous system.

1.3.4 Heart rate

The heart rate, the frequency at which cardiac contractions occur, is under the instantaneous influence of the autonomic nervous system. Apart from influencing the contraction strength of the heart muscle, the sympathetically controlled release of noradrenaline through the nervi accelerantes also has an accelerating effect on heart rate. The parasympathetic nervous system on the other hand, has a decelerating effect on heart rate. The parasympathetic nervous system controls the release of acetylcholine in the branches of the nervi vagi. Through the right nervus vagus, the parasympathetic nervous system can slow down the excitation of the sinoatrial node, which initiates the depolarization wave that leads to a cardiac contraction. Furthermore, the conductivity of the atrioventricular node can be controlled through the left nervus vagus, slowing down the propagation of the depolarization wave from the atria to the ventricles of the heart. In addition to the neural regulation of the heart rate, also hormones are of influence on the heart rate. In contrast to the short term regulation of the heart rate by the sympathetic and parasympathetic nervous system, hormones play an important role in the long term regulation of the heart rate. One of these hormones is noradrenaline, which is used as neurotransmitter for the sympathetic nervous system, and due to the synapses of the sympathetic nervous system is released in the blood in small amount, where it acts as a hormone.

1.3.5 Cardiovascular control centers

The cardiovascular control centers that regulate blood pressure, stroke volume and heart rate are located in the medulla oblongata. The control centers receive information from various types of sensors in the body. Very important are the pressure sensitive baroreceptors, which are located in the walls of the arteries and in the heart. These baroreceptors sense changes in blood pressure and in response change the neural stimulation of the afferent nerves to the control centers in the medulla oblongata. Consequently, through the sympathetic and parasympathetic nervous systems, heart rate and peripheral vascular resistance are adjusted. This way, the cardiovascular system more or less compensates the change in blood pressure that occurred. This mechanism is called the baroreceptor reflex and is characteristic for short term control of cardiovascular function. By mechanisms like the baroreceptor reflex, the cardiovascular system is capable of buffering fluctuations in blood pressure and flow. Within reasonable limits cardiovascular homeostasis can be maintained, ensuring a constant perfusion of tissues, which is essential for adequate oxygen supply. Figure 1.2 displays a simplified schematic overview of the pathways through which the sympathetic and parasympathetic nervous systems regulate the cardiovascular system.

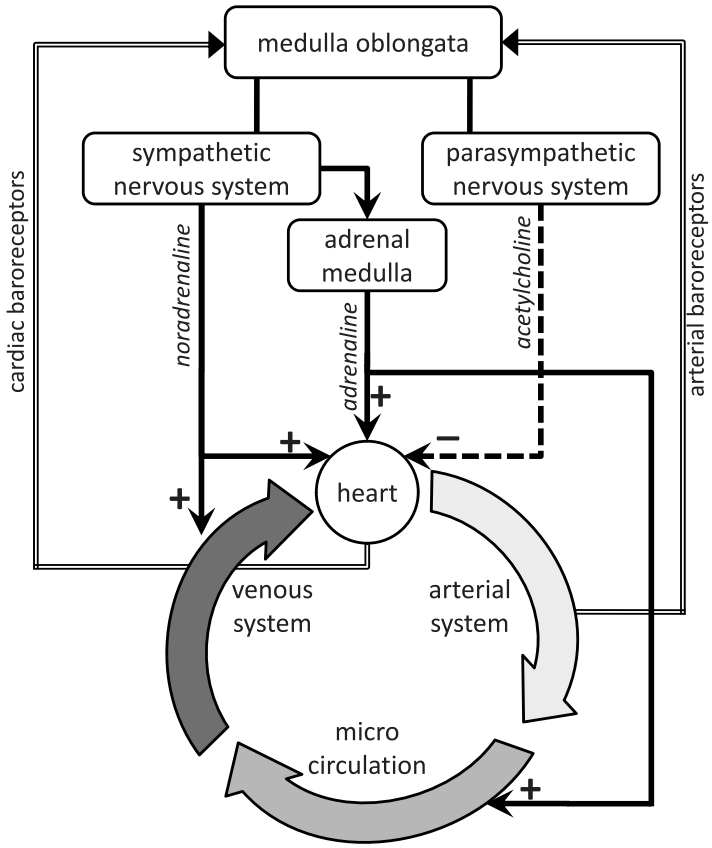

Figure 1.2:*Simplified schematic overview of cardiovascular control by the autonomic nervous system*

1.4 The fetal cardiovascular system

1.4.1 Development

In the fetus, the first blood vessels are formed in the fifth week of gestation. A few days later, one of these blood vessels bends, which is the very first onset of the formation of the heart. Eventually, the blood vessel loops, and from this loop the atria and later on also the ventricles of the heart will be formed. Due to the presence of pacemaker cells, the blood vessel starts to pulsate at a constant frequency. During further development of the fetal heart, these pulsations evolve into cardiac contractions. The frequency of these contractions initially rises

from approximately 100 to approximately 175 contractions per minute [39], [40]. Around the tenth week of gestation the fetal heart rate starts to decrease and also becomes more variable, which is the result of the innervation of the fetal heart. Also the contraction strength of the fetal heart increases, which is primarily due to an maturational increase of myocardial contractility.

1.4.2 Circulatory system

The fetal circulatory system regulates the supply of blood to the organs and other tissues. Essential for the health of the fetus, is adequate fetal perfusion of the placenta, which can be considered a very special organ. In the placenta, deoxygenated fetal blood disposes of carbon dioxide and other waste products and is resupplied with oxygen and nutrients. For the supply of oxygen, the fetus depends entirely on the mother and therefore difficulties in either the oxygenation of maternal blood, the maternal blood flow towards the placenta or the functioning of the placenta might affect fetal wellbeing.

In case of reduced oxygenation of the fetal blood, as a first response the capability of tissues to extract oxygen from the blood will be increased. Also, in an attempt to minimize the consumption of oxygen, the level of activity of the fetus will decrease. A healthy fetus can sustain this condition called hypoxemia, for a relative long time. In case of a further decrease of oxygenation of the fetal blood, activation of the sympathetic nervous system will lead to vasoconstriction in the peripheral circulation, causing redistribution of the blood flow to ensure perfusion of the brain, heart, adrenals, and placenta. This redistribution will further increase with increasing oxygen deficiency and forces peripheral tissues to use anaerobic metabolism, which results in the build up of metabolic acid. This condition called hypoxia, generally can be sustained for a few hours as the metabolic acid is buffered through fetal hemoglobin and partially excreted via the placenta, but will eventually lead to acidosis.

In case of persistent hypoxia, anaerobic metabolism will also occur in the central organs. In this condition of severe oxygen deficiency, which is called asphyxia, failure of central organs may occur which can lead to permanent fetal damage. In a final defense reaction, the sympathetic nervous system is activated maximally in an attempt to provide oxygen to the heart and to the brain. Severe asphyxia will cause brain damage within minutes and can only be sustained for short time, as it eventually will lead to fetal death.

The actual response to hypoxia will depend on the health of the individual fetus. Fetuses with reduced placental reserve (e.g. due to fetal growth restriction or due to maternal hypertension) will experience more difficulties in maintaining oxygenation of the tissues during persisting hypoxemia than uncompromised fetuses. Consequently, the fetal response to hypoxia displays wide biological vari-

ation, which complicates reliable evaluation of fetal condition. The essence of fetal monitoring therefore is to discriminate between physiological adaptation and pathological effects.

1.5 Spectral analysis of fetal heart rate variability

1.5.1 Heart rate variability

The sympathetic and parasympathetic nervous systems play an important role in the regulation of blood supply to the fetal brain and other organs. The availability of information on fetal sympathetic and parasympathetic nervous activity in addition to the already available cardiotocographic information, might contribute to a more reliable assessment of fetal condition. Indirect information on sympathetic and parasympathetic nervous activity is contained in the variability of the fetal heart rate, as the fetal heart rate is one of the cardiovascular parameters that is controlled by the autonomic nervous system. Due to more direct innervation of the heart, the parasympathetic nervous system is capable to act on a relatively short time scale on which the sympathetic nervous system cannot act.

Spectral analysis is the decomposition of a signal into sinoids of different frequencies. Spectral analysis of heart rate variability shows a characteristic spectrum in which a high frequency band can be distinguished, in which solely the parasympathetic nervous system is active, and also a low frequency band can be distinguished, in which both the sympathetic and the parasympathetic nervous systems are active [41]. In human adults, the low frequency band ranges from approximately 0.04 Hz to 0.15 Hz and the high frequency band ranges from 0.15 Hz to 0.4 Hz [42]. In newborns however, it has been demonstrated that the parasympathetic nervous system acts in a variable, but significantly higher frequency range than 0.15 Hz to 0.4 Hz. The high frequency band for newborns therefore has been defined as ranging from 0.4 to 1.5 Hz [43] and this definition is also accepted for studying heart rate variability in fetuses.

1.5.2 Clinical value

Several studies have demonstrated changes in the power of fetal heart rate variability within the low and high frequency bands to be correlated with fetal hypoxemia or acidemia, although there are some inconsistencies between the results of these studies [44], [45], [46], [47], [48], [49], [50]. More recently, the ratio between the power of the fetal heart rate variability in the low frequency range and the power in the entire frequency range between 0.04 Hz and 1.5 Hz has been demonstrated to be inversely correlated with the pH of fetal blood samples obtained from the

umbilical artery directly after birth [51]. These results illustrate the potential that spectral analysis of fetal heart rate variability has for the evaluation of fetal condition and also might have for the early detection of fetal distress. However, spectral analysis of fetal heart rate variability requires accurately detected inter beat intervals. With currently available technology, accurate beat-to-beat fetal heart rates can only be obtained from fetal scalp ECG recordings. As these recordings require the application of an electrode directly to the fetal scalp, beat-to-beat fetal heart rates can only be obtained when the amniotic membrane has ruptured and the fetal scalp is accessible. Therefore, the application of spectral analysis of fetal heart rate variability is currently limited to labor.

1.5.3 Future perspective

The availability of satisfactory methods for obtaining a beat-to-beat fetal heart rate antepartum, would be highly appreciated as this allows for spectral analysis of fetal heart rate variability earlier in pregnancy. Firstly, this would allow for the application of spectral analysis for a more reliable evaluation of fetal condition earlier than labor. Secondly, spectral analysis of fetal heart rate variability is also expected to provide more insight in the functioning of the autonomic nervous system. Small fluctuations in the supply of oxygenated fetal blood naturally occur during pregnancy, even when the fetus is in rest. Under normal conditions, these fluctuations in blood flow will be buffered by the fetal circulatory system. Spectral analysis of fetal heart rate variability will then provide information on the modulation by the sympathetic and parasympathetic nervous systems under non-stress conditions. During labor, relatively large fluctuations in the supply of oxygenated blood will be induced. Consequently, labor can be considered as a stress test for the fetal circulatory system. Information on the functioning of the autonomic nervous system under non-stress conditions earlier in pregnancy might predict how well the fetal circulatory system is capable of dealing with the challenges induced by labor.

Finally, spectral analysis of antepartum fetal heart rate variability might be useful for characterizing the development of the fetal autonomic nervous system. Parameters like approximate entropy, which can be used to quantify regularity in heart rate patterns, have been shown to increase with gestational age [52]. These findings indicate that a gradual development of cardiovascular control occurs during pregnancy, however, it remains unclear how the sympathetic and parasympathetic nervous systems develop specifically . Analysis of heart rate and blood pressure variability in preterm infants has demonstrated that the baroreceptor reflex sensitivity increases with gestational age [53]. This maturational effect of the baroreceptor reflex sensitivity has been attributed to the development of the parasympathetic nervous system. It is expected that in fetal life a similar matu-

ration of the parasympathetic nervous system occurs, however, accurate tools to characterize the development of autonomic cardiovascular control in the human fetus have lacked so far.

Various studies have associated low birth weight with increased risk of cardiovascular disease at adult age [54], [55]. As vascular growth is closely related to tissue growth, one of the suggested underlying physiological mechanisms for this association is dysfunction of cardiovascular autonomic regulation [56], [57]. A restriction in fetal growth is likely to cause a mismatch in the development of cardiovascular function. This mismatch in the programming of cardiovascular function in utero, appears to have consequences that stretch far beyond birth. These consequences can only be controlled by appropriate intervention if the underlying mechanisms are fully understood. Spectral analysis of antepartum fetal heart rate variability may make a modest, but valuable contribution to studying these mechanisms.

1.6 Outline of the thesis

1.6.1 Goals

Nowadays a large clinical need exists for additional information that can be used to reliably evaluate fetal condition. A method that provides information on sympathetic and parasympathetic nervous activity antepartum, would be highly appreciated. Spectral analysis of fetal heart rate variability holds the potential to provide this information, however, this method requires a beat-to-beat fetal heart rate. Unfortunately, clinical measurement of the beat-to-beat fetal heart rate is currently only possible during labor. The first goal of this thesis therefore is to:

1. *Obtain the beat-to-beat fetal heart rate throughout pregnancy*

The development of a method to obtain the fetal heart rate on a beat-to-beat basis during earlier stages of pregnancy than labor, is the necessary first step towards antepartum spectral analysis of fetal heart rate variability. Considering the lack of success that previous attempts have had, it might well be expected that the resulting heart rate will contain significantly more artifacts than the fetal heart rate obtained from scalp ECG measurements during labor does. Consequently, standard techniques for spectral analysis of fetal heart rate, such as the fast Fourier transform, most likely do not provide accurate spectral information. The fast Fourier transform based method that has been applied successfully for the analysis of fetal scalp ECG heart rate variability and also for the analysis of neonatal heart rate and blood pressure variability, therefore is not suitable for analysis of the

antepartum fetal heart rate variability. To resolve this issue, the second goal of the thesis is to:

2. *Obtain accurate spectral information on antepartum fetal heart rate variability*

By developing a method for spectral analysis of heart rate variability that is less sensitive to artifacts in the input data, accurate information on the activity of the sympathetic and parasympathetic nervous systems can be obtained.

1.6.2 Outline

To measure fetal heart activity antepartum and during labor, a dedicated data-acquisition system and measurement setup has been developed. Chapter 2 contains an overview of this work and also shortly describes the method that is used to retrieve fetal ECG traces from electrophysiological measurements on the abdomen of a pregnant woman.

To achieve the first goal of the thesis, chapter 3 describes the development of an algorithm to obtain the beat-to-beat heart rate from multichannel ECG recordings with poor signal-to-noise ratio. This method can directly be applied to the fetal ECG traces retrieved from non-invasive electrophysiological recordings on the maternal abdomen to obtain the beat-to-beat fetal heart rate.

A more theoretical approach towards obtaining the beat-to-beat fetal heart rate from multichannel abdominal ECG recordings is presented in chapter 4. By exploiting the spatial correlation of the fetal electrocardiogram that is measured on the maternal abdomen, the source signals of the fetal ECG are obtained from which the fetal QRS complex can be detected elegantly. Nevertheless, this approach will only be successful for recordings with reasonable signal-to-noise ratios and the method is currently not suitable for online implementation.

Chapter 5 evaluates the performance of the developed prototype electrophysiological fetal monitor on non-invasive fetal ECG recordings obtained during various stages of pregnancy. The performance of the system is characterized by the success rate of determining the fetal heart rate, the amplitude of the fetal ECG that is retrieved from the measurements and the noise level in the retrieved traces.

Chapter 6 presents an alternative method to obtain the beat-to-beat fetal heart rate antepartum. This method uses Doppler ultrasound signals and can be applied in stages of pregnancy in which the non-invasive fetal ECG measurement is not capable of providing accurate results.

To realize the second goal of the thesis, chapter 7 introduces a method for spectral analysis that is based on the continuous wavelet transform. The chapter illustrates the effect that artifacts in the beat-to-beat heart rate have on spectral estimates of heart rate variability that are calculated by Fourier based methods

and demonstrates that the developed continuous wavelet transform based method is much less sensitive to artifacts.

In chapter 8, the continuous wavelet transform based method of the previous chapter is used for spectral analysis of the beat-to-beat fetal heart rate obtained from non-invasive fetal ECG recordings. This chapter illustrates the clinical value of the developed technology as it provided new insights in the functional development of the sympathetic nervous system.

Chapter 9 completes the thesis by reflecting on the realization of the goals set and discussing future perspective.

References

[1] J. Pinkerton, "Fetal auscultation–some aspects of its history and evolution," *Ir Med J.*, vol. 69, pp. 363–8, Sep 1976.

[2] R. Goodlin, "History of fetal monitoring," *Am J Obstet Gynecol.*, vol. 133, pp. 323–52, Feb 1979.

[3] P. Dunn, "Adolphe Pinard (1844-1934) of Paris and intrauterine paediatric care," *Arch Dis Child Fetal Neonatal Ed.*, vol. 91, pp. F231–2, May 2006.

[4] M. O'Dowd and E. Philipp, *The History of Obstetrics and Gynaecology*. Parthenon Publishing Group, 1994.

[5] A. Gunn and M. Wood, "The amplification and recording of fœtal heart sounds," *Proc R Soc Med.*, vol. 46, pp. 85–91, Feb 1953.

[6] M. Cremer, "Über die direkte Ableitung der Aktionströme des menschlichen Herzens vom Oesophagus und über das Elektrokardiogramm des Fötus," *Münch Med Wochenschr.*, vol. 53, pp. 811–3, Apr 1906.

[7] C. Smyth, "Experimental electrocardiography of the foetus," *Lancet*, vol. 1, pp. 1124–6, Jun 1953.

[8] E. Hon, R. Paul, and R. Hon, "Electronic evaluation of fetal heart rate. XI. Description of a spiral electrode," *Obstet Gynecol.*, vol. 40, pp. 362–5, Sep 1972.

[9] E. Hon and O. Hess, "Instrumentation of fetal electrocardiography," *Science*, vol. 125, pp. 553–4, Mar 1957.

[10] A. Favret and A. Caputo, "Application of computer techniques to the fetal electrocardiogram," *Biomed Sci Instrum.*, vol. 1, pp. 317–23, 1963.

[11] F. Offner and B. Moisand, "A coincidence technique for fetal electrocardiography," *Am J Obstet Gynecol.*, vol. 95, pp. 676–80, Jul 1966.

[12] E. Bishop, "Instrument & method: the Doppler ultrasonic motion sensor," *Obstet Gynecol.*, vol. 28, pp. 712–2, Nov 1966.

[13] E. Hon, "The electronic evaluation of the fetal heart rate; Preliminary report," *Am J Obstet Gynecol.*, vol. 75, pp. 1215–30, Jun 1958.

[14] E. Hon, "Classification of fetal heart rate. I. A working classification," *Obstet Gynecol.*, vol. 22, pp. 137–46, Aug 1963.

[15] R. Kennedy, "Electronic fetal heart rate monitoring: retrospective reflections on a twentieth-century technology," *J R Soc Med.*, vol. 91, pp. 244–50, May 1998.

[16] F. Boehm, "Intrapartum fetal heart rate monitoring," *Obstet Gynecol Clin North Am.*, vol. 26, pp. 623–39, Dec 1999.

[17] H. Banta and S. Thacker, "Assessing the costs and benefits of electronic fetal monitoring," *Obstet Gynecol Surv.*, vol. 34, pp. 627–42, Aug 1979.

[18] R. Beard, P. Edington, and J. Sibanda, "The effects of routine intrapartum monitoring on clinical practice," *Contrib Gynecol Obstet*, vol. 3, pp. 14–21, 1977.

[19] F. Johnstone, D. Campbell, and G. Hughes, "Has continuous intrapartum monitoring made any impact on fetal outcome?," *Lancet*, vol. 1, pp. 1298–300, Jun 1978.

[20] A. Haverkamp, H. Thompson, J. McFee, and C. Cetrulo, "The evaluation of continuous fetal heart rate monitoring in high-risk pregnancy," *Am J Obstet Gynecol.*, vol. 125, pp. 310–20, Jun 1976.

[21] A. Haverkamp, M. Orleans, S. Langendoerfer, J. McFee, J. Murphy, and H. Thompson, "A controlled trial of the differential effects of intrapartum monitoring," *Am J Obstet Gynecol.*, vol. 134, pp. 399–412, Jun 1979.

[22] J. Parer, "Fetal heart-rate monitoring," *Lancet*, vol. 2, pp. 632–3, Sep 1979.

[23] D. MacDonald, A. Grant, M. Sheridan-Pereira, P. Boylan, and I. Chalmers, "The dublin randomized controlled trial of intrapartum fetal heart rate monitoring," *Am J Obstet Gynecol.*, vol. 152, pp. 524–39, Jul 1985.

[24] R. Beard, "The detection of fetal asphyxia in labor," *Pediatrics*, vol. 53, pp. 157–69, Feb 1974.

[25] G. Dawes, M. Moulden, and C. Redman, "System 8000: computerized antenatal FHR analysis," *J Perinat Med.*, vol. 19, no. 1-2, pp. 47–51, 1991.

[26] D. A. de Campos, J. Bernardes, A. Garrido, J. M. de Sá, and L. Pereira-Leite, "SisPorto 2.0: a program for automated analysis of cardiotocograms," *J Matern Fetal Med.*, vol. 9, pp. 311–8, Sep-Oct 2000.

[27] M. Mohajer, D. Sahota, N. Reed, A. Chang, E. Symonds, and D. James, "Cumulative changes in the fetal electrocardiogram and biochemical indices of fetal hypoxia," *Eur J Obstet Gynecol Reprod Biol.*, vol. 55, pp. 63–70, May 1994.

[28] N. Reed, M. Mohajer, D. Sahota, D. James, and E. Symonds, "The potential impact of PR interval analysis of the fetal electrocardiogram (FECG) on intrapartum fetal monitoring," *Eur J Obstet Gynecol Reprod Biol.*, vol. 68, pp. 87–92, Sep 1996.

[29] B. Strachan, W. van Wijngaarden, D. Sahota, A. Chang, and D. James, "Cardiotocography only versus cardiotocography plus PR-interval analysis in intrapartum surveillance: a randomised, multicentre trial. FECG study group," *Lancet*, vol. 355, pp. 456–9, Feb 2000.

[30] R. Luzietti, R. Erkkola, U. Hasbargen, L. Mattson, J. Thoulon, and K. Rosén, "European Community Multicentre Trial "Fetal ECG Analysis During Labour": the P-R interval," *J Perinat Med.*, vol. 25, no. 1, pp. 27–34, 1997.

[31] J. Westgate, A. Gunn, L. Bennet, M. Gunning, H. de Haan, and P. Gluckman, "Do fetal electrocardiogram PR-RR changes reflect progressive asphyxia after repeated umbilical cord occlusion in fetal sheep?," *Pediatr Res.*, vol. 44, pp. 297–303, Sep 1998.

[32] I. Amer-Wåhlin, S. Arulkumaran, H. Hagberg, K. Marsál, and G. Visser, "Fetal electrocardiogram: ST waveform analysis in intrapartum surveillance," *BJOG*, vol. 114, pp. 1191–3, Oct 2007.

[33] J. Westgate, L. Bennet, C. Brabyn, C. Williams, and A. Gunn, "ST waveform changes during repeated umbilical cord occlusions in near-term fetal sheep," *Am J Obstet Gynecol*, vol. 184, pp. 743–51, Mar 2001.

[34] J. Westgate, M. Harris, J. Curnow, and K. Greene, "Plymouth randomized trial of cardiotocogram only versus ST waveform plus cardiotocogram for intrapartum monitoring in 2400 cases," *Am J Obstet Gynecol.*, vol. 169, pp. 1151–60, Nov 1993.

[35] I. Amer-Wåhlin, C. Hellsten, H. Norén, H. Hagberg, A. Herbst, I. Kjellmer, H. Lija, C. Lindoff, M. Månsson, L. Mårtensson, P. Olofsson, A. Sundström, and K. Marsál, "Cardiotocography only versus cardiotocography plus ST analysis of fetal electrocardiogram for intrapartum fetal monitoring: a Swedish randomised controlled trial," *Lancet*, vol. 358, pp. 534–8, Aug 2001.

[36] K. Ojala, M. Vääräsmäki, K. Mäkikallio, M. Valkama, and A. Tekay, "A comparison of intrapartum automated fetal electrocardiography and conventional cardiotocography–a randomised controlled study," *BJOG*, vol. 113, pp. 419–23, Apr 2006.

[37] M. Westerhuis, G. Visser, K. Moons, E. van Beek, M. Benders, S. Bijvoet, H. van Dessel, A. Drogtrop, H. van Geijn, G. Graziosi, F. Groenendaal, J. van Lith, J. Nijhuis, S. Oei, H. Oosterbaan, M. Porath, R. Rijnders, N. Schuitemaker, L. Sopacua, I. van der Tweel, L. Wijnberger, C. Willekes, N. Zuithoff, B. Mol, and A. Kwee, "Cardiotocography plus ST analysis of fetal electrocardiogram compared with cardiotocography only for intrapartum monitoring: a randomized controlled trial," *Obstet Gynecol*, vol. 115, pp. 1173–80, Jun 2010.

[38] M. Westerhuis, K. Moons, E. van Beek, S. Bijvoet, A. Drogtrop, H. van Geijn, J. van Lith, B. Mol, J. Nijhuis, S. Oei, M. Porath, R. Rijnders, N. Schuitemaker, I. van der Tweel, G. Visser, C. Willekes, and A. Kwee, "A randomised clinical trial on cardiotocography plus fetal blood sampling versus cardiotocography plus ST-analysis of the fetal electrocardiogram (STAN) for intrapartum monitoring," *BMC Pregnancy Childbirth*, vol. 7, p. 13, Jul 2007.

[39] T. DuBose, J. Cunyus, and L. Johnson, "Embryonic heart rate and age," *J Diagn Med Sonography*, vol. 6, pp. 151–7, 1990.

[40] R. Schats, C. Jansen, and J. Wladimiroff, "Embryonic heart activity: appearance and development in early human pregnancy," *Br J Obstet Gynaecol.*, vol. 97, pp. 989–94, Nov 1990.

[41] S. Akselrod, D. Gordon, F. Ubel, D. Shannon, A. Berger, and R. Cohen, "Power spectrum analysis of heart rate fluctuation: a quantitative probe of beat-to-beat cardiovascular control," *Science*, vol. 213, pp. 220–2, Jul 1981.

[42] Task force of the European society of cardiology and the North American society of pacing electrophysiology, "Heart rate variability: standards of measurement, physiological interpretation, and clinical use," *Circulation*, vol. 93, pp. 1043–65, 1996.

[43] E. Rosenstock, Y. Cassuto, and E. Zmora, "Heart rate variability in the neonate and infant: analytical methods, physiological and clinical observations," *Acta Paediatr.*, vol. 88, pp. 477–82, May 1999.

[44] D. Chun, Y. Sim, K. Park, S. Yi, J. Shin, and S. Kim, "Spectral analysis of fetal heart rate variability as a predictor of intrapartum fetal distress," *Int J Gynaecol Obstet.*, vol. 73, pp. 109–16, May 2001.

[45] T. Rantonen, E. Ekholm, S. Siira, T. Metsälä, R. Leino, U. Ekblad, and I. Välimäki, "Periodic spectral components of fetal heart rate variability reflect the changes in cord arterial base deficit values: a preliminary report," *Early Hum Dev.*, vol. 60, pp. 233–8, Jan 2001.

[46] T. Suzuki, Y. Kimura, J. Murotsuki, T. Murakami, S. Uehara, and K. Okamura, "Detection of a biorhythm of human fetal autonomic nervous activity by a power spectral analysis," *Am J Obstet Gynecol.*, vol. 185, pp. 1247–52, Nov 2001.

[47] E. Salamalekis, E. Hintipas, I. Salloum, G. Vasios, C. Loghis, N. Vitoratos, C. Chrelias, and G. Creatsas, "Computerized analysis of fetal heart rate variability using the matching pursuit technique as an indicator of fetal hypoxia during labour," *J Matern Fetal Neonatal Med.*, vol. 19, pp. 165–9, Mar 2006.

[48] S. Siira, T. Ojala, T. Vahlberg, J. Jalonen, I. Välimäki, K. Rosén, and E. Ekholm, "Marked fetal acidosis and specific changes in power spectrum analysis of fetal heart rate variability recorded during the last hour of labour," *BJOG*, vol. 112, pp. 418–23, Apr 2005.

[49] S. Siira, T. Ojala, E. Ekholm, T. Vahlberg, S. Blad, and K. Rosén, "Change in heart rate variability in relation to a significant st-event associates with newborn metabolic acidosis," *BJOG*, vol. 114, pp. 819–23, May 2007.

[50] J. van Laar, M. Porath, C. Peters, and S. Oei, "Spectral analysis of fetal heart rate variability for fetal surveillance: review of the literature," *Acta Obstet Gynecol Scand.*, vol. 87, no. 3, pp. 300–6, 2008.

[51] J. van Laar, C. Peters, R. Vullings, S. Houterman, J. Bergmans, and S. Oei, "Fetal autonomic response to severe acidaemia during labour," *BJOG*, vol. 117, pp. 429–37, Mar 2010.

[52] S. Pincus and R. Viscarello, "Approximate entropy: a regularity measure for fetal heart rate analysis," *Obstet Gynecol.*, vol. 79, pp. 249–55, Feb 1992.

[53] P. Andriessen, S. Oetomo, C. Peters, B. Vermeulen, P. Wijn, and C. Blanco, "Baroreceptor reflex sensitivity in human neonates: the effect of postmenstrual age," *J Physiol.*, vol. 568, pp. 333–41, Oct 2005.

[54] C. Law and A. Shiell, "Is blood pressure inversely related to birth weight? the strength of evidence from a systematic review of the literature," *J Hypertens*, vol. 14, pp. 935–41, Aug 1996.

[55] R. Huxley, A. Shiell, and C. Law, "The role of size at birth and postnatal catch-up growth in determining systolic blood pressure: a systematic review of the literature," *J Hypertens*, vol. 18, pp. 815–31, Jul 2000.

[56] D. Phillips and D. Barker, "Association between low birthweight and high resting pulse in adult life: is the sympathetic nervous system involved in programming the insulin resistance syndrome?," *Diabet Med.*, vol. 14, pp. 673–7, Aug 1997.

[57] R. IJzerman, C. Stehouwer, E. de Geus, M. van Weissenbruch, H. D. van de Waal, and D. Boomsma, "Low birth weight is associated with increased sympathetic activity: dependence on genetic factors," *Circulation*, vol. 108, pp. 566–71, Jul 2003.

Chapter 2

Technical background

2.1 Electrocardiography

2.1.1 Physiological background

Electrocardiography is the recording of electrical potentials on the skin that change with the contractions of the heart. During each cardiac contraction, the muscle cells in the heart contract in a synchronized way and relax again. This synchronized contraction of heart muscles is caused by depolarization of the charges that exist across the cell membranes of the cardiac muscle cells. The depolarization is triggered by the sino-atrial node and progresses from the atria through specialized electrical-conduction muscle cells towards the ventricles. During depolarization of the muscle cells in the ventricles, repolarization has already started across the cell membranes of the muscle cells in the atria. Consequently, this process of depolarization and repolarization of cardiac muscle cells produces very characteristic patterns of changes in electrical potential that are measurable on the skin: the electrocardiogram (ECG). The size of the changes in electrical potential depends among others on the number of muscle cells that is involved, and therefore on the size of the heart muscle. The amplitude of the electrocardiogram strongly varies between individuals and depends on the measurement position and direction, but typically is in the mV range.

2.1.2 Clinical application

In 1903 Willem Einthoven invented the string galvanometer, which was much more sensitive than the galvanometers that had been devised before. His invention facilitated the first practical measurement of the electrocardiogram and Einthoven was awarded the Nobel prize in physiology or medicine in 1924. Eventually, his invention led to the indispensable role that electrocardiography has in modern medicine. Also the standardized placement of electrodes and the terminology that is used today to describe the different complexes in the electrocardiogram, originate from Willem Einthoven. Nowadays, electrocardiography is essential for the diagnosis

of cardiovascular and other diseases, but also for monitoring the condition of a patient, for instance in an intensive care unit. Additionally, measurement of the electrocardiogram is the golden standard for obtaining the heart rate, which is relevant in numerous applications in medicine. Figure 2.1 shows an illustration of a electrocardiographic recording in clinical practice.

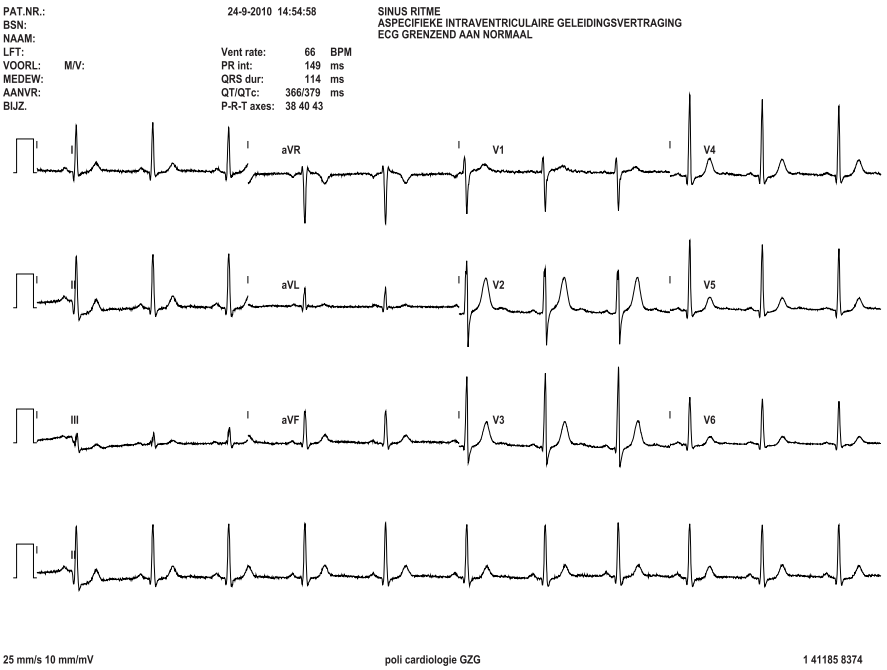

Figure 2.1: *Illustration of a clinical electrocardiographic recording in cardiology. The recording shows a representative part (12 x 2.5 s) of a 12-lead ECG and a 10 seconds part of one of these leads (lead II, bottom plot). From left to right in the graph, the 12-lead ECG consists of the limb leads (I, II and III), the augmented limb leads (aVR, aVL and aVF) and the precordial leads (V1–V6). These leads represent projections of the electrical activity of the heart on specific angles and provide insight in the conductive characteristics of the heart.*

2.1.3 The fetal electrocardiogram

In obstetrics, measurement of the fetal electrocardiogram provides very valuable information on fetal condition. For decades, measurement of the direct electrocar-

diogram from the fetal scalp has been the standard method for obtaining the fetal heart rate during labor. More recently, analysis of the fetal ECG waveform was introduced successfully to provide additional information to assess fetal wellbeing. However, a significant drawback of the direct fetal electrocardiogram is that the measurement is only possible during delivery. Also, due to its invasive character, the measurement method contains risks of infection and serious harm to the fetus. Consequently, a safer alternative to direct measurement of the fetal electrocardiogram that also can be applied earlier in pregnancy, is highly appreciated.

Non-invasive measurement of the fetal electrocardiogram at the maternal abdomen might offer this alternative. As the fetal heart is very small when compared to the adult heart, the amplitude of the fetal ECG waveform is 10 to 100 times smaller than the amplitude of the adult ECG waveform. Nevertheless, under the right circumstances, the fetal electrocardiogram can be measured on the skin of the maternal abdomen. Electrical measurements on the abdomen of a pregnant woman provide a mixture of electrophysiological signals and noise, in which the fetal electrocardiogram is largely obscured by signals as the maternal electrocardiogram and maternal muscle activity. Figure 2.2 shows a typical example of the signal that is measured on the abdomen of a pregnant woman. This figure nicely illustrates the challenge of retrieving the fetal electrocardiogram from the measured mixture of electrophysiological signals.

2.2 Non-invasive measurement of the fetal electrocardiogram

2.2.1 Electrical conduction

In addition to being obscured by the maternal electrocardiogram, the fetal electrocardiogram measured on the maternal abdomen is also much smaller than the fetal electrocardiogram that is measured directly on the fetal scalp. In the electrical conduction from the fetus to the skin of the maternal abdomen, the amplitude of the electrical signal is significantly reduced. Further, the amplitude of the fetal component in the measured mixture of electrophysiological signals, varies with the position of the measurement electrodes on the abdomen. To a large extent, this is determined by the orientation of the fetus in the uterus, but to a smaller extent this is also influenced by the composition of the tissue between the fetus and the maternal skin.

The amplitude of the fetal electrocardiogram is highest if the measurement vector – which is the vector that connects two electrodes on the maternal abdomen– is directed along the electrical axis of the heart, which is the general direction in which the depolarization wave propagates. This direction depends on the

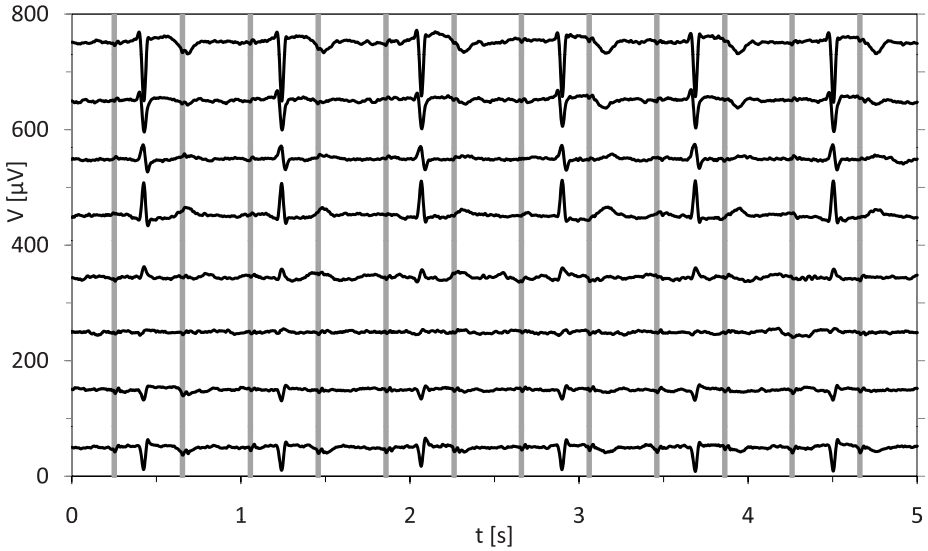

Figure 2.2: *Example of an eight channels electrical recording on the abdomen of a pregnant woman. The recording is dominated by the maternal electrocardiogram. The grey vertical bars in the figure denote fetal heart beats. Note that (a) the fetal heart rate is about twice as high as the maternal heart rate and that (b) the amplitude of the fetal electrocardiogram is 5–20 times smaller than the amplitude of the maternal electrocardiogram.*

orientation of the fetal heart and therefore is influenced by the position of the fetus. During a certain part of pregnancy, the fetal skin is covered by an isolating layer, the vernix caseosa, which strongly reduces the conduction of the fetal electrocardiogram towards the maternal abdomen. Literature reports that later in pregnancy, gaps appear in this isolating layer, which results in the conduction of the fetal electrocardiogram to the maternal abdomen through distinct pathways that are determined by the size and location of the gaps in the vernix caseosa [1]. This heterogeneous character of the electrical conduction from fetal heart to maternal skin may influence the favorable positions at the maternal abdomen for non-invasive measurement of the fetal electrocardiogram.

2.2.2 Multi-lead recordings

For non-invasive abdominal measurement of the fetal electrocardiogram it is required to record multiple electrophysiological leads, i.e. potential differences between different electrodes. First of all, multi-lead recordings allow for combining

different leads to increase the quality of the resulting fetal electrocardiogram. Second, apart from increasing the quality of the signal, recombination of leads can also be used to reconstruct the standard leads that are used in cardiology, which significantly increases the diagnostic value of the obtained fetal electrocardiogram. Finally, a priori it is unknown in which leads the fetal electrocardiogram will be present, although knowledge of fetal position and orientation may often provide an acceptable prediction.

Use of multiple electrodes will increase the chances of picking up a useful fetal ECG signal. However, the use of too many electrodes will reduce the patient friendliness of the measurement, and also requires too much calculation power in the processing of the recorded signals. Early experiments learned that, with the right selection of electrode positions, the use of eight measurement leads should provide adequate results, without seriously affecting the patient friendliness of the non-invasive measurement method. Also the use of maximum eight different measurement leads allows real-time processing of the measured signals.

2.2.3 Prototype development

A prototype of a non-invasive electrophysiological fetal monitoring system was built for the acquisition of abdominal electrical recordings on pregnant women in clinical practice. This system consisted of an eight channel data-acquisition device (MPAQ, Maastricht Instruments BV) and a panel PC (POC-174, Advantech). Figure 2.3 shows the prototype as used in clinical practice in the obstetric high-care unit of Máxima Medical Center in Veldhoven.

The MPAQ data-acquisition device is a multi-functional programmable amplifier system for acquiring physiological and non-physiological signals in clinical settings. The device has been developed according to the requirements in the medical device directive MDD 93/42/EEC for type IIa devices and is classified as type BF applied part according to IEC 60601-1. The front-end of the eight channel MPAQ was slightly modified to meet the requirements for abdominal fetal ECG recordings. By default, for each channel the difference between two input signals is amplified. However, for the abdominal fetal ECG recordings, the use of a common reference signal was desired. Therefore the signal from the electrode that was used as a reference, was buffered to function as reference for each of the channels. To reduce the effect of external disturbances such as power line interference, the electrode leads were actively shielded and an active patient ground lead was used. Figure 2.4 schematically represents the configuration of electrodes that was used.

The gain of the amplifier was set to 200 and signals were digitized at 1000 Hz with 20 bits precision. The MPAQ hardware filtered the input signals with a 0.01 – 75 Hz band-pass filter to remove high-frequency noise and low-frequency

Figure 2.3: *Prototype of an electrophysiological fetal monitoring system being used in the obstetric high-care unit of Máxima Medical Center in Veldhoven, the Netherlands. Photo: Bart van Overbeeke.*

electronic drift and a 50 Hz notch filter to reduce power line interference. The MPAQ was controlled by the POC-174 panel PC. The POC-174 is a medical grade touch-screen personal computer that communicates with the MPAQ through a USB 2.0 interface. The computer runs the data-acquisition software and software for processing of the recorded signals to retrieve the fetal electrocardiogram.

2.3 Maternal ECG removal

2.3.1 History

Half a century after the first abdominal recording of the fetal electrocardiogram in 1906 [2], the application of an electrode directly to the fetal scalp [3] was a clinical breakthrough that enabled fetal monitoring during labor. The success of measuring the direct fetal electrocardiogram during labor, increased the interest of using non-invasive abdominal recordings for fetal monitoring before labor. Several

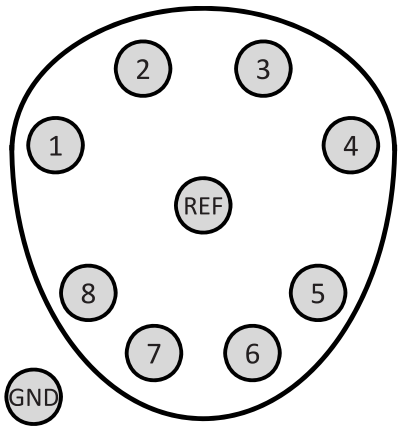

Figure 2.4: *Schematic view of the configuration of electrodes that was used for the abdominal recordings. The envelope marks the part of the abdomen that is directly above the uterus. Due to the expanding size of the uterus, the distance between the electrodes increases with gestation. The ground electrode GND is placed on the patient's right-hand side.*

techniques were developed to remove the dominating maternal electrocardiogram from these recordings. Most of these early techniques were based on detection and blanking of maternal QRS complexes or on cancelation with the electrocardiogram measured on the maternal chest [4], [5], [6]. The performance of blanking techniques is rather limited, as blanking of the maternal QRS complexes also removes large parts of the fetal ECG signal. Cancelation of the maternal ECG component with the maternal chest ECG requires matching of the amplitude and phase of both signals. In general, a residual maternal signal will remain, which limits the value of cancelation techniques in clinical practice.

Although large improvements were achieved in the processing of abdominal recordings, the results are rather unsatisfactory. With the introduction of autocorrelation techniques to calculate the fetal heart rate from Doppler ultrasound recordings in the early 1980's, abdominal fetal electrocardiography disappeared from clinical practice almost entirely. However, research continued in the following decades and several new techniques have been developed to improve the quality of maternal ECG removal from abdominal recordings. Most of these techniques incorporate algorithms that benefited from the exponentially increased computational power of computers [7], [8].

In the 2000's, clinical use of ST analysis of the direct fetal electrocardiogram during labor clearly demonstrated the added value of fetal ECG waveform analysis

for fetal monitoring [9]. Non-invasive fetal ECG measurements from the maternal abdomen hold the potential to expand fetal ECG waveform analysis to periods of pregnancy earlier than labor. Therefore, abdominal measurement of the fetal electrocardiogram has recently received renewed and increasing interest [10], [11], [12].

2.3.2 Current methods

Six different techniques for obtaining the fetal electrocardiogram from electrical recordings on the maternal abdomen are discussed in this section. Four of these techniques (paragraphs A to D) are commonly applied methods for removing the maternal electrocardiogram from abdominal electrophysiological recordings [10], [11], [12], [13], [14]. The fifth technique (paragraph E) is a novel method for removing the maternal ECG [15] that has been developed in a joint project of Máxima Medical Center and Eindhoven University of Technology, which was sponsored by the Dutch technology foundation STW. The sixth technique (paragraph F) is a commonly applied blind source separation technique that can be used to retrieve components of the fetal electrocardiogram directly from multi-lead abdominal recordings [8].

A. Spatial filtering

Both the maternal and fetal electrocardiograms are represented as electrical dipoles in a conductive volume. Consequently, each measurement channel contains the projection of these dipoles on the measurement vector that corresponds to the electrode pair of that channel. This can be written as:

$$V_i(t) = \vec{a}_i \cdot \vec{M}(t) + \vec{b}_i \cdot \vec{F}(t). \tag{2.1}$$

Here, $\vec{M}(t)$ and $\vec{F}(t)$ are the maternal and fetal electrocardiogram, respectively, and $\vec{a}_i$ and $\vec{b}_i$ the transfer vectors which represent the electrical conduction towards the measurement electrodes on the skin of the maternal abdomen. By properly choosing a linear combination of leads from different measurement channels, a new ECG lead can be obtained in which the maternal electrocardiogram is eliminated:

$$Y(t) = \sum_{i=1}^{N} \lambda_i V_i(t) \qquad \text{with } \sum_{i=1}^{N} \lambda_i \vec{a}_i \cdot \vec{M}(t) = \vec{0}. \tag{2.2}$$

The coefficients λ_i can be calculated by means of singular value decomposition [14]. A disadvantage of spatial filtering is that the resulting ECG lead $Y(t)$ will not always contain a significant fetal ECG component. The presence of a significant fetal ECG component depends on the actual orientation of the fetus with respect

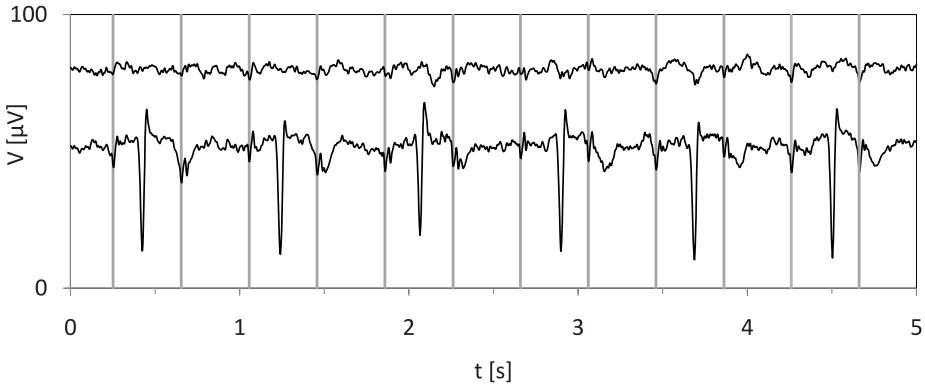

Figure 2.5: *Removal of the maternal electrocardiogram by spatial filtering. The lower graph shows one of the recorded leads from figure 2.2 and the upper graph shows the filtered ECG lead in which the maternal electrocardiogram is reduced. The grey bars mark the location of fetal QRS complexes.*

to the electrical main axis of the maternal heart. Figure 2.5 illustrates maternal ECG removal by means of spatial filtering.

B. Adaptive filtering

In this approach, a reference maternal ECG waveform is created either by averaging a number of consecutive maternal ECG waveforms that are recorded on the maternal abdomen or by recording the maternal ECG on the chest. This reference ECG waveform is then passed through a variable filter, and the output of this filter is subtracted from the original recording to remove the maternal electrocardiogram. The concept of adaptive filtering is illustrated in figure 2.6. The

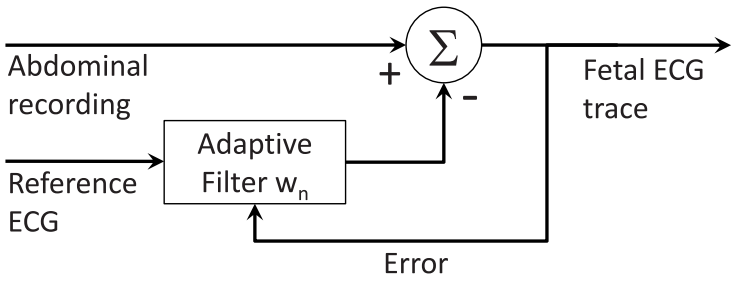

Figure 2.6: *The concept of adaptive filtering of abdominal fetal ECG recordings.*

transfer-function of the filter is adjusted with each new maternal ECG waveform, to minimize the residue of the maternal electrocardiogram after subtraction. Nevertheless, adaptive filtering can not entirely account for the continuously occurring changes in amplitude and shape of the maternal electrocardiogram. Consequently, the obtained signals may still contain some maternal ECG residue.

C. Template subtraction

Similar to adaptive filtering, a template of the maternal ECG waveform is built by averaging a number of consecutive maternal ECG waveforms that are synchronized on the QRS complex. Before subtraction, the maternal ECG template is linearly scaled to minimize the mean squared error with respect to the maternal ECG waveform that is estimated. This way, template subtraction accounts for changes in the amplitude of the maternal ECG waveform, which reduces the residue of the maternal electrocardiogram in the retrieved signals. The maternal ECG template is defined as:

$$\widehat{Z}_{i,j}(t) = \frac{A}{N} \sum_{k=1}^{N} Z_{i-k,j}(t - \theta_{i-k}), \tag{2.3}$$

with $\widehat{Z}_{i,j}(t)$ the scaled maternal ECG template for estimating for the i$^{\text{th}}$ maternal ECG waveform in the j$^{\text{th}}$ measurement channel, $Z_{i-k,j}(t)$ the k$^{\text{th}}$ preceding maternal ECG waveform, θ_{i-k} the time shift that is necessary to synchronize this ECG waveform on the QRS complex and A the constant that is used to scale the constructed template. The accuracy of maternal ECG removal by means of template subtraction can be further improved by accounting also for changes in the shape of the ECG waveform. This is achieved by segmenting the maternal ECG waveform and scaling each segment of the maternal ECG template separately before subtracting the template, as given by:

$$\widehat{Z}'_{i,j}(t_s) = \frac{A_s}{N} \sum_{k=1}^{N} Z_{i-k,j}(t_s - \theta_{i-k}), \tag{2.4}$$

with s the index indicating the segments in which the maternal ECG template has been cut.

D. Linear prediction

A drawback of template subtraction techniques is that the ECG waveforms that are used to build the maternal ECG template, all contribute equally to this template. Artifacts, but also fetal ECG waveforms that are present in the recording, affect the template that is built and therefore reduce the accuracy of the maternal ECG removal. In linear prediction, the template is built by weighted averaging of the

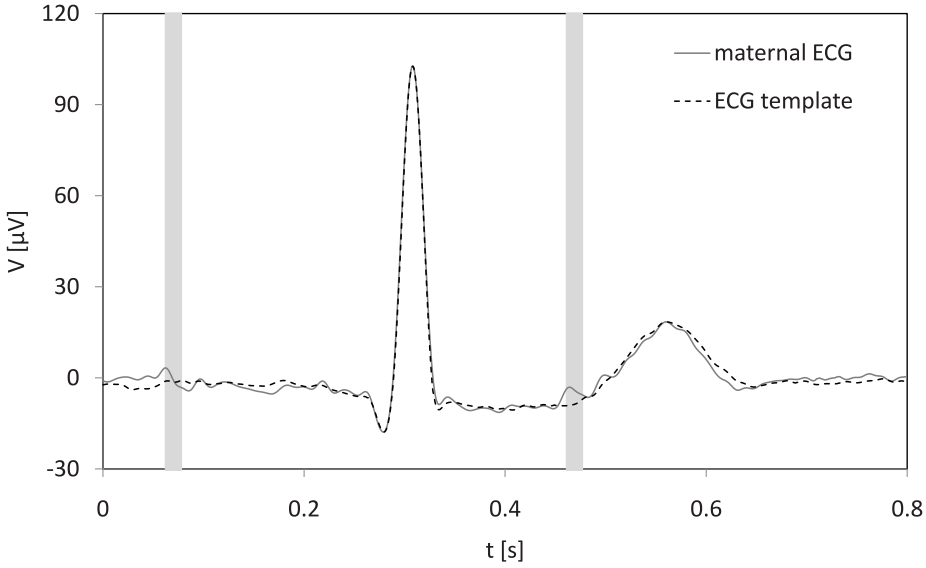

Figure 2.7: *Segmented ECG template and corresponding maternal ECG complex to be estimated. Note the clearly visible presence of fetal QRS complexes at t = 0.07 s and t = 0.47 s, as indicated by the grey vertical lines.*

synchronized maternal ECG waveforms. Weights are calculated by minimizing the mean squared deviation with respect to the maternal ECG waveform that is estimated. The maternal ECG template that is obtained this way is less affected by disturbances in the measured signal. The template is given by:

$$\widehat{Z}''_{i,j}(t) = \sum_{k=1}^{N} w_{i-k} Z_{i-k,j}(t - \theta_{i-k}), \tag{2.5}$$

with $\widehat{Z}''_{i,j}(t)$ the scaled maternal ECG template for estimating the i$^{\text{th}}$ maternal ECG waveform in the j$^{\text{th}}$ measurement channel, $Z_{i-k,j}(t)$ the k$^{\text{th}}$ preceding maternal ECG waveform, w_{i-k} the weight that is attributed to this ECG waveform and θ_{i-k} the time shift that is necessary to synchronize this ECG waveform on the QRS complex.

E. Weighted averaging of maternal ECG segments

The previous techniques fail to provide results that are sufficiently robust for clinical applications. The measured signals generally contain interferences that do not completely satisfy the assumptions that are implicitly made by the methods used.

Consequently, either the resulting fetal ECG traces will contain a considerable amount of maternal ECG residue or the fetal ECG waveforms in these traces are significantly affected by the maternal ECG removal. To overcome these limitations and increase the clinical applicability of non-invasive fetal ECG measurements, a new technique is introduced that adequately removes the maternal electrocardiogram from abdominal recordings. This new technique, weighted averaging of maternal ECG segments, is an extension of MECG template subtraction, combined with linear prediction. The most important features that have been added are:

1. *Dynamic segmentation:* in addition to scaling the individual segments of the maternal ECG template, segments are also synchronized, offset corrected and interpolated. This offers more flexibility in constructing waves to estimate the specific segments of the electrocardiogram, which allows to take into account morphological changes in the ECG waveform.

2. *Linear prediction of segments:* instead of attributing weight to the entire maternal ECG waveform, different weights are attributed to the individual segments of the maternal ECG waveform. This results in the construction of a template that contains closer estimates of the actual segments in the ECG waveform.

3. *Exclusion of segments with artifacts:* segments that are likely to contain artifacts, are excluded in the construction of the maternal ECG template from individually weighted segments. This results in a closer estimate of the actual ECG segment, but also prevents the obtained fetal electrocardiogram to be affected by maternal ECG removal, as segments that contain a fetal QRS complex are automatically excluded.

4. *Interpolation of segment transitions:* To reduce maternal ECG residue in the obtained fetal traces, the transitions between the segments of the template are interpolated before subtracting the template from the measured signal.

The performance of this approach has been compared directly to the existing techniques, both by using modeled abdominal recordings and actual clinical recordings [15]. For each of the techniques, figure 2.8 displays the results for removing the maternal electrocardiogram from a typical modeled abdominal recording. The figure clearly shows the pronounced differences in the residue of the maternal ECG and the distortion of the fetal QRS complex for the different techniques. For the analyzed recordings, weighted averaging of maternal ECG segments outperforms the other techniques and has the promise of becoming a valuable new technique for filtering abdominal recordings.

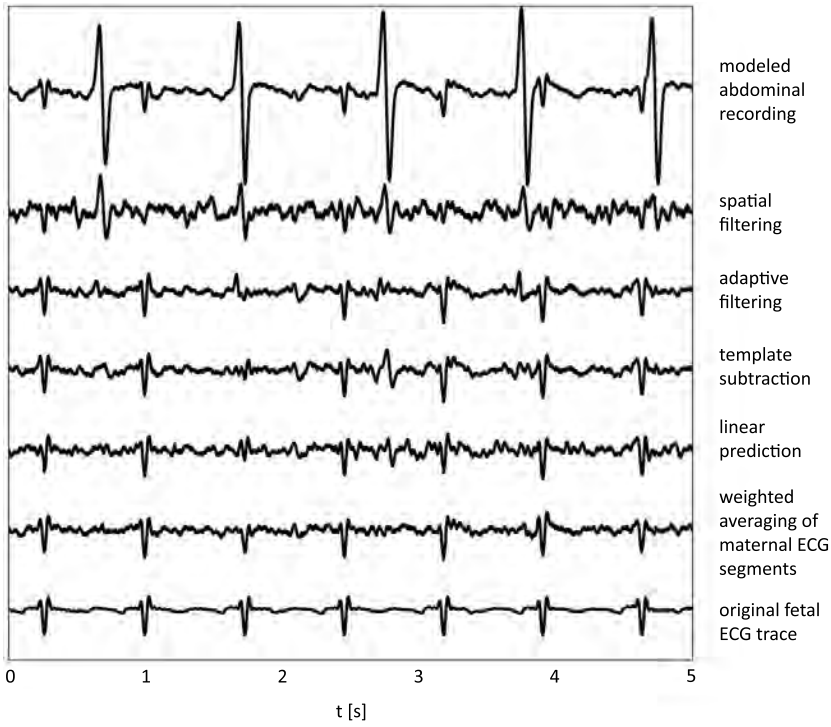

Figure 2.8: *Comparison of five different techniques for removing the maternal electrocardiogram from abdominal recordings. The upper curve shows the modeled abdominal recording that was used as input and the lower curve the fetal ECG trace that was used to generate this input. Note the coincidence of a maternal and fetal QRS complex at t = 1.7 s. (Adapted from [15]).*

F. Independent component analysis

Another common technique for retrieving the fetal electrocardiogram from abdominal recordings is independent component analysis (ICA). ICA is a statistical signal processing technique that can be used to identify and retrieve independent components from measured signals that consist of a mixture of statistically independent source signals. As the electrical signals that are measured on the maternal abdomen consist of a mixture of electrophysiological signals from mother and fetus and noise, ICA can be applied to obtain the fetal electrocardiogram. It is expected that for detecting the fetal heart rate in low amplitude fetal ECG recordings, the performance of ICA will be higher than the performance of weighted averaging of maternal ECG segments.

A drawback of the use of ICA for retrieving the fetal electrocardiogram, is that it is a priori unknown which independent components will contain fetal ECG. Also, it cannot be guaranteed that any of the identified independent components will actually contain fetal ECG. Increasing the number of measurement channels, will increase the chance that the fetal electrocardiogram is retrieved. However, an additional drawback of ICA is that the retrieved fetal ECG generally will be a non-physiological lead. This drawback may seriously limit the clinical applicability of ICA for obtaining the fetal electrocardiogram and therefore weighted averaging of maternal ECG segments was selected for further use in this work.

2.4 Beat-to-beat implementation

To realize a fully functional prototype of an electrophysiological fetal monitor for research use, an online implementation of the selected algorithm for maternal ECG removal was developed. The weighted averaging of maternal ECG segments technique was implemented on a beat-to-beat basis using National Instruments Labview 7.1 and Mathworks Matlab 2006a. The software runs on the POC-174 touch-screen personal computer, as used for data-acquisition from the eight channel M-PAQ. The software processes the signals from the eight channels in real-time and on a sample-by-sample basis.

First, the acquired signals are filtered to remove high-frequency noise, electronic drift of the inputs and power line interference. Next, the software determines to which part of the maternal cardiac cycle, the received samples correspond. Whenever a complete maternal cardiac cycle has been acquired, the software calculates the estimate of the maternal ECG waveform in each of the eight channels. Finally, these estimates are subtracted from the measured input signals to provide eight filtered traces from which the maternal electrocardiogram has been removed.

2.5 Conclusion

The real-time implementation of the algorithm for maternal ECG removal completes the development of the prototype and fulfills the starting conditions for realizing the goals from Chapter 1. The following chapters will focus on retrieving information on fetal condition from the fetal ECG components that are present in the filtered traces.

References

[1] T. Oostendorp, A. van Oosterom, and H. Jongsma, "The effect of changes in the conductive medium on the fetal ECG throughout gestation," *Clin Phys Physiol Meas.*, vol. 10, no. Suppl B, pp. 11–20, 1989.

[2] M. Cremer, "Über die direkte Ableitung der Aktionströme des menschlichen Herzens vom Oesophagus und über das Elektrokardiogramm des Fötus," *Münch Med Wochenschr.*, vol. 53, pp. 811–3, Apr 1906.

[3] C. Smyth, "Experimental electrocardiography of the foetus," *Lancet*, vol. 1, pp. 1124–6, Jun 1953.

[4] E. Hon and O. Hess, "Instrumentation of fetal electrocardiography," *Science*, vol. 125, pp. 553–4, Mar 1957.

[5] A. Favret and A. Caputo, "Application of computer techniques to the fetal electrocardiogram," *Biomed Sci Instrum.*, vol. 1, pp. 317–23, 1963.

[6] F. Offner and B. Moisand, "A coincidence technique for fetal electrocardiography," *Am J Obstet Gynecol.*, vol. 95, pp. 676–80, Jul 1966.

[7] S. Cerutti, G. Baselli, S. Civardi, E. Ferrazzi, A. Marconi, A. Pagani, and G. Pardi, "Variability analysis of fetal heart rate signals as obtained from abdominal electrocardiographic recordings," *J Perinat Med.*, vol. 14, no. 6, pp. 445–52, 1986.

[8] L. de Lathauwer, B. de Moor, and J. Vandewalle, "Fetal electrocardiogram extraction by blind source subspace separation," *IEEE Trans Biomed Eng.*, vol. 47, pp. 567–72, May 2000.

[9] I. Amer-Wåhlin, C. Hellsten, H. Norén, H. Hagberg, A. Herbst, I. Kjellmer, H. Lija, C. Lindoff, M. Månsson, L. Mårtensson, P. Olofsson, A. Sundström, and K. Marsál, "Cardiotocography only versus cardiotocography plus ST analysis of fetal electrocardiogram for intrapartum fetal monitoring: a Swedish randomised controlled trial," *Lancet*, vol. 358, pp. 534–8, Aug 2001.

[10] M. Ungureanu, J. Bergmans, S. Oei, and R. Strungaru, "Fetal ECG extraction during labor using an adaptive maternal beat subtraction technique," *Biomed Tech (Berl).*, vol. 52, pp. 56–60, Feb 2007.

[11] V. Zarzoso and A. Nandi, "Noninvasive fetal electrocardiogram extraction: blind separation versus adaptive noise cancellation," *IEEE Trans Biomed Eng.*, vol. 48, pp. 12–8, Jan 2001.

[12] M. Taylor, M. Smith, M. Thomas, A. Green, F. Cheng, S. Oseku-Afful, L. Wee, N. Fisk, and H. Gardiner, "Non-invasive fetal electrocardiography in singleton and multiple pregnancies," *BJOG*, vol. 110, pp. 668–78, Jul 2003.

[13] B. Widrow, J. G. Jr., J. McCool, J. Kaunitz, C. Williams, R. Hearn, J. Zeidler, E. D. Jr., and R. Goodlin, "Adaptive noise cancelling: principles and applications," *Proc IEEE*, vol. 63, pp. 1692–716, Dec 1975.

[14] A. van Oosterom, "Spatial filtering of the fetal electrocardiogram," *J Perinat Med.*, vol. 14, no. 6, pp. 411–9, 1986.

[15] R. Vullings, C. Peters, R. Sluijter, M. Mischi, S. Oei, and J. Bergmans, "Dynamic segmentation and linear prediction for maternal ECG removal in antenatal abdominal recordings," *Physiol Meas.*, vol. 30, pp. 291–307, Mar 2009.

Chapter 3

Beat-to-beat heart rate detection in multi-lead abdominal fetal ECG recordings

Abstract

Reliable monitoring of fetal condition often requires more information than is provided by cardiotocography, the standard technique for fetal monitoring. Abdominal recording of the fetal electrocardiogram may offer valuable additional information, but unfortunately is troubled by poor signal-to-noise ratios during certain parts of pregnancy. To increase the usability of abdominal fetal ECG recordings, an algorithm was developed that enhances fetal QRS complexes in these recordings and thereby provides a promising method for detecting the beat-to-beat fetal heart rate in recordings with poor signal-to-noise ratios. The method was evaluated on generated recordings with controlled signal-to-noise ratios and on actual recordings that were performed in clinical practice and were annotated by two independent experts. The evaluation on the generated signals demonstrated excellent results (sensitivity of 0.98 for SNR $\geq$ 1.5). Only for SNR $<$ 2, the inaccuracy of the fetal heart rate detection exceeded 2 ms, which may still suffice for cardiotocography but is unacceptable for analysis of the beat-to-beat fetal heart rate variability. In actual recordings, small deviations ($<$ 10 ms) from the actual timing of the fetal QRS complex occurred occasionally, which significantly reduced the performance of the method on these recordings. It is expected that fine-tuning of the algorithm minimizes these deviations and improves the performance of the method.

3.1 Introduction

Reliable monitoring of fetal condition remains one of the largest challenges in obstetrics nowadays. The information provided by cardiotocography, the standard technique for fetal monitoring, is limited and often additional information is

submitted for publication

required for accurate evaluation of fetal condition. Traditionally, this additional information is obtained from fetal blood sampling [1]. Unfortunately, fetal blood sampling only provides information on fetal condition at a single moment. Further disadvantages of fetal blood sampling are its invasiveness and the difficulty of the procedure. More recently, ST analysis of the fetal scalp electrocardiogram (ECG) has been introduced as addition to cardiotocography [2]. Although ST analysis provides information on a semi-continuous basis, the invasiveness of the method is still a disadvantage, as it can only be applied during labor and is not free of risks [3], [4], [5]. Apart from ST analysis, spectral analysis of fetal heart rate variability has also been shown to be a potential predictor for fetal condition [6], [7]. Accurate spectral analysis of fetal heart rate variability requires a beat-to-beat measurement of the heart rate and this more or less has restricted the application of spectral analysis to fetal scalp ECG recordings. To overcome this restriction, the availability of a reliable method to record the fetal electrocardiogram non-invasively would be highly appreciated. This would allow for antepartum application of ECG waveform analysis and spectral analysis of fetal heart rate variability.

The fetal electrocardiogram can be measured non-invasively from the maternal abdomen during large parts of pregnancy and the measurement is completely safe for both mother and fetus. Ever since the first measurement of the fetal electrocardiogram by Max Cremer in 1906 [8], it has remained a challenge to retrieve the fetal ECG from the mix of physiological signals and noise that is measured on the maternal abdomen. As the main interference is the maternal electrocardiogram, several techniques have been developed to remove the maternal electrocardiogram from the measurements, but with varying success [9], [10], [11]. In the 1970's clinical applications of the abdominal fetal electrocardiogram have been introduced, but these have disappeared with the growing success of Doppler ultrasound for antepartum cardiotocography. Recently, abdominal measurement of the fetal electrocardiogram has regained interest [12], [13], [14] and nowadays is commercially available (AN24, Monica Healthcare Ltd., UK). Due to the use of multi-lead recordings and advances in signal processing techniques, interference of the maternal electrocardiogram is no longer an issue, and the additional information that potentially can be obtained is of high clinical importance [15], [16].

Despite all technological improvements, retrieving the fetal electrocardiogram remains a challenge as the amplitude of the measured fetal signal varies during pregnancy and also varies between patients. The various methods that have been developed to separate the fetal electrocardiogram from the measured signals all yield one or multiple channels that contain fetal ECG components. Due to the small amplitude of the fetal electrocardiogram, the signal-to-noise ratio (SNR) of the fetal ECG components in these channels is often relatively poor. Consequently,

standard techniques for detecting QRS complexes fail to provide a reliable heart rate for these signals. Averaged heart rates can often be obtained [17], but provide less information and are not suitable for accurate spectral analysis of heart rate variability. Evidently, a need exists for a method that can obtain the beat-to-beat fetal heart rate from fetal ECG recordings with poor signal-to-noise ratio. This need has initiated the development of an algorithm that incorporates a priori knowledge on the fetal electrocardiogram to detect the beat-to-beat heart rate. This work describes this algorithm and evaluates its performance on both generated signals with controlled signal-to-noise ratios and actual measurements that were performed in clinical practice.

3.2 Algorithm description

The algorithm is intended for detecting the beat-to-beat fetal heart from multi-lead electrophysiological recordings on the abdomen of a pregnant woman. The input of the algorithm consists of multiple channels of abdominal electrophysiological recordings from which the maternal electrocardiogram has been removed. The output that the algorithm provides, contains the recording times at which fetal QRS complexes have been detected.

3.2.1 Fetal ECG enhancement

The strength of the fetal ECG components in multi-lead abdominal recordings depends among others on the position of the fetus and the electrical conduction towards the maternal abdominal skin, and varies strongly from channel to channel. Calculating linear combinations of these channels, generally improves the signal-to-noise ratio of the fetal ECG. In the fetal vectorcardiogram, of which the various channels are all different projections, the QRS complex is represented by a loop. Due to this loop, phase differences will exist between the fetal ECG components in different channels. These phase differences will widen the QRS complex when calculating linear combinations of different channels and therefore limit the improvement of the signal-to-noise ratio. In our approach, we correct for this phase difference before calculating the linear combinations. Linear combination of phase difference corrected signals will not only reduce noise, but will also enhance the QRS complex, when compared to standard linear combination. The transformation of the multi-lead input signals $S_i(t)$ into new, non-physiological leads $V_j(t)$ is given by:

$$V_j(t) = \sum_i W_{j,i} \cdot S_i(t - \tau_i). \tag{3.1}$$

Here, W is the j by i matrix with the weights for calculating the specific linear combinations and τ_i is the inter-channel phase difference calculated by cross-correlating a selected input signal $S_k(t)$ with each of the other input signals:

$$\tau_i = \underset{t}{\operatorname{argmax}} \left| \sum_{t'} (S_k(t') S_i(t+t') \right| . \tag{3.2}$$

Here, $S_k(t)$ is the channel that makes the largest contribution to the average of all input channels. The algorithm calculates a reduced set of four enhanced ECG leads for further processing to determine the beat-to-beat fetal heart rate. For the used electrode configuration, which is shown in figure 3.1 (left), we define W as:

$$W = \frac{1}{\sum w_i} \begin{pmatrix} w_1 & w_2 & w_3 & w_4 & -w_5 & -w_6 & -w_7 & -w_8 \\ 0 & 0 & \frac{2w_3}{a} & \frac{2w_4}{a} & 0 & 0 & \frac{-2w_7}{a} & \frac{-2w_8}{a} \\ -w_1 & -w_2 & w_3 & w_4 & w_5 & w_6 & -w_7 & -w_8 \\ \frac{-2w_1}{b} & \frac{-2w_2}{b} & 0 & 0 & \frac{2w_5}{b} & \frac{2w_6}{b} & 0 & 0 \end{pmatrix}, \tag{3.3}$$

with $a = \frac{\sum_{i=3,4,7,8} w_i}{\sum w_i}$ and $b = \frac{\sum_{i=1,2,5,6} w_i}{\sum w_i}$ and w_i the absolute value of the maximum in the cross-correlation that was calculated to determine the inter channel phase difference:

$$w_i = \max \left| \sum_{t'} S_k^*(t') S_i(t+t') \right| . \tag{3.4}$$

For equal weights w_i the calculated set of ECG leads is displayed in figure 3.1 (right). By enhancing the fetal ECG components in the recording, the signal-to-noise ratio of the resulting four leads has significantly improved. Before processing these leads to detect the fetal heart rate, noise is further reduced by applying a band pass filter that matches the spectral content of the fetal QRS complexes (fourth order Butterworth filter, 12 – 42 Hz).

3.2.2 Fetal heart rate detection

To detect the beat-to-beat fetal heart rate from the calculated ECG leads, the absolute first derivatives of the four filtered signals $\widetilde{V}_j(t)$ are calculated and convoluted with a square function that matches the width of the fetal QRS complex. Then, the results are squared and summed over the four leads to provide the function $L(t)$:

$$L(t) = \sum_{j=1}^{4} \left(H(t) * \left| \frac{d\widetilde{V}_j(t)}{dt} \right| \right)^2 , \tag{3.5}$$

with $H(t)$ a square function that was set to a width of 21 ms. To remove the DC-offset, $L(t)$ is high-pass filtered using a fourth order Butterworth filter with

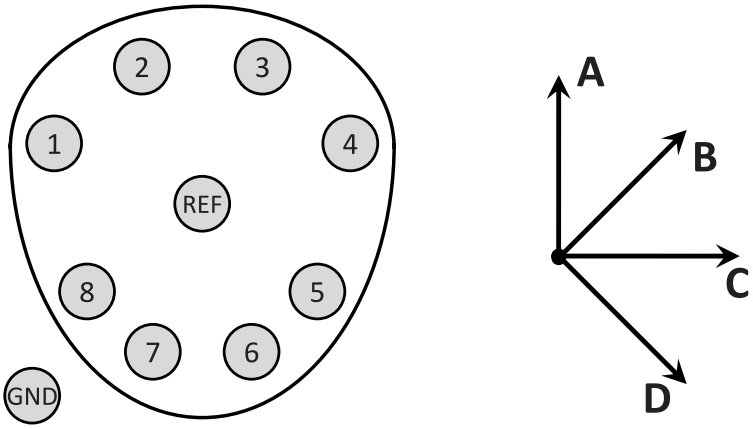

Figure 3.1: *Used electrode configuration (left) and calculated ECG leads A, B, C, D for equal weights w_i (right).*

a cut-off frequency of 1 Hz. In the resulting signal, peaks are detected using a quadratic fit, which provides a first estimate of the times at which fetal QRS complexes are present in the recording. Based on these first estimates, the polarity of the QRS complex in each of the four filtered ECG leads is determined and the four leads are combined to detect the exact location of the QRS complexes in the recording. Figure 3.2 illustrates the operation of the algorithm by showing the four enhanced fetal ECG leads after filtering $\widetilde{V}_1(t)$ to $\widetilde{V}_j(4)$, as well as the calculated function $L(t)$ and the detected fetal QRS complexes.

3.3 Methods

The signal-to-noise ratio of abdominal fetal ECG recordings varies during pregnancy, between patients, and often also during the recording. Ideally, the performance of the algorithm is evaluated by determining the accuracy of QRS complex detection for various signal-to-noise ratios. Such an evaluation would require the availability of a golden standard to which the method can be validated. The golden standard for fetal heart rate detection is the fetal scalp ECG, which can only be applied during labor. However, at the end of pregnancy, when the fetal scalp ECG can be recorded, the signal-to-noise ratio of abdominal recordings is generally high. Therefore, direct comparison to the fetal scalp ECG will only provide information on the performance of the algorithm for recordings with relatively high SNR.

To evaluate the performance of the algorithm over a wider range of signal-to-

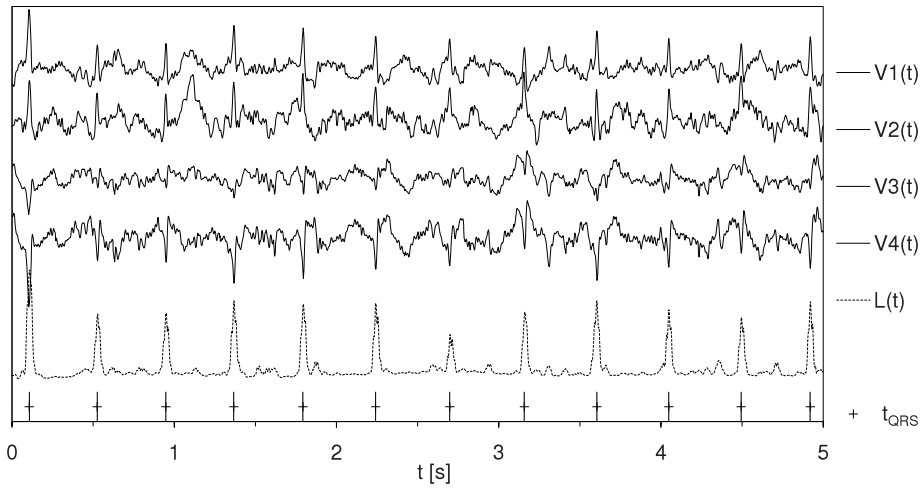

Figure 3.2: *Illustration of the algorithm. The four upper curves are the calculated non-physiological leads $\widetilde{V}_1(t)$–$\widetilde{V}_j(4)$, the dashed line represents $L(t)$ calculated from $\widetilde{V}_1(t)$–$\widetilde{V}_j(4)$. The vertical lines at the bottom of the graph mark the actual times at which QRS complexes occur and the plus-signs mark the times at which QRS complexes have been detected by the algorithm.*

noise ratios, a controlled amount of noise is added to generated signals. These generated signals with various signal-to-noise ratios, are analyzed by the algorithm and the results are compared to the actual QRS locations in the original noise free signals. Additionally, actual clinical abdominal ECG recordings were analyzed and the results of the algorithm were evaluated visually by experts.

3.3.1 Generated recordings

Multi-lead electrocardiographic recordings were performed on the abdomen of a pregnant patient using a prototype non-invasive fetal ECG monitor (NEMO, Eindhoven University of Technology). The maternal ECG component in these recordings was estimated by means of weighted averaging of maternal ECG segments [16]. The amplitude and timescale of the maternal ECG estimates were scaled to generate noise free multi-lead signals that represent abdominally measured fetal ECG components. Next, actual measurement noise from abdominal recordings was amplified and added to the noise free multi-lead signals, to provide artificial fetal ECG recordings at the desired signal-to-noise ratios. Signals were generated for signal-to-noise ratios of 10, 5, 4, 3, 2.5, 2, 1.5 and 1, where the SNR of the

fetal ECG is defined as [17]:

$$SNR = \frac{\frac{1}{8}V_{pp,QRS}^2}{V_{rms,noise}^2}, \tag{3.6}$$

with $V_{pp,QRS}$ the mean peak-to-peak amplitude of the QRS complexes in the noise-free multi-lead signals and $V_{rms,noise}$ the rms amplitude of the noise that is added to the signals. The added measurement noise was different for each of the channels, but the signal-to-noise ratio was kept equal for all channels. Note that in actual abdominal fetal ECG measurements the signal-to-noise ratio will vary between channels. Figure 3.3 displays a generated multi-lead fetal ECG recording with a signal-to-noise ratio of 1. The performance of the algorithm was

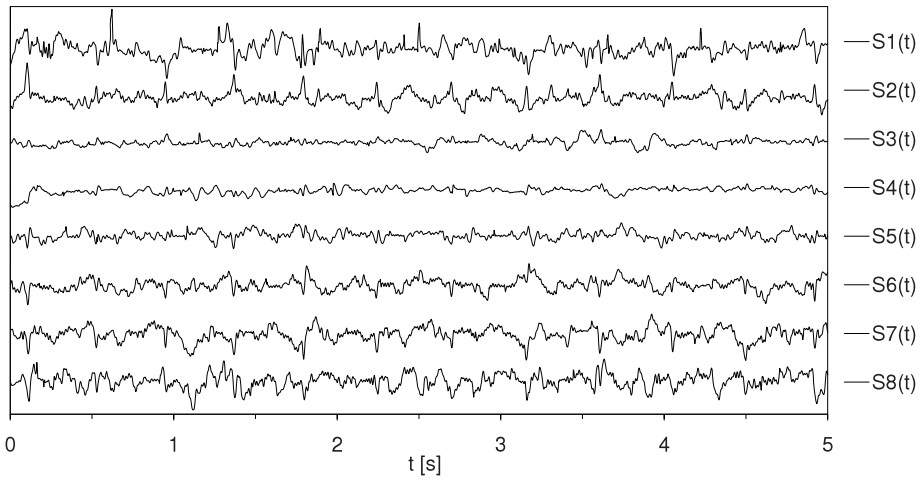

Figure 3.3: *Five seconds example of an eight channel generated fetal ECG recording with a signal-to-noise ratio of 1. This recording was used to illustrate the algorithm in figure 3.2.*

evaluated by comparing the times at which QRS complexes were detected in the generated signals, to the times at which QRS complexes were detected in the noise free signals. For each signal-to-noise ratio, 360 seconds of multi-lead fetal ECG recording were generated and the generation and analysis of the signals was repeated up to 16 times.

3.3.2 Actual recordings

Abdominal fetal ECG recordings were performed on pregnant patients at the Máxima Medical Center in Veldhoven, the Netherlands using a prototype of a

non-invasive fetal ECG monitor (NEMO, Eindhoven University of Technology). Measurements were performed during various stages of pregnancy. From these measurements, a selection of recordings with different signal-to-noise characteristics was processed by the algorithm. The detected fetal QRS complexes in a one minute subset of each of these recordings were evaluated visually by two independent expert observers. A five seconds segment of one of the analyzed recordings is displayed in figure 3.4. The figure shows the eight measurement channels that each have a different signal-to-noise ratio. For the displayed segment, the mean signal-to-noise ratio of the channels is 3.0.

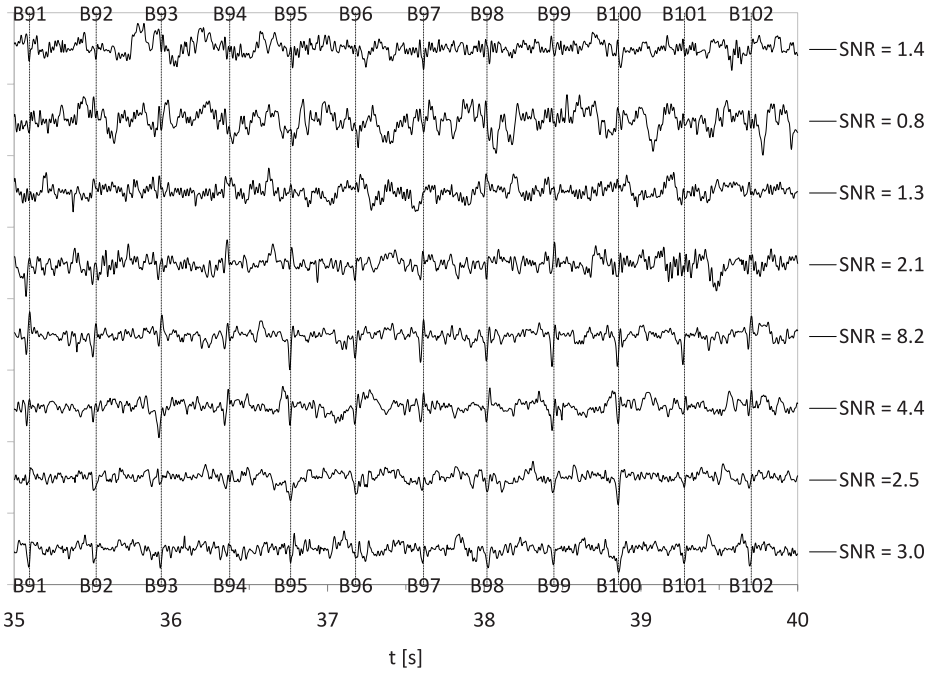

Figure 3.4: *Five second segment of an actual abdominal fetal ECG recording. The mean SNR of this segment is 3.0, but the SNR of the individual channels fluctuates between 0.8 (channel 2) and 8.2 (channel 5). The vertical dashed lines B91 – B102 denote the detection of fetal QRS complexes by the developed method.*

3.4 Results

3.4.1 Generated recordings

The noise-free signals that were used to generate the artificial abdominal fetal ECG recordings, contained 884 QRS complexes. The exact times at which QRS complexes were present in these signals were determined with an accuracy of 0.5 ms (i.e. $0.5 \cdot T_s$, with T_s the sampling interval of the recording). These times were used to validate the times at which the algorithm detected QRS complexes in the generated abdominal fetal ECG recordings. The mean absolute error in the timing of the detected QRS complexes was calculated. Additionally, the number of missed QRS complexes was determined, as well as the number of extra, falsely detected, QRS complexes. Table 3.1 displays the results for each of the signal-to-noise ratios.

Table 3.1: *Results of QRS detection for the generated abdominal fetal ECG recordings with various signal-to-noise ratios.*

SNR	Missed [%]	Extra [%]	Sensitivity	PPV	Error [ms]
10	2.1 ± 0.5	1.1 ± 0.3	0.98 ± 0.01	0.99 ± 0.00	0.08 ± 0.08
5	2.2 ± 0.6	1.1 ± 0.3	0.98 ± 0.01	0.99 ± 0.00	1.00 ± 0.07
4	2.1 ± 0.5	1.1 ± 0.4	0.98 ± 0.01	0.99 ± 0.00	1.04 ± 0.09
3	2.2 ± 0.6	1.2 ± 0.4	0.98 ± 0.01	0.99 ± 0.00	1.21 ± 0.10
2.5	2.1 ± 0.8	1.5 ± 0.5	0.98 ± 0.01	0.99 ± 0.01	1.23 ± 0.11
2	2.0 ± 0.6	1.8 ± 0.7	0.98 ± 0.01	0.98 ± 0.01	1.57 ± 0.51
1.5	2.4 ± 0.7	3.4 ± 1.9	0.98 ± 0.01	0.97 ± 0.02	2.32 ± 0.66
1	4.0 ± 1.0	12.7 ± 5.6	0.96 ± 0.01	0.89 ± 0.04	6.97 ± 3.70

3.4.2 Actual recordings

All QRS complexes that have been detected in the one minute subsets of the actual recordings were evaluated visually. On average, these subsets contained 149 fetal QRS complexes. Extra, falsely detected, and missing QRS complexes were annotated in the recordings. These annotations were used to evaluate the performance of the algorithm, similar to the evaluation for the generated recordings. The inaccuracy of the QRS detection expressed in the mean absolute error could not be determined as there was no information available on the exact times at

which the QRS complexes are present in the recordings. Instead, it was annotated when the detection deviated slightly (less than 10 ms) from the visually detected timing of the QRS complex. In figure 3.4 these deviations occurred in detections B94, B96 and B98. Based on the correctly detected QRS complexes, the signal-to-noise ratio was estimated for each of the recordings. Table 3.2 shows the results for each of the recordings. The detections that deviated slightly were considered as falsely detected. The values in the table that are between parentheses, are the results that would have been achieved if these slightly deviating detections had been detected successfully. The inter-observer agreement was evaluated by comparing the annotations from both experts. Table 3.2 shows the overall proportion of agreement p_O and κ value for the recordings.

Table 3.2: *Results of QRS detection for actual abdominal fetal ECG recordings with various signal-to-noise ratios.*

SNR	Missed [%]	Extra [%]	Sensitivity	PPV	p_O	κ
7.2	0	0	97.0 (100)	97.0 (100)	99.3	0.94
4.0	1.4	0	79.7 (99.3)	80.3 (100)	93.8	0.81
2.4	7.2	12.5	81.2 (93.9)	75.7 (87.5)	86.2	0.63
1.8	5.3	6.0	86.5 (94.7)	85.1 (93.2)	67.5	0.11
1.3	5.1	5.1	89.9 (93.3)	89.9 (93.3)	73.7	0.38

3.5 Discussion

3.5.1 Generated recordings

The results for the generated recordings show that even for relatively high signal-to-noise ratios, some QRS complexes remain undetected and also extra detections occur. The number of undetected QRS complexes remains relatively constant for signal-to-noise ratios of 1.5 and above and the sensitivity of the method is very high (0.98). For generated signals with SNR < 3, the number of extra detected QRS complexes slightly increases with decreasing signal-to-noise ratio. Consequently, the positive predictive value of the method decreases for lower signal-to-noise ratios. Additionally, the increased amount of noise in the generated recordings will affect the accuracy of the detection of fetal QRS complexes. For signal-to-noise ratios below 2, the inaccuracy of the QRS complex detection exceeds 2 ms,

which may suffice for standard cardiotocography but is unacceptable for analysis of the beat-to-beat fetal heart rate variability [18].

3.5.2 Actual recordings

For the actual measurements with relatively high signal-to-noise ratios (mean SNR of 4 and 7.2), the number of both undetected and extra detected QRS complexes is much lower than for the generated recordings. However, this may be due to the relatively small number of QRS complexes in the subsets that were analyzed. For the actual measurements with low signal-to-noise ratios (mean SNR of 2.4 and lower), the numbers of undetected and extra detected QRS complexes are by average 3.5 times higher than for the generated recordings with comparable signal-to-noise ratios. Consequently, both the sensitivity and the positive predictive value of the method are lower than for generated signals. Also, for the recordings with mean signal-to-noise ratios of 1.3 and 1.8 the inter-observer agreement is rather poor (κ values of 0.11 and 0.38). Due to their low signal-to-noise ratio, these recordings are difficult to interpret visually.

The largest contribution to the reduction in sensitivity and positive predictive value is made by the large number of small deviations (< 10 ms) from the actual QRS timing. When these deviations occur, the initial detection of the fetal QRS complex has been successful, but the algorithm is inaccurate in determining the exact timing of the QRS complex. It is expected that fine-tuning of the algorithm may minimize this inaccuracy and thereby increase the performance of the method to a level that is only just below the performance on generated recordings, as indicated by the values between brackets in table 3.2.

Interestingly, there is no evident relationship between the mean signal-to-noise ratio of the actual recordings on one hand and the sensitivity and the positive predictive of the method on the other hand. The observed fluctuation in sensitivity and positive predictive value of the method may result from the rather limited length of analysis. However, it is more likely that the mean signal-to-noise ratio of a recording does not characterize the quality of the signal sufficiently to quantify the performance of the method on actual recordings. As displayed in figure 3.3, the signal-to-noise ratio strongly fluctuates over the channels of the recording. The mean signal-to-noise ratio of a recording therefore is not necessarily a good indicator for the performance of the method on that recording.

3.6 Conclusions

By incorporating a priori knowledge on the physiology of the fetal heart, the developed algorithm enhances fetal QRS complexes in multi-lead fetal ECG recordings.

This provides a promising method for detecting the beat-to-beat fetal heart rate in recordings with poor signal-to-noise ratio. Evaluation of the method on generated fetal ECG signals with controlled signal-to-noise ratios showed excellent results for SNR ≥ 2. For signal-to-noise ratios below 2, the inaccuracy in the detection of the fetal QRS complex exceeds 2 ms, which prohibits analysis of the fetal heart rate variability in these signals. In the detection of the fetal QRS complexes in the actual recordings, small deviations (< 10 ms) from the actual fetal QRS complex occur occasionally. This significantly reduces the performance of the method on these recordings. However, it is expected that fine-tuning of the algorithm will minimize the occurrence of these small deviations and increase the sensitivity and positive predictive value of the method.

References

[1] R. Beard, "The detection of fetal asphyxia in labor," *Pediatrics*, vol. 53, pp. 157–69, Feb 1974.

[2] I. Amer-Wåhlin, S. Arulkumaran, H. Hagberg, K. Marsál, and G. Visser, "Fetal electrocardiogram: ST waveform analysis in intrapartum surveillance," *BJOG*, vol. 114, pp. 1191–3, Oct 2007.

[3] A. Riskin, L. Beni-Adani, I. Chistiekov, A. Kugelman, M. Abend-Weinger, and D. Bader, "Cerebrospinal fluid leak in a premature neonate," *Am J Perinatol.*, vol. 22, pp. 57–9, Jan 2005.

[4] M. Miyashiro and H. Mintz-Hittner, "Penetrating ocular injury with a fetal scalp monitoring spiral electrode," *Am J Ophthalmol.*, vol. 128, pp. 526–8, Oct 1999.

[5] B. Eggink, C. Richardson, and J. Rowen, "Gardnerella vaginalis-infected scalp hematoma associated with electronic fetal monitoring," *Pediatr Infect Dis J.*, vol. 23, pp. 276–8, Mar 2004.

[6] J. van Laar, M. Porath, C. Peters, and S. Oei, "Spectral analysis of fetal heart rate variability for fetal surveillance: review of the literature," *Acta Obstet Gynecol Scand.*, vol. 87, no. 3, pp. 300–6, 2008.

[7] J. van Laar, C. Peters, R. Vullings, S. Houterman, J. Bergmans, and S. Oei, "Fetal autonomic response to severe acidaemia during labour," *BJOG*, vol. 117, pp. 429–37, Mar 2010.

[8] M. Cremer, "Über die direkte Ableitung der Aktionströme des menschlichen Herzens vom Oesophagus und über das Elektrokardiogramm des Fötus," *Münch Med Wochenschr.*, vol. 53, pp. 811–3, Apr 1906.

[9] E. Hon and O. Hess, "Instrumentation of fetal electrocardiography," *Science*, vol. 125, pp. 553–4, Mar 1957.

[10] A. Favret and A. Caputo, "Application of computer techniques to the fetal electrocardiogram," *Biomed Sci Instrum.*, vol. 1, pp. 317–23, 1963.

[11] F. Offner and B. Moisand, "A coincidence technique for fetal electrocardiography," *Am J Obstet Gynecol.*, vol. 95, pp. 676–80, Jul 1966.

[12] L. de Lathauwer, B. de Moor, and J. Vandewalle, "Fetal electrocardiogram extraction by blind source subspace separation," *IEEE Trans Biomed Eng.*, vol. 47, pp. 567–72, May 2000.

[13] V. Zarzoso and A. Nandi, "Noninvasive fetal electrocardiogram extraction: blind separation versus adaptive noise cancellation," *IEEE Trans Biomed Eng.*, vol. 48, pp. 12–8, Jan 2001.

[14] M. Ungureanu, J. Bergmans, S. Oei, and R. Strungaru, "Fetal ECG extraction during labor using an adaptive maternal beat subtraction technique," *Biomed Tech (Berl).*, vol. 52, pp. 56–60, Feb 2007.

[15] M. Taylor, M. Smith, M. Thomas, A. Green, F. Cheng, S. Oseku-Afful, L. Wee, N. Fisk, and H. Gardiner, "Non-invasive fetal electrocardiography in singleton and multiple pregnancies," *BJOG*, vol. 110, pp. 668–78, Jul 2003.

[16] R. Vullings, C. Peters, R. Sluijter, M. Mischi, S. Oei, and J. Bergmans, "Dynamic segmentation and linear prediction for maternal ECG removal in antenatal abdominal recordings," *Physiol Meas.*, vol. 30, pp. 291–307, Mar 2009.

[17] C. Peters, R. Vullings, J. Bergmans, G. Oei, and P. Wijn, "Heart rate detection in low amplitude non-invasive fetal ECG recordings," *Conf Proc IEEE Eng Med Biol Soc.*, vol. 1, pp. 6092–4, 2006.

[18] G. Dawes, M. Moulden, and C. Redman, "System 8000: computerized antenatal FHR analysis," *J Perinat Med.*, vol. 19, no. 1-2, pp. 47–51, 1991.

Chapter 4

A physiology based source separation method for QRS detection in non-invasive fetal ECG recordings

Abstract

The use of the non-invasively obtained fetal electrocardiogram (ECG) in fetal monitoring is complicated by the low signal to noise ratio (SNR) of the ECG signals. Even after removal of the predominant interference (i.e. the maternal ECG), the SNR is generally too low for medical diagnostics and hence, additional signal processing is still required. To this end, several methods for exploiting the spatial correlation of multi-channel fetal ECG recordings from the maternal abdomen have been proposed in literature, of which principal component analysis (PCA) and independent component analysis (ICA) are the most prominent.Both PCA and ICA, however, suffer from the drawback that they are blind source separation (BSS) techniques and as such suboptimum in that they do not consider *a priori* knowledge on the abdominal electrode configuration and fetal heart activity. In this paper we propose a source separation technique that is based on the physiology of the fetal heart and on knowledge of the electrode configuration. This technique operates by calculating the spatial fetal vectorcardiogram (VCG) and approximating the VCG for several overlayed heartbeats by an ellipse. By subsequently projecting the VCG onto the long axis of this ellipse, a source signal of the fetal ECG can be obtained. To evaluate the developed technique, its performance is compared to that of both PCA and ICA and to that of augmented versions of these techniques (aPCA and aICA; PCA and ICA applied on preprocessed signals) in generating a fetal

published as R. Vullings, C.H.L. Peters, M.J.M. Hermans, P.F.F Wijn, S.G. Oei and J.W.M. Bergmans, "A robust physiology-based source separation method for QRS detection in low amplitude fetal ECG recordings," *Physiol Meas.*, vol. 31, pp. 935-51, Jun 2010. The idea of exploiting the spatial correlation contained in the VCG and the solution found in fitting an ellipse to the QRS-loop, originate from C.H.L. Peters. M.J.M. Hermans implemented and fine-tuned the method under supervision of R. Vullings who evaluated the method and was main author of the publication.

ECG source signal with enhanced SNR that can be used to detect fetal QRS complexes. The evaluation shows that the developed source separation technique performs slightly better than aPCA and aICA and outperforms PCA and ICA and has the main advantage that, with respect to aPCA/PCA and aICA/ICA, it performs more robustly. This advantage renders it favorable for employment in automated, real-time fetal monitoring applications.

4.1 Introduction

High-risk pregnancies are becoming more prevalent because of the progressively higher age at which women get pregnant. Ten to twenty percent of all pregnancies are complicated by preterm delivery, fetal hypoxia, fetal growth restriction, or hypertension, yielding a large need for pregnancy monitoring technologies. For monitoring of the well-being of the fetus, the cardiotocogram (CTG; a recording of fetal heart rate in combination with uterine contractions) is commonly used. Subtle changes in fetal heart rate variability may occur as the first signs of fetal distress [1], which could still be reversible at this point if appropriately treated. Extensive studies have, however, shown that the diagnostic predictive value of the CTG is low [2]. To improve this predictive value, additional information is needed, either from more sophisticated analysis of the CTG, such as spectral analysis of the fetal heart rate variability [3], or from other sources such as the fetal electrocardiogram (ECG).

With respect to fetal ECG monitoring as an additional source of information, the currently available technique has one important limitation. This limitation is that recording of the fetal ECG is currently only possible during labor, by applying an electrode to the fetal scalp. Applying this electrode is cumbersome for both patient and clinician. As an alternative, the fetal ECG can also be recorded non-invasively from the maternal abdomen. In contrast to the invasive ECG, this abdominal ECG recording can be performed in all stages of pregnancy, but due to the typically low signal to noise ratio (SNR) of the abdominal fetal ECG, this non-invasive technique has not found its way to clinical practice yet.

The maternal ECG is generally the dominant interference in the abdominal fetal ECG recordings. Numerous methods to remove this maternal ECG have been proposed in literature [4], [5], [6], [7], [8], of which many perform reasonably well. Even so, because the fetal ECG recordings are also corrupted by other interferences and noise, even after removal of the maternal ECG, the SNR of the fetal ECG is generally still relatively low. The most straightforward approach to overcome this problem is to enhance the SNR of the fetal ECG by averaging several consecutive ECG complexes, all synchronized on their QRS complex. Unfortunately, this approach requires knowledge on the locations of QRS complexes, which are difficult to determine from the low SNR fetal ECG recordings [9], [10].

Consequently, in order to fully exploit the time correlation of the fetal ECG, the abdominal fetal ECG recordings need additional processing – next to maternal ECG removal – to facilitate detection of the QRS complexes. In a simplified model, the electrical activity of the heart can be assumed to be represented by a single electrical field vector that varies in amplitude and orientation over time [11], [12]. The time-path of this field vector is referred to as the vectorcardiogram (VCG). In this model, each ECG signal corresponds to the projection of the VCG onto the lead vector indicating the electrode position with which the ECG signal is obtained. This projection constitutes a linear combination of the three orthogonal components into which the VCG can be decomposed. As a consequence all abdominal fetal ECG signals have to be spatially related to one another.

To exploit this spatial relation, several powerful mathematical techniques are available, of which *principal component analysis* (PCA) and *independent component analysis* (ICA) are the most prominent [13], [14]. These techniques operate by linearly combining the fetal ECG signals in such way that the resulting combinations exhibit either maximum variances (PCA) or maximum statistical independency (ICA) [15]. A disadvantage of these techniques is that the resulting linear combinations are randomly ordered, requiring additional processing to determine which combination should be attributed to the fetal ECG.

Another disadvantage is that PCA and ICA, although they are categorized as source separation techniques, in general do not provide all three independent, orthogonal components (i.e. separate sources) of the VCG, but usually only one or two [16]. In addition, they do not include physiological considerations and, hence, are generally referred to as blind source separation (BSS) techniques. This lack of physiological basis can render the BSS techniques less effective in separating the fetal ECG signals from a mixture of these ECG signals and noise. In fact, typically in case of low SNR, it occurs frequently that the BSS techniques are not capable of extracting the fetal ECG signals. To overcome this problem of robustness against noise – and as a side effect, also the problem of unknown order of the generated linear combinations – in this paper a physiology-based source separation (PBSS) technique is developed.

The PBSS technique operates by spatially combining the abdominal signals, based on knowledge about the positions of the recording electrodes, to obtain a three-dimensional representation of the signals. This three-dimensional representation is related to the fetal VCG and, although it is still corrupted by noise, typically exhibits a higher SNR than the signals that were available before the spatial combining. The main advantage of this SNR enhancement is that it is based on physiology and as a result is robust to noise. After spatial combination of the fetal ECG signals, the three-dimensional representation is approximated by fitting an ellipse to the combined data points. The paradigm of fitting a two-dimensional

ellipse to three-dimensional data is explained in Section 4.2. The sources that are associated to the fetal ECG can, subsequently, be obtained by projecting the three-dimensional representation of the abdominal signals onto the long axis, the short axis and the normal vector of this ellipse.

To recapitulate, in this paper a PBSS technique is developed that overcomes robustness issues that are associated with blind techniques such as PCA and ICA. The PBSS technique is used to generate a linear combination of fetal ECG signals in such way that it exhibits increased SNR with respect to the original fetal ECG signals, thus facilitating detection of the QRS complexes. By averaging consecutive ECG complexes, synchronized on the QRS complexes, in turn, the non-invasive fetal ECG signals can be enhanced, potentially providing them with sufficient quality to support clinical decision-making.

The PBSS technique is evaluated by assessing its performance in spatially combining fetal ECG signals obtained from real abdominal recordings on women with various gestational ages and detecting the QRS complexes from the spatially combined signal. The performance is gauged by comparing it to the performance of both PCA and ICA on the same abdominal signals. More specifically, the performance of the PBSS technique is compared to that of PCA and ICA on unprocessed abdominal recordings (i.e. without removal of the maternal ECG) and to that of PCA and ICA on preprocessed abdominal recordings (i.e. after removal of the maternal ECG). The latter two approaches are expected to improve the performance of the respective BSS techniques PCA and ICA in the sense that the maternal ECG does not longer play a role in the source separation. The PCA and ICA technique are briefly discussed in Section 4.3, while the methodology for the comparison is discussed in Section 4.4. The results are presented in Section 4.5 and finally discussed in Section 4.6.

4.2 Physiology based source separation

The PBSS technique is discussed in separate parts, each in a different subsection. The mutual connection between these parts of the PBSS technique is schematically depicted in figure 4.1.

4.2.1 VCG estimation

The abdominal fetal ECG signals can be assumed linear combinations of three orthogonal signals that together constitute the VCG. This implies that three independent ECG signals are enough to fully describe the VCG, meaning that all additional ECG signals are redundant, yet can be used to enhance the robustness of the VCG determination against noise. Taking the VCG to be represented by

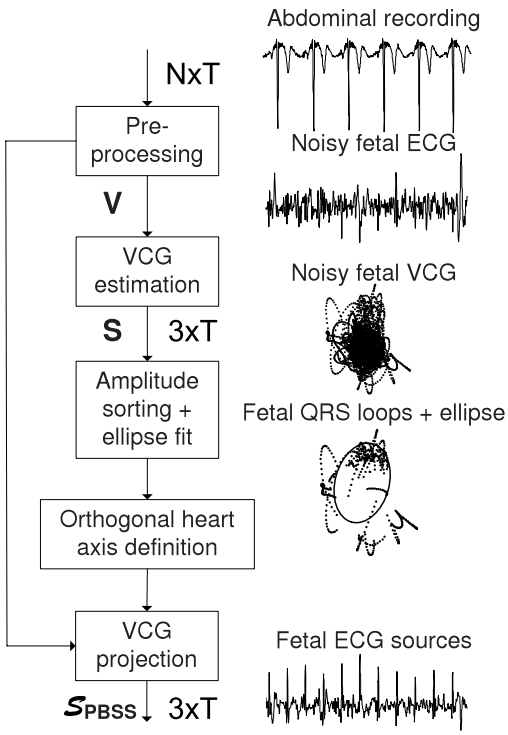

Figure 4.1: *Block scheme of the informed source separation technique. Each of the blocks is discussed in detail in Section 4.2 with the exception of the Preprocessing block, which is discussed in Section 4.4. On the right, typical examples of the signals that are used as inputs for the various blocks are depicted.*

the $[3 \times T]$ matrix $\mathbf{S}$, where each row represents one of the orthogonal signals of length T, and taking the N abdominal fetal ECG signals to be represented by the $[N \times T]$ matrix $\mathbf{V}$, the relation between the VCG and ECG can be described by:

$$\mathbf{V} = \mathbf{D}\mathbf{S}, \tag{4.1}$$

with $\mathbf{D}$ the $[N \times 3]$ matrix containing electrode positions. This matrix is determined from analysis of photographs of the abdomen, taken from several, orthogonal directions. The linear combination of the three orthogonal signals is, thus, described by the projection of the VCG $\mathbf{S}$ onto the electrode position vector, as mentioned in Section 4.1. Inverting equation 4.1 gives:

$$\mathbf{S} = \left(\mathbf{D}^T\mathbf{D}\right)^{-1}\mathbf{D}^T\mathbf{V} = \mathbf{D}^\dagger\mathbf{V}, \tag{4.2}$$

where $\mathbf{D}^{\dagger}$ is the Moore-Penrose inverse of the matrix $\mathbf{D}$, also referred to as the inverse Dower matrix [17]. The calculation of the VCG is illustrated in figure 4.1 as *VCG estimation*. It has to be noted, here, that the ECG signals $\mathbf{V}$ comprise several heartbeats and that the VCG $\mathbf{S}$ therefore shows the time path of the electrical field vector for several heartbeats overlayed on one another.

In addition, it has to be noted that the VCG estimation limits the SNR gain that can be potentially reached by the PBSS technique. That is, by the weighted combination of individual ECG signals – as done, albeit in different forms, by PCA and ICA – the possible increase in SNR is larger than can be reached from the projection of $\mathbf{S}$ onto any vector. However, since the goal of the PBSS technique is not to obtain a maximum SNR but to provide a means for robustly detecting QRS complexes, this limitation of the PBSS technique is of minor concern. In fact, the reason for adopting the VCG estimation approach in the PBSS technique is to ensure that spatial correlation is exploited in all cases – even when this correlation cannot be directly assessed from the ECG signals themselves – to, at least, some extent.

4.2.2 Amplitude sorting

The QRS complexes of the ECG generally entail the parts with the largest amplitude. However, because these QRS complexes also comprise only a small fraction of the ECG signals, the fetal VCG $\mathbf{S}$ usually represents itself as a scatter plot in which most points in the plot will be focused near the origin of the axes system. Since these points (i.e. the points near the origin) are not associated to the QRS complexes, omitting these points from the scatter plot results in a scatter plot in which most points are associated the QRS complexes. This omission is justified since the purpose of the PBSS technique is to spatially combine the fetal ECG signals in such way that the SNR of the QRS complexes is enhanced, rather than that the SNR of the complete ECG signals is enhanced. As the QRS complex of a fetus lasts about 40 ms [18] and the time between two heartbeats lasts about 400 ms (i.e. a heartrate of 150 beats per minute), only the top 10 % of the points needs to be retained (i.e. the points with the largest distance from the origin of the scatter plot). To prevent potentially present artifacts from affecting the further processing of the data points, any point that is further away from the origin than twice the mean distance, determined over the points remaining after omission of the bottom 90 %, is omitted as well. The omission of the low amplitudes and potential artifacts in the VCG scatter plot is indicated in figure 4.1 as *amplitude sorting*.

Besides the fact that the QRS complexes exhibit a superior SNR with respect to the rest of the ECG, they have another property that renders them advantageous to the purpose of the PBSS technique: they have an almost planar shape

[19]. As a consequence of this planar shape, the scatter plot of the overlayed QRS complexes can be approximated by a two-dimensional mathematical function. Since random noise would cause the scatter plot to have a circular shape (i.e. a spherical shape in three dimensions), any spatial correlation would interfere with the symmetrical shape of this circle, causing it to obtain a preferential direction. This preferentially directed scatter plot of overlayed QRS complexes is approximated here by an ellipse.

4.2.3 Ellipse fitting

To facilitate the fitting of the two-dimensional ellipse to the three-dimensional scatter plot, each point in the scatter plot can be projected onto the three orthogonal planes of a Cartesian coordinate system. In each of these planes, the scatter plot can again be approximated by an ellipse, but now in a two-dimensional plane. At first sight this might pose a problem to the ellipse approximation in the three-dimensional scatter plot, as the three orthogonal ellipses fitted in the two-dimensional planes cannot readily be combined to yield a single ellipse in three-dimensional space. However, the main interest in the PBSS technique is to find the preferential direction of the scatter plot (i.e. the direction of the long axis of the ellipse) and this direction can be readily obtained from combination of the preferential directions in the three two-dimensional ellipse fits. In addition, as in each of the orthogonal planes two components of the three-dimensional preferential direction are determined, each component is determined twice. That is, in the *xy*-plane, the x and y component of the preferential direction are determined and in the *xz*-plane the x component is determined a second time. The match between these two independent determinations yields a direct way to assess the reliability of the ellipse fits; good correspondence between the various components signifies an accurate ellipse fit in each of the orthogonal planes, whereas poor correspondence signifies an inaccurate ellipse fit and thus an inaccurate estimation of the preferential direction in the scatter plot.

The ellipses are fitted in the two-dimensional planes using a least squares approach. In this approach the ellipse is described by the conic equation:

$$f\left(\vec{x},\vec{a}\right) = a_1x^2 + a_2xy + a_3y^2 + a_4x + a_5y + a_6 = 0. \tag{4.3}$$

For given $\vec{a}$, the ellipse is fully described and only for points $\vec{x}_i$ that lie exactly on the ellipse the conic equation of equation 4.3 will equal zero. Any deviation in the conic equation for $\vec{x}_i$ will therefore yield a measure for the error of the ellipse fit. By minimizing the summed square of this error ϵ:

$$\sum_i^T \epsilon_i^2 = \sum_i^T \left(a_1x_i^2 + a_2x_iy_i + a_3y_i^2 + a_4x_i + a_5y_i + a_6\right)^2, \tag{4.4}$$

the optimal estimate $\hat{\vec{a}}$ for the ellipse parameters can be assessed.

Prior to estimation of the ellipse parameters, the potential bias of the ellipse is removed by subtracting the mean value of the scatter points across each dimension. The fitting of an ellipse to the scatter plot is indicated in figure 4.1 as *ellipse fit*.

4.2.4 Orthogonal heart axis definition

As mentioned previously, the preferential direction of the scatter plot is approximated by the direction of the long axis of the ellipse. In the two-dimensional planes onto which the scatter plot is projected, the direction and the amplitude of this long axis can be readily assessed by determining the distance $|\vec{r}_{\text{long}}|$ and the orientation α_{long} between the origin of the fitted ellipse and the point on the ellipse for which the distance to the origin is largest.

With the amplitude and orientation of the long axis determined for each orthogonal plane, the long axis can be decomposed into two components; e.g. for the *xy*-plane it can be decomposed into:

$$r^x_{\text{long}} = |\vec{r}_{\text{long}}| \cos \alpha_{\text{long}} \qquad \text{and} \qquad r^y_{\text{long}} = |\vec{r}_{\text{long}}| \sin \alpha_{\text{long}}. \tag{4.5}$$

The direction of the long axis in three-dimensional space follows from fitting the ellipse in all three orthogonal planes and subsequent averaging of each of the twice determined (as discussed in Section 4.2.3) long axis components, i.e. r^x_{long}, r^y_{long}, and r^z_{long}.

By projecting the scatter plot onto this three-dimensional long axis, one of the three fetal ECG sources $\boldsymbol{\mathcal{S}}_{\text{PBSS}}$ can be obtained. The other two sources can be determined straightforwardly, i.e. by projecting the scatter plot onto the short axis of the fitted ellipse and onto the normal vector of the ellipse plane. The direction of the short axis of the ellipse is determined similarly as the direction of the long axis, except that the length $|\vec{r}_{\text{short}}|$ and orientation α_{short} of the short axis are determined from the point on the ellipse at orientation $\alpha_{\text{short}} = \alpha_{\text{long}} + \frac{\pi}{2}$. The direction of the normal vector, in turn, is determined by:

$$\vec{r}_{\text{normal}} = \vec{r}_{\text{long}} \times \vec{r}_{\text{short}}, \tag{4.6}$$

where $\bullet \times \bullet$ denotes the vector-product. The determination of the directions of these three axes (i.e. the long axis, short axis, and normal vector) are indicated in figure 4.1 as *orthogonal heart axis definition*.

4.2.5 VCG projection

Although the projection of the scatter plot onto the three axes of the fitted ellipse provides three linearly independent sources of the fetal ECG, the method as

described in this section may not seem a source separation technique. However, when recalling that the scatter plot of the fetal VCG is obtained by multiplying the ECG signals matrix $\mathbf{V}$ with $\mathbf{D}^{\dagger}$, the mixing matrix $\mathbf{M}_{\mathrm{PBSS}}$ that maps the ECG signals onto the independent sources can be expressed as:

$$\mathbf{M}_{\mathrm{PBSS}} = \begin{pmatrix} \vec{r}_{\mathrm{long}} \\ \vec{r}_{\mathrm{short}} \\ \vec{r}_{\mathrm{normal}} \\ \vdots \end{pmatrix} \mathbf{D}^{\dagger}. \tag{4.7}$$

Here, the dots on the bottom rows indicate potential projections onto other directions. These latter projections, however, do not represent any of the fetal ECG sources. The independent sources $\boldsymbol{\mathcal{S}}_{\mathrm{PBSS}}$ are subsequently determined as:

$$\boldsymbol{\mathcal{S}}_{\mathrm{PBSS}} = \mathbf{M}_{\mathrm{PBSS}}\mathbf{V}. \tag{4.8}$$

The projection of the VCG onto the axes of the fitted ellipse is indicated in figure 4.1 as *VCG projection*.

In figure 4.2, the PBSS method is illustrated by means of three examples. These examples comprise some of the original fetal ECG signals, the amplitude sorted VCGs and their corresponding ellipse fits, and the fetal ECG signals originating from the VCG projection. The three depicted examples each have different SNR; the first has relatively high SNR, the second has average SNR, and the last has an SNR of zero (i.e. the fetal ECG signals are replaced by Gaussian noise signals).

From the examples in figure 4.2 it can be seen that, as expected, the fitted ellipse becomes more and more spherical with lower SNR. That is, the VCG scatter plot loses its preferential direction when the noise becomes more dominant.

4.3 Blind source separation

4.3.1 Principal component analysis

In PCA the correlated fetal ECG signals $\mathbf{V}$ are transformed into a number of uncorrelated signals called principal components. The first principal component accounts for as much of the variability in $\mathbf{V}$ as possible. In turn, each succeeding components accounts for as much of the remaining variability as possible.

The principal components can be calculated using the covariance method [20]. In this method, the fetal ECG signals $\mathbf{V}$ are multiplied with an orthonormal transformation matrix $\mathbf{P}$ such that the resulting sources $\boldsymbol{\mathcal{S}}_{\mathrm{PCA}}$ are uncorrelated:

$$\boldsymbol{\mathcal{S}}_{\mathrm{PCA}} = \mathbf{P}^{T}\mathbf{V}, \tag{4.9}$$

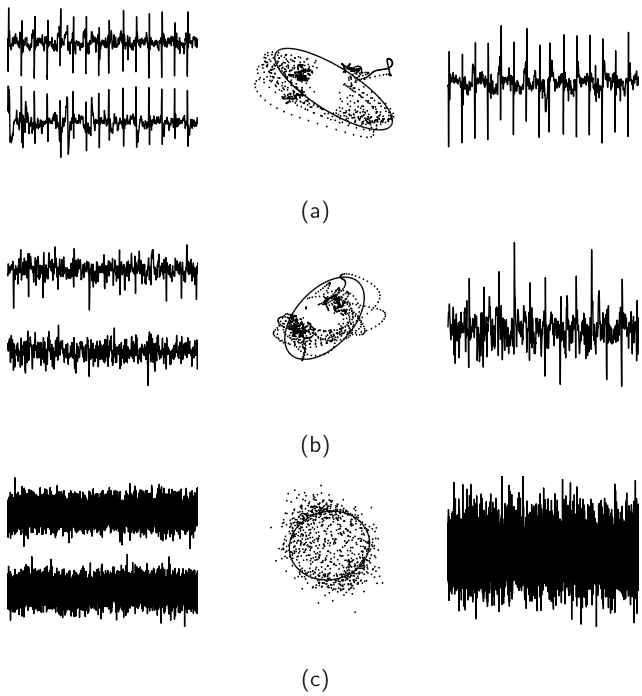

Figure 4.2: *Illustration of the PBSS method. In (a) the method is applied on fetal ECG signals with a relatively high SNR, in (b) the method is applied on signals with an average SNR, and in (c) the method is applied on Gaussian noise signals. For each of the examples, the graphs on the left show two of the N recorded fetal ECG signals. The center plot shows the scatter plot of the amplitude sorted VCG and its associated ellipse fit. The right plot shows the source signal resulting from projection of the VCG onto the long axis of the ellipse.*

with the constraints that $\mathrm{cov}(\boldsymbol{\mathcal{S}}_{\mathrm{PCA}})$ is a diagonal matrix and that $\mathbf{P}^T = \mathbf{P}^{-1}$. Consequently, with substitution of equation 4.9:

$$\begin{aligned} \mathrm{cov}\left(\boldsymbol{\mathcal{S}}_{\mathrm{PCA}}\right) &= \mathbb{E}\left[\boldsymbol{\mathcal{S}}_{\mathrm{PCA}}\boldsymbol{\mathcal{S}}_{\mathrm{PCA}}^T\right] \\ &= \mathbf{P}^T\mathbb{E}\left[\mathbf{V}\mathbf{V}^T\right]\mathbf{P} \\ &= \mathbf{P}^T\mathrm{cov}\left(\mathbf{V}\right)\mathbf{P}. \end{aligned} \tag{4.10}$$

Since $\mathrm{cov}(\boldsymbol{\mathcal{S}}_{\mathrm{PCA}})$ is a diagonal matrix, equation 4.10 is nothing more than an Eigenvector problem:

$$\mathbf{P}\mathrm{cov}\left(\boldsymbol{\mathcal{S}}_{\mathrm{PCA}}\right) = \mathrm{cov}\left(\mathbf{V}\right)\mathbf{P}. \tag{4.11}$$

Thus, by solving the Eigenvector problem of equation 4.11, the orthonormal transformation matrix $\mathbf{P}$ can be assessed and, using equation 4.9, the sources $\boldsymbol{\mathcal{S}}_{\mathrm{PCA}}$ determined.

The source that represents the fetal ECG is selected from the N sources by visual inspection.

4.3.2 Independent component analysis

The assumption of uncorrelated source signals in PCA is extended by the assumption of statistical independency for ICA. ICA operates by estimating both the independent sources of the fetal ECG $\boldsymbol{\mathcal{S}}_{\mathrm{ICA}}$, defined as:

$$\boldsymbol{\mathcal{S}}_{\mathrm{ICA}} = \mathbf{M}_{\mathrm{ICA}}\mathbf{V}, \tag{4.12}$$

and the mixing matrix $\mathbf{M}_{\mathrm{ICA}}$ by linearly combining the fetal ECG signals $\mathbf{V}$ in such way that the resulting combinations exhibit a distribution that is as little Gaussian as possible. The Central Limit Theorem states that the distribution of a sum of random variables tends towards a Gaussian distribution [21]. Thus, a combination of two random variables exhibits a distribution that is closer to a Gaussian distribution than the distribution of any of the two original variables. Hence, minimizing the Gaussianity of the source signals, maximizes their statistical independency.

In fact, the ICA approach is to some extent similar to the developed PBSS technique. Since signals containing only Gaussian noise would yield a spherical scatter plot in the PBSS technique, the search for a preferential direction in the scatter plot can be regarded as the maximization of the non-Gaussianity of the source signals. The main difference between the two techniques, however, is that the PBSS technique, before maximizing the non-Gaussianity, uses physiological knowledge on the spatial correlation of the signals by calculating the VCG, reducing the dimension of the problem from N to 3.

For implementation of ICA implementation, the FastICA algorithm [22] is used. As with PCA, the source representing the fetal ECG is selected from the calculated independent sources by visual inspection.

4.3.3 Application of BSS techniques

The PCA and ICA techniques are both applied on the fetal ECG signals in two different ways. In the first way, they are applied similar to the PBSS technique: both PCA and ICA are applied on fetal ECG signals that have been preprocessed to remove the maternal ECG. The results of these approaches are labeled as augmented PCA (aPCA) and augmented ICA (aICA). In the second way, both BSS technique are applied on fetal ECG signals in which the maternal ECG has not

yet been removed. The reason for using this second approach as well is that both PCA and ICA are capable of extracting a fetal ECG source signal from unprocessed abdominal fetal ECG recordings [13], [14]. The source signals resulting from this approach might differ significantly from the ones determined from the preprocessed ECG recordings as potential negative aspects of the maternal ECG removal do no longer play a role. The source signals resulting from the second approach are labeled PCA and ICA.

It has to be noted the comparison between the PBSS technique, aPCA, and aICA on the one hand and PCA and ICA on the other hand at first sight seems to be unfair as PCA and ICA have to deal with more interferences (i.e. the maternal ECG) than PBSS, aPCA, and aICA. However, as most applications of PCA and ICA in the field of fetal monitoring are used in the way that PCA and ICA are used here, the application of PCA and ICA is included in this paper for reasons of completeness.

As with the aPCA and aICA approach, also for PCA and ICA the source signal that represents the fetal ECG is selected from the calculated sources by visual inspection.

4.4 Evaluation

4.4.1 Fetal ECG signals

Data acquisition and preprocessing

The fetal ECG signals are recorded from the maternal abdomen using eight contact electrodes on the maternal abdomen with a common reference near the umbilicus (see figure 4.3). The signals recorded with these electrodes are digitized using the NEMO device (Maastricht Instruments BV, the Netherlands), an 8-channel dedicated amplifier with programmable gain and sampling frequency, set at 500 and 1 kHz, respectively, and high input impedance.

The signals acquired from the maternal abdomen contain a mixture of fetal ECG, maternal ECG, muscular activity, and other interferences. The maternal ECG, being the predominant interference, is removed by a dynamic template subtraction technique [8]. The other interferences are partly removed using frequency selective filtering, but due to the overlap with the frequency content of the fetal ECG [23] a significant fraction of these interferences remains. The filtering and the removal of the maternal ECG are referred to in figure 4.1 as *preprocessing*.

Figure 4.3: *Photograph of the electrode configuration and the NEMO data acquisition system. The common reference electrode near the umbilicus is not attached in this photograph. Photo: Bart van Overbeeke.*

Patient demographics

In total, 17 recordings of 5 minutes each are performed on 17 different patients, ranging between 21 weeks of gestational age and term. For one of the recordings at term, also the invasive fetal scalp ECG was simultaneously recorded. All women were healthy and had uncomplicated singleton pregnancies.

4.4.2 Evaluation criteria

The performance of the developed PBSS technique is evaluated by comparing it to the performance of the BSS techniques aPCA and aICA (and PCA and ICA). To quantify the performance, the quality of the determined linear combination (i.e. source signal) of the fetal ECG signals, two approaches are used.

In the first way, the percentage of fetal QRS complexes that are detected correctly in the linear combination serves as measure of the performance. The percentage of correctly detected peaks is expressed here by the sensitivity Se and positive predictive value PPV:

$$\mathrm{Se}\ (\%) = \frac{\mathrm{TP}}{\mathrm{TP}+\mathrm{FN}} \cdot 100 \tag{4.13}$$

$$\mathrm{PPV}\ (\%) = \frac{\mathrm{TP}}{\mathrm{TP}+\mathrm{FP}} \cdot 100, \tag{4.14}$$

with TP the number of correctly detected fetal QRS complexes (true positives), FN the number of undetected QRS complexes (false negatives), and FP the

number of falsely detected QRS complexes (false positives). For the first four recordings mentioned above, these numbers are assessed by visual analysis, while for the last recordings they are assessed from the comparison to the simultaneously performed invasive scalp ECG recording. The QRS complexes are detected in the linearly combined signal as peaks exceeding an adaptive threshold [24], [8].

For the second way of quantifying the performance, the SNR of the determined linear combination is estimated. This is achieved by using the detected QRS complexes to calculate an average ECG complex for the linear combination. By comparing this average ECG complex $\hat{\vec{V}}$ to the various ECG complexes $\vec{V}_i$ in the linear combination, a measure σ for the SNR can be obtained:

$$\sigma \ (\mathrm{dB}) = 10 \log \frac{1}{K} \sum_{i=1}^{K} \frac{\hat{\vec{V}} \hat{\vec{V}}^T}{\left(\vec{V}_i - \hat{\vec{V}}\right)\left(\vec{V}_i - \hat{\vec{V}}\right)^T}, \tag{4.15}$$

with K the number of ECG complexes in the 5 minute long signals. Note that both the averaged ECG and the individual ECG complexes are represented by a $[1 \times T]$ row vector here instead of by a $[N \times T]$ matrix as in equation 4.1 because the linear combination yields only one signal.

4.5 Results

In figure 4.4(a) an example of an eight lead fetal ECG recording is shown for the patient at term, for which also the invasive fetal ECG was recorded simultaneously. In figure 4.4(b) the calculated sources for each source separation technique (i.e. PBSS, aPCA, aICA, PCA, and ICA) are shown, together with the simultaneously recorded fetal scalp ECG signal. The circles in the plot indicate the detected QRS complexes and for the PBSS technique only the source along the long axis of the fitted ellipse is depicted. Note that for the aPCA method, at about 8.7 s, one of the fetal QRS complexes is missed by the peak detection algorithm. The graphs in figure 4.4 only show the signals for a period of 10 s and for one patient.

The results of the evaluation of either method in terms of the sensitivity, the positive predictive value, and the SNR for all recordings is shown in figures 4.5, 4.6, and 4.7.

The results in figures 4.5–4.7 indicate that PCA and ICA perform worse than the other techniques for almost all recordings. Intuitively, this difference in performance can be explained by the fact that both PCA and ICA can maximally calculate eight source signals from the eight-channel abdominal fetal ECG recordings [20], [21]. Without prior removal of the maternal ECG and other interferences, most of the eight calculated source signals still are a linear combination of the actual source signals. That is, if each of the abdominal signals constitutes a

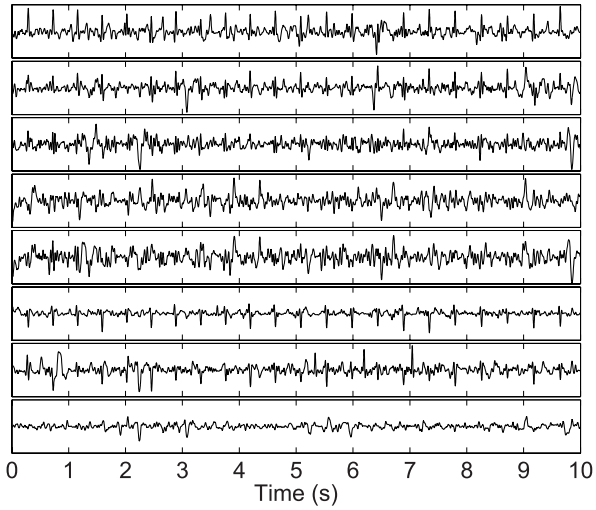

(a)

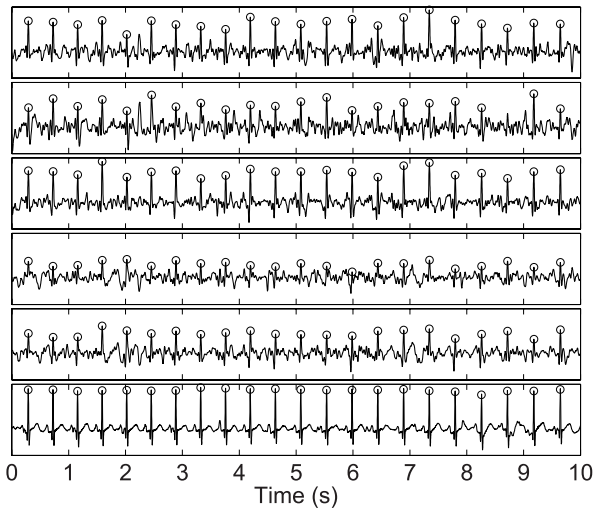

(b)

Figure 4.4: *Example of (a) eight lead fetal ECG signals obtained with the electrode configuration of figure 4.3 and (b) the calculated sources signals from PBSS (top graph), aPCA (second graph), aICA (third graph), PCA (fourth graph), and ICA (fifth graph) plus the simultaneously recorded invasive fetal scalp ECG (bottom graph). The detected fetal QRS complexes are indicated with the circles.*

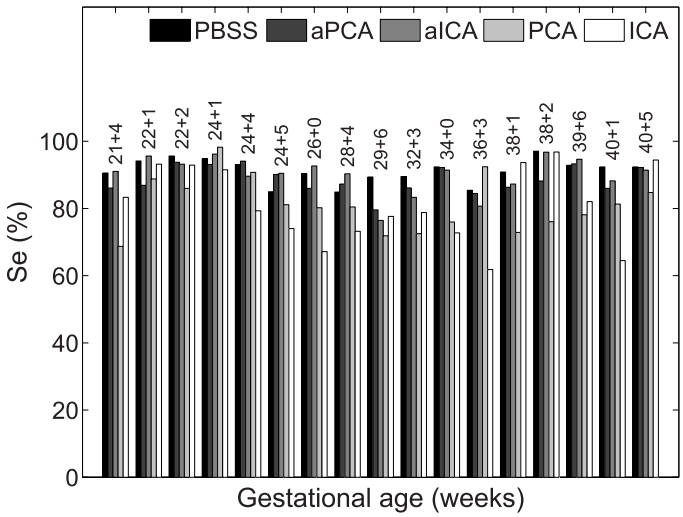

Figure 4.5: *Sensitivity of the QRS detection for all 17 recordings and for each of the source separation techniques.*

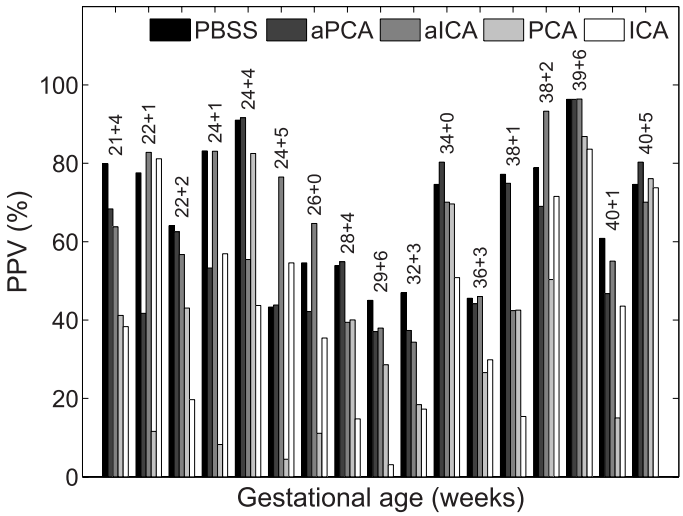

Figure 4.6: *Positive predictive value of the QRS detection for all 17 recordings and for each of the source separation techniques.*

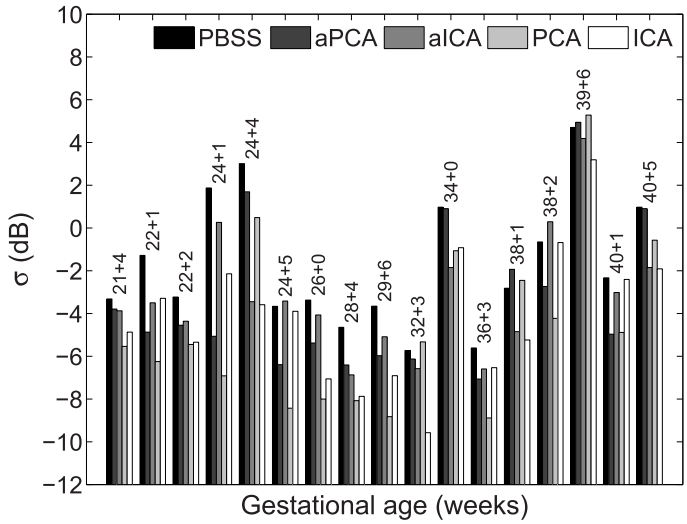

Figure 4.7: *SNR σ of the source signals for all 17 recordings and for each of the source separation techniques.*

linear combinations of e.g. ten independent source signals, the $[8 \times T]$ matrix $\mathbf{V}$ cannot be fully decomposed into a $[10 \times T]$ matrix $\mathbf{S}$ but only into a $[8 \times T]$ matrix. Hence, the eight source signals calculated by PCA and ICA cannot fully correspond to the ten original independent sources signals. This implies that the source signal representing the fetal ECG will be a linear combination of the actual fetal ECG and noise. For PBSS, aPCA, and aICA, on the other hand, some of the independent source signals (i.e. maternal ECG and part of other interferences) are *a priori* removed from $\mathbf{V}$, facilitating improved decomposition of $\mathbf{V}$ into the original source signals.

From figures 4.5–4.7 it can also be seen that where aPCA and aICA show occasional reductions in Se, PPV, or σ, the performance of PBSS is rather constant. Moreover, the performance of the PBSS technique is in most cases larger, albeit marginally, than the performance of aPCA and aICA. From this finding it can, therefore, be concluded that the PBSS technique performs similarly well as, or even better than, the aPCA and aICA techniques and has the additional advantage that its performance is more robust.

Finally, figures 4.5–4.7 show that the performance of all methods exhibits a reduction between 26 and 32 weeks of gestation. This reduction in performance can be explained by the development of the vernix caseosa, a waxy layer that electrically isolates the fetus from its surroundings, develops around 28 weeks of gestation, and start to shed around 32 weeks of gestation. In addition, it can be seen that, whereas the performance in terms of the Se is rather constant, the

performance in terms of σ and PPV value fluctuates more and shows a relation between σ and PPV. That is, for high σ also the PPV is relatively high; for low σ, also the PPV is low. This relation can be explained by the fact that a small σ signifies more noise in the ECG signal. This higher noise level, in turn, increases the possibility of the noise to be (incorrectly) detected as a QRS complex. The fact that Se is less affected by noise can be explained by the fact that the Se is governed by the ratio between the correctly detected QRS complexes (TP) and the missed QRS complexes (FN). These missed complexes not only occur as a result of increased noise levels, but also occur due to the fact that during the removal of the maternal ECG some of the fetal QRS complexes are removed or affected as well. The latter effect is independent of noise levels and hence explains the relation between Se and σ.

As mentioned in Section 4.1, a side effect of the developed PBSS technique is that it also overcomes the problem of unknown order of the source signals determined by aPCA and aICA (and PCA and ICA). Due to this problem, these techniques required additional signal processing to identify which of the calculated source signals represents the fetal ECG. Although this is a triviality in source signals with a relatively high SNR, for signals with a low SNR this can impose a significant problem to automated applications of the techniques. In addition, neither of these BSS techniques provides all three orthogonal sources of the ECG in all situations. The PBSS technique, on the other hand, is capable of calculating all three sources, as shown in figure 4.8 for the patient at 28 weeks of gestation.

In each of the three sources in figure 4.8 the fetal ECG can be distinguished, although the projection normal to the ellipse plane shows significant artifacts. These artifacts are caused by residues of the maternal ECG, originating from imperfections in the dynamic template subtraction technique [8].

4.6 Discussion and conclusions

The developed PBSS technique provides a method for linearly combining low SNR fetal ECG signals in such way that the linear combination has an improved SNR, thus facilitating detection of the fetal QRS complexes. The method performs more robustly than the BSS techniques aPCA and aICA and has the additional advantages that no additional signal processing for identifying the source signal that represents the fetal ECG is required and that it always provides three linearly independent sources of the fetal ECG. In addition, the PBSS technique (and also aPCA and aICA) significantly outperform PCA and ICA for all abdominal fetal ECG recordings.

In terms of the SNR of the determined source signals, the PBSS technique does not perform optimally. The reason for this suboptimal performance is the

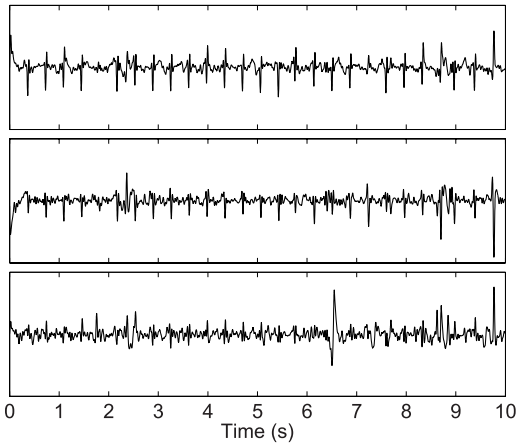

Figure 4.8: *Three source signals determined for the fetal ECG recording at 28 weeks of gestation. The top graph shows the projection of the VCG onto the long axis of the fitted ellipse. The middle graph shows the projection on the short axis of the ellipse and the bottom graph show the projection onto the normal vector of the ellipse plane.*

fact that the technique is aimed to enhance the SNR of the QRS complexes alone and does not consider the other features of the ECG. Consequently, in some situations aPCA and aICA outperform the PBSS technique as these techniques do consider the whole ECG complex, rather than the QRS complex alone. So when the interest of the source separation is not on QRS complex detection alone, but on ECG segment or interval analysis, it can be advantageous to use the source signals determined by aPCA and aICA. To overcome the problem of unknown order of the source signals in these situations, the source signals from the PBSS technique can be used as reference. That is, the aPCA and aICA source signal that shows maximum correlation with the PBSS source signals is most likely the source signal that represents the fetal ECG.

Since the amplitude of the fetal ECG is expected to rise with progressing pregnancy due to the growth of the fetus and its heart, the SNR of the abdominally recorded fetal ECG signals is also expected to rise. Naturally, with the exception of the period between 28 and 32 weeks, in which the fetus is covered by the vernix caseosa. Taking this expectation into account, then from figures 4.7 it can be concluded that the difference between the SNR of the source signals determined by the PBSS technique on the one hand, and the SNR of the source signals determined by aPCA and aICA on the other hand decreases with increasing SNR of the abdominal recordings. This effect can be explained by the fact that aPCA

and aICA operate by maximizing the variance and statistical independency of the source signals, respectively. Although these approaches suffer from significant inaccuracies for low SNR recordings, they are relatively accurate for high SNR recordings. The ellipse fit employed by PBSS, on the other hand, suffers less from inaccuracies in low SNR recordings as it uses prior, physiology based information to spatially combine the abdominal ECG signals and enhance the SNR. However, in all cases, also for high SNR recordings, the ellipse fit in PBSS is not completely accurate, reducing the performance of PBSS. This reduction in performance becomes more evident for the high SNR recordings.

The inaccuracies in the ellipse fit originate from the fact that the least squares fitting employed does not guarantee an optimal fit as fitting errors can be unwillingly weighted and are generally biased [25]. These problems can be resolved using a geometric fitting approach in which the mean orthogonal distance between the ellipse and each data point is minimized. This method, however, requires an iterative approach and significantly larger computation times. The latter is the main reason why in our technique the less accurate, yet faster, least squares fit is preferred; With this least squares fit approach, the PBSS technique requires, on average and on a standard-issue desktop computer, 1.2 seconds to calculate the source signals for fetal ECG recordings with lengths of 1 minute.

Besides the fact that the performance of the PBSS technique depends on the SNR of the recorded fetal ECG signals, the performance is also expected to depend, albeit less strongly, on the orientation of the fetus within the maternal uterus. Variations in the orientation of the fetus mostly result in rotations of the VCG and, thus, also in rotations of the fitted ellipse and its associated orthogonal axes. The projection of the rotated VCG onto these rotated axes will nevertheless be the same as before the fetal rotation. However, for each orientation of the fetus, the distances between the fetal heart and the abdominal electrodes will be different. These differences, in turn, result in different signal attenuations for each ECG signal and, as a result, in distortion of the VCG [26]. This distortion can affect the performance of the PBSS technique to some extent. However, as the shape of the QRS loop is expected to remain planar and will therefore still allow for elliptic fits, this effect is expected to be small. Naturally, larger signal attenuations will reduce the SNR of the fetal ECG signals and, as such, still affect the performance of the PBSS technique.

In future, for developing real-time fetal monitoring applications, the PBSS technique can be used for estimating which of the abdominal fetal ECG signals has the largest SNR. That is, by determining which signals contribute most to the linear combination, it can be assessed which abdominal signal contains the most fetal ECG. This abdominal signal "ordering" can be used to reduce computation times (i.e by omitting signals that do not contain a fetal ECG with sufficient

SNR) or improve patient comfort by reducing the number of electrodes on the abdomen, and is therefore subject of ongoing research. Next to this ongoing research, another subject for research is to explore whether the improved accuracy of a geometric ellipse fitting approach outweighs the associated increase in computational complexity.

Acknowledgments

This work was supported by the Dutch Technology Foundation STW.

References

[1] H. Lilja, K. Karlsson, I. Kjellmer, K. Lindecrantz, T. Olsson, and K. Rosen, "Heart rate variability and electrocardiogram changes in the fetal lamb during hypoxia and beta-adrenoceptor stimulation," *J Perinat Med.*, vol. 12, no. 3, pp. 115–25, 1984.

[2] Z. Alfirevic, D. Devane, and G. Gyte, "Continuous cardiotocography (CTG) as a form of electronic fetal monitoring (EFM) for fetal assessment during labor," *Cochrane Database of Systematic Reviews*, vol. Issue 3, 2006.

[3] S. Siira, T. Ojala, T. Vahlberg, J. Jalonen, I. Välimäki, K. Rosén, and E. Ekholm, "Marked fetal acidosis and specific changes in power spectrum analysis of fetal heart rate variability recorded during the last hour of labour," *BJOG*, vol. 112, pp. 418–23, Apr 2005.

[4] S. Cerutti, G. Baselli, S. Civardi, E. Ferrazzi, A. Marconi, A. Pagani, and G. Pardi, "Variability analysis of fetal heart rate signals as obtained from abdominal electrocardiographic recordings," *J Perinat Med.*, vol. 14, no. 6, pp. 445–52, 1986.

[5] L. de Lathauwer, B. de Moor, and J. Vandewalle, "Fetal electrocardiogram extraction by blind source subspace separation," *IEEE Trans Biomed Eng.*, vol. 47, pp. 567–72, May 2000.

[6] V. Zarzoso and A. Nandi, "Noninvasive fetal electrocardiogram extraction: blind separation versus adaptive noise cancellation," *IEEE Trans Biomed Eng.*, vol. 48, pp. 12–8, Jan 2001.

[7] M. Ungureanu, J. Bergmans, S. Oei, and R. Strungaru, "Fetal ECG extraction during labor using an adaptive maternal beat subtraction technique," *Biomed Tech (Berl).*, vol. 52, pp. 56–60, Feb 2007.

[8] R. Vullings, C. Peters, R. Sluijter, M. Mischi, S. Oei, and J. Bergmans, "Dynamic segmentation and linear prediction for maternal ECG removal in antenatal abdominal recordings," *Physiol Meas.*, vol. 30, pp. 291–307, Mar 2009.

[9] C. Peters, R. Vullings, J. Bergmans, G. Oei, and P. Wijn, "Heart rate detection in low amplitude non-invasive fetal ECG recordings," *Conf Proc IEEE Eng Med Biol Soc.*, vol. 1, pp. 6092–4, 2006.

[10] M. Kotas, J. Jezewski, T. Kupka, and K. Horoba, "Detection of low amplitude fetal QRS complexes," *Conf Proc IEEE Eng Med Biol Soc.*, vol. 2008, pp. 4764–7, 2008.

[11] H. Burger and J. Van Milaan, "Heart-vector and leads," *Br Heart J.*, vol. 8, pp. 157–61, Jul 1946.

[12] E. Frank, "An accurate, clinically practical system for spatial vectorcardiography," *Circulation*, vol. 13, pp. 737–49, 1956.

[13] E. Karvounis, M. Tsipouras, and D. Fotiadis, "Detection of fetal heart rate through 3-D phase space analysis from multivariate abdominal recordings," *IEEE Trans Biomed Eng.*, vol. 56, pp. 1394–406, May 2009.

[14] S. Waldert, M. Bensch, M. Bogdan, W. Rosenstiel, B. Schölkopf, C. Lowery, H. Eswaran, and H. Preissl, "Real-time fetal heart monitoring in biomagnetic measurements using adaptive real-time ICA," *IEEE Trans Biomed Eng*, vol. 54, pp. 1867–74, Oct 2007.

[15] C. Bishop, *Pattern recognition and machine learning*. New York: Springer Science+Business Media LLC, 2006.

[16] S. Harmeling, F. Meinecke, and K. Müller, "Analysing ICA components by injecting noise," in *4th International Symposium on Independent Component Analysis and Blind Signal Separation*, (Nara, Japan), pp. 149–154, Apr 2003.

[17] G. Dower, H. Machada, and J. Osborne, "On deriving the electrocardiogram from vectorcardiographic leads," *Clin Cardiol.*, vol. 3, pp. 87–95, 1980.

[18] J. Stinstra, E. Golbach, P. van Leeuwen, S. Lange, T. Menendez, W. Moshage, E. Schleussner, C. Kaehler, H. Horigome, S. Shigemitsu, and M. Peters, "Multicentre study of fetal cardiac time intervals using magnetocardiography," *BJOG*, vol. 109, pp. 1235–1243, Nov. 2002.

[19] F. Shellong, *Grundzüge einer klinischen Vektorcardiographie des Herzens*. Berlin: Springer-Verlag, 1939.

[20] I. Jolliffe, *Principal Component Analysis*. New York: Springer-Verlag, 2nd ed., 2002.

[21] A. Hyvärinen and E. Oja, "Independent component analysis: algorithms and applications," *Neural Netw.*, vol. 13, pp. 411–30, 2000.

[22] A. Hyvärinen, "Fast and robust fixed point algorithms for independent component analysis," *IEEE Trans On Neural Networks*, vol. 10, no. 3, p. 62634, 1999.

[23] S. Abboud and D. Sadeh, "Spectral analysis of the fetal electrocardiogram," *Comput Biol Med.*, vol. 19, no. 6, pp. 409–15, 1989.

[24] F. Gritzali, G. Frangakis, and G. Papakonstantinou, "Detection of the P and T waves in an ECG," *Comput Biomed Res.*, vol. 22, pp. 83–91, Feb 1989.

[25] S. Ahn, W. Rauh, and H. Warnecke, "Least-squares orthogonal distances fitting of circle, sphere, ellipse, hyperbola, and parabola," *Pattern Recognition*, vol. 34, pp. 2283–303, 2001.

[26] R. Vullings, C. Peters, I. Mossavat, S. Oei, and J. Bergmans, "Bayesian approach to patient-tailored vectorcardiography," *IEEE Trans Biomed Eng.*, vol. 57, pp. 586–95, Mar 2010.

Chapter 5

Evaluation of the suitability of experimental non-invasive fetal ECG measurements for fetal monitoring in clinical practice

5.1 Introduction

5.1.1 Non-invasive fetal ECG measurements

Since the introduction of auscultation of fetal heart tones in 1820 [1], fetal heart activity has rapidly grown into one of the most important indicators of fetal health. Cardiotocography (CTG), the recording of the fetal heart rate along with the uterine activity, has been the world-wide standard in fetal monitoring for decades. The success of cardiotocography is to a large extent due to the inaccessibility of the fetus in the womb, which makes it virtually impossible to obtain physiological parameters that are more directly related to fetal wellbeing. During each cardiac contraction, the muscle cells in the heart depolarize in a synchronized manner and repolarize again. The changes that occur in charges across the cell membranes, result in voltage differences that are measurable on the skin (electrocardiography). Although electrocardiography is routine clinical practice for postnatal life, the measurement is rather challenging for fetal life, as the amplitude of the fetal electrocardiogram (ECG) is 10 to 100 times smaller than the amplitude of the adult ECG, and the fetus is safely contained in the maternal uterus. Nevertheless, the first abdominal measurement from which the fetal electrocardiogram could just be distinguished, was reported already in 1906 [2].

Advances in electronics in the following decades did improve the quality of the recordings, but the largest breakthrough was obtained by applying an electrode directly to the fetal scalp in 1953 [3]. Since then, the invasive measurement of the direct fetal ECG has become the golden standard for fetal heart rate measurements during delivery. For antepartum measurements however, still no adequate

method was available. Besides the abdominal measurement of the fetal ECG, also fetal phonocardiography, the registration of fetal heart sounds, was attempted [4], but never really grew to success. In the late 1960's, Doppler ultrasound was introduced to measure fetal heart activity [5] and since the 1970's Doppler ultrasound has become the standard technique for antenatal measurement of fetal heart activity. The introduction of autocorrelation techniques in the 1980's significantly increased the performance of Doppler ultrasound cardiotocography and caused abdominal measurement of the fetal ECG and fetal phonocardiography to disappear from the market quickly.

Unfortunately, the information that cardiotocography provides, is often insufficient for reliably assessing fetal condition. More in particular, cardiotocography has a low predictive value for bad fetal outcome [6]. Therefore, in modern obstetrics any additional information that may contribute to reliable evaluation of fetal condition is highly appreciated. Possible valuable sources of additional clinical information include beat-to-beat fetal heart rate variability and fetal ECG waveform analysis. The beat-to-beat fetal heart rate contains information on fetal cardiovascular control that cardiotocography currently does not reveal [7], [8]. Fetal ECG waveform analysis has already been demonstrated to be of significant clinical value for fetal monitoring during labor [9]. Abdominal fetal ECG measurements hold the potential to provide both beat-to-beat fetal heart rate and fetal ECG waveform information already antepartum. This is one of the major reasons for technological research on abdominal fetal ECG measurement to continue during the past three decades [10], [11]. The advances in computer technology have enabled real-time analysis of recordings using advanced or time-consuming signal processing techniques, such as blind source separation techniques and adaptive filtering [12], [13], [14]. This has resulted in a growing number of publications from several research groups reporting successful results [15], [16] and into the reintroduction of commercial abdominal fetal ECG measurement technology (AN24, Monica Healthcare Ltd, UK). However, most of the measurements in the reported studies were not performed in a routine clinical setting, but in research settings varying from measurements in outpost clinics to home measurements overnight. Therefore, from these studies, it is difficult to assess the actual suitability of abdominal fetal ECG measurements for fetal monitoring during routine clinical practice.

5.1.2 Patient study

In 2007 a longitudinal patient study was started in Máxima Medical Center in Veldhoven, the Netherlands. In this study, abdominal fetal ECG measurements were repeatedly performed on pregnant patients during outpost visits to the maternity ward. The main goal of the study was to gain insight into the clinical value of new fetal monitoring parameters that can be derived from the beat-to-beat fetal heart

rate. To obtain information on the normal values of these heart rate variability parameters, non-invasive abdominal fetal ECG recordings were performed in healthy pregnancies. From these recordings, the dominating maternal electrocardiogram was removed by means of weighted averaging of maternal ECG segments [16]. The resulting traces were used to retrieve the fetal electrocardiogram, which was further processed to obtain the beat-to-beat fetal heart rate [17] and calculate the heart rate variability parameters.

As all measurements were performed in a routine clinical setting, this study provided an excellent opportunity to evaluate the clinical use of non-invasive fetal ECG measurements. To assess the suitability of the experimental abdominal ECG measurements for routine fetal monitoring, the success rate of the maternal ECG subtraction and the performance of the fetal heart rate detection were evaluated. Also, the signal to noise ratio of the retrieved fetal ECG waveforms was calculated. To a certain extent, the results of this evaluation are biased by limitations of the specific experimental setup that was used. Nevertheless, these results provide insight into the clinical usability of non-invasive fetal ECG measurements in general. In particular, valuable insight is gained into the suitability of abdominal fetal ECG measurements for fetal monitoring throughout the various stages of pregnancy.

5.2 Methods

5.2.1 Clinical measurements

Between January 2007 and January 2009, non-invasive fetal ECG measurements were performed on pregnant women, during a longitudinal patient study at Máxima Medical Center. The goal of this study was to obtain insight into the development of fetal heart rate variability parameters during the various stages of pregnancy and to establish normal values for these parameters. The study was approved by the medical ethics committee of the hospital. In total, 40 healthy singleton pregnancies were included in the study. Each of the subjects visited the maternity ward of the Máxima Medical Center at approximately 18, 22, 24, 26, 30, 34, 36, 38, and 40 weeks of gestation. During each visit, abdominal electrophysiological recordings were performed for at least 30 minutes. For these recordings, a prototype of a non-invasive electrophysiological fetal monitoring system (NEMO) was used, which incorporated an 8-channel M-PAQ universal physiological data acquisition system (Maastricht Instruments BV, The Netherlands). During the recordings, the position and movements of the fetus were monitored using ultrasonic imaging (Aloka ProSound SSD-1000). The measurements took place under normal conversation between patient and operator and in settings that were similar to routine clinical practice.

5.2.2 Signal processing

Each of the eight channels of the recorded electrophysiological signals was digitized at 1000 Hz and all channels were processed simultaneously and in real-time by dedicated software. In this software, the signals are band-pass filtered between 1.5 and 70 Hz using a FIR filter. After filtering, the software removes the dominating maternal ECG signal from the recordings by estimating each individual waveform of the maternal electrocardiogram and subtracting this estimate from the recorded signal [16]. The eight resulting traces are then used to calculate four weighted linear combinations in which the fetal ECG signal is enhanced [17]. From these linear combinations, the precise timing of QRS-complexes in the fetal electrocardiogram is detected, from which the true beat-to-beat fetal heart rate is calculated. Additionally, from the same linear combinations, averaged fetal heart rates are calculated by an algorithm that has been developed for fetal ECG recordings with poor signal-to-noise characteristics [18].

5.2.3 Evaluation

To assess the suitability of the abdominal ECG measurements for routine fetal monitoring, the performance of the system's measurement and processing chain is evaluated on different levels. First, for each recording, the performance of the maternal ECG estimation algorithm is characterized by the success rate, i.e. the number of maternal ECG waveforms that is estimated successfully divided by the total number of maternal ECG waveforms in the recording. This success rate provides information on the robustness of the algorithm but also on the quality of the electrophysiological recordings. Second, the performance of both the averaged heart rate detection and the beat-to-beat heart rate detection are evaluated. For this purpose, the calculated heart rate patterns are analyzed by a logical algorithm to detect non-physiological patterns and other artifacts. The performance of both algorithms for fetal heart rate detection is expressed by the percentage of the recording that is not marked as artifact. Finally, for all the correctly detected fetal heart beats, the peak-to-peak amplitudes of the QRS complexes and the rms-amplitudes of the entire ECG waveforms are determined. These amplitudes are used to estimate the signal-to-noise ratio of the measured fetal electrocardiograms. These signal-to-noise ratios can be used to characterize the quality of the recordings throughout pregnancy. This way, specific insight is gained into the reliability of the fetal heart rate calculations and the suitability of the measured fetal electrocardiogram for diagnostic interpretation during the various stages of pregnancy.

The difficulty of characterizing the signal-to-noise ratio of an ECG waveform is that the QRS complex, the part of the waveform that is of interest for heart beat

detection, contains only a very small part of the energy in the recorded signal. A suitable way of expressing the signal-to-noise ratio of the electrocardiogram is by considering the QRS complex as one period of a sine function. As the root-mean-square amplitude of a sine function $V_{rms} = \frac{1}{\sqrt{2}}\frac{V_{pp}}{2}$, the signal-to-noise ratio of an ECG waveform can be characterized by [18]:

$$SNR = \frac{\frac{1}{8}V_{pp,QRS}^2}{V_{rms,noise}^2}, \tag{5.1}$$

with $V_{pp,QRS}$ the peak-to-peak amplitude of the QRS complex in the ECG waveform and $V_{rms,noise}^2$ the power of the noise in the recorded signal. However, the noise component in the recorded signal cannot easily be separated, and therefore $V_{rms,noise)}^2$ cannot be measured directly. Instead the total power V_{rms}^2 of the recorded signal is measured. The total power consists of the power P_{QRS} in the QRS complex and the power in the remaining signal, which is considered as noise P_{noise}:

$$P_{total} = V_{rms}^2 = P_{QRS} + P_{noise}. \tag{5.2}$$

The power of the noise in the recording is expressed as:

$$P_{noise} = V_{rms,noise}^2 = \frac{1}{8}V_{pp,noise}^2, \tag{5.3}$$

with $V_{pp,noise}$ the peak-to-peak amplitude of the noise in the recorded signal.

To estimate the power in the QRS complex, we model the QRS complex as one period of a cosine wave with duration T_{QS} at an offset of $\frac{V_{pp,QRS}-V_{pp,noise}}{2}$ with respect to the baseline of the recording:

$$\widetilde{V}_{QRS}(t) = \frac{V_{pp,QRS} - V_{pp,noise}}{2} - \frac{V_{pp,QRS}}{2}\cos\left(\frac{2\pi t}{T_{QS}}\right), \tag{5.4}$$

with T_{QS} the duration of the QRS complex. Figure 5.1 illustrates the modeling of the QRS complex. In the recording, fetal QRS complexes have a duration of T_{QS} and two consecutive complexes are separated T_{RR}. Using equation 5.4, the power of the QRS complexes in the signal can be expressed as:

$$P_{QRS} = \frac{1}{T_{RR}}\int_0^{T_{QS}} \widetilde{V}_{QRS}^2(t)dt = \frac{T_{QS}}{T_{RR}}\left(\frac{V_{pp,QRS}^2}{8} + \left(\frac{V_{pp,QRS} - V_{pp,noise}}{2}\right)^2\right), \tag{5.5}$$

which by inserting equation 5.3 can be written as:

$$P_{QRS} = \frac{T_{QS}}{T_{RR}}\left(\frac{V_{pp,QRS}^2}{8} + \left(\frac{V_{pp,QRS} - \sqrt{8}V_{rms,noise}}{2}\right)^2\right). \tag{5.6}$$

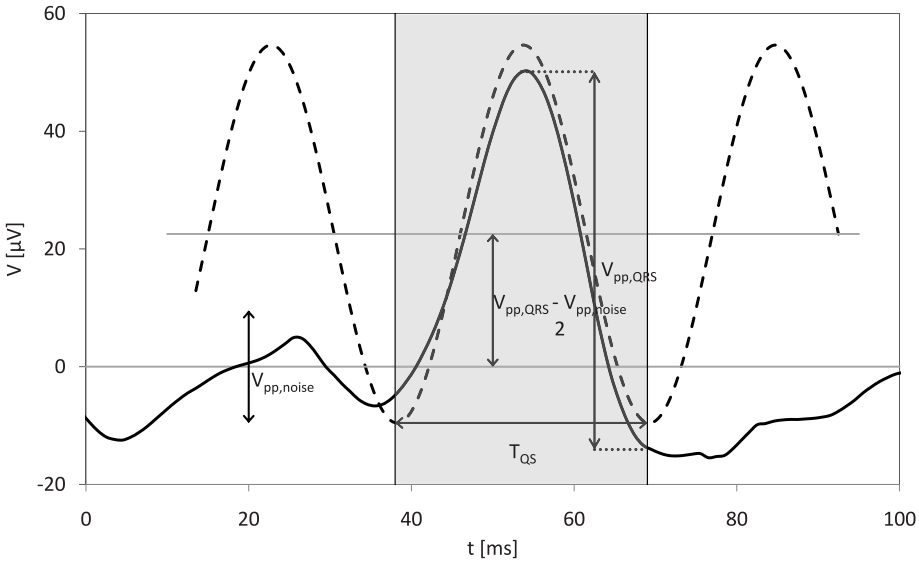

Figure 5.1: *Modeling of the QRS complex of an ECG waveform by a cosine wave. The solid line represents a part of the ECG waveform, in which the grey area marks the QRS complex. The dashed line represents the cosine wave that is fitted to the QRS complex.*

The total power P_{total} then becomes:

$$\begin{aligned} P_{total} = V_{rms}^2 &= \frac{T_{QS}}{T_{RR}} \left(\frac{V_{pp,QRS}^2}{8} + \left(\frac{V_{pp,QRS} - \sqrt{8} V_{rms,noise}}{2} \right)^2 \right) + V_{rms,noise}^2 \\ &= \left(2\frac{T_{QS}}{T_{RR}} + 1 \right) V_{rms,noise}^2 - \sqrt{2}\frac{T_{QS}}{T_{RR}} V_{pp,QRS} V_{rms,noise} + \frac{3}{8}\frac{T_{QS}}{T_{RR}} V_{pp,QRS}^2. \end{aligned} \tag{5.7}$$

Under normal conditions, the latter two terms in equation 5.7 cancel out each other almost entirely. Consequently, we may write:

$$V_{rms}^2 \approx \left(2\frac{T_{QS}}{T_{RR}} + 1 \right) V_{rms,noise}^2. \tag{5.8}$$

Typically, T_{QS}, the duration of the fetal QRS complex, is around 25 ms. By using equations 5.1 and 5.8, the signal to noise ratio of each individual fetal ECG waveform can be calculated from the peak-to-peak amplitude of the QRS complex

$(V_{pp,QRS})$, the total power of the recorded signal (V_{rms}^2) and the time between two consecutive QRS complexes (T_{RR}), which can all be determined from the recorded signals.

5.3 Results

5.3.1 Maternal ECG estimation

In the real-time processing of the electrophysiological measurements, each maternal heart beat is detected individually. In each channel, the corresponding maternal ECG waveform is estimated from segments of the preceding ECG waveforms. Failure of the algorithm to estimate the maternal ECG waveforms is logged, which provides accurate insight in the performance of the maternal ECG estimation. Failure may occur due to implementation errors in the algorithm and due to the presence of disturbances in the measured signals. The latter will particularly occur, when the quality of the recording is poor due to poor electrical contact between skin and electrode. The success rate of the maternal ECG estimation was calculated for each of the recordings. Figure 5.2 shows the success rate, plotted against the gestational age at which the recording was performed.

5.3.2 Fetal heart rate detection

All successfully estimated maternal ECG complexes were subtracted from the original recordings. The resulting traces were processed by two algorithms to obtain the fetal heart rate. One of these algorithms detects the exact timing of QRS complexes in the fetal ECG waveforms, to obtain the true beat-to-beat heart rate which is required for additional analysis [17]. For traces with poor signal-to-noise ratio, this algorithm will fail to provide a beat-to-beat fetal heart rate. Therefore, the fetal ECG traces are also processed by an algorithm that detects the 2.5 seconds averaged fetal heart rate [18]. This averaged fetal heart rate is similar to the heart rate in standard Doppler ultrasound cardiotocography and can even be calculated from fetal ECG traces with poor signal-to-noise ratios. The performance of both algorithms, defined as the percentage of the recording for which the heart rate was obtained successfully, is displayed in figure 5.3.

5.3.3 Signal-to-noise ratio

For all QRS complexes in the recordings that were successfully detected by the beat-to-beat heart rate detection algorithm, the peak-to-peak amplitude $(V_{pp,QRS})$ was measured. Also the total power of the recorded signal (V_{rms}^2) was measured. From these measurements and the time between two consecutive QRS complexes

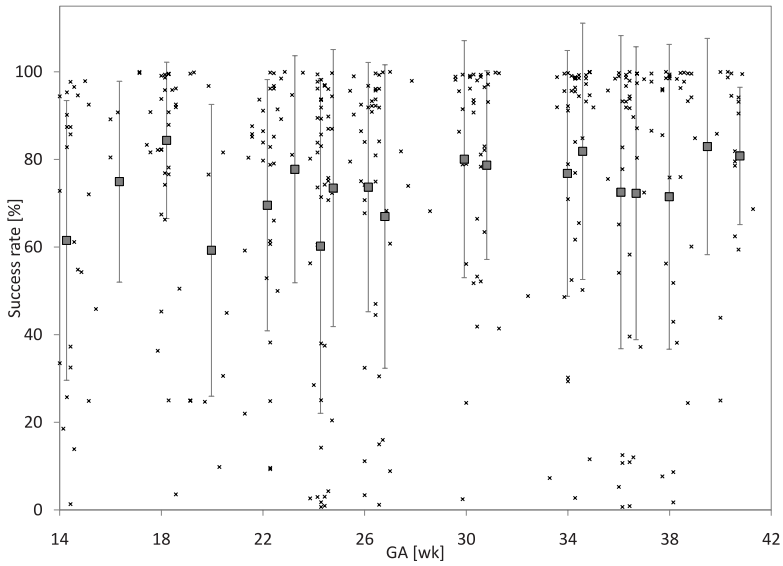

Figure 5.2: *Performance of the maternal ECG estimation algorithm. In the plot, the crosses represent individual abdominal recordings while the squares display the average performance over 20 measurements and their standard deviation.*

(T_{RR}), the signal-to-noise ratio of each ECG waveform was calculated as described in section 5.2.3. Only for recordings in which the performance of the beat-to-beat fetal heart rate detection exceeded 40 %, the average signal-to-noise ratio was calculated to characterize the signal quality of that recording. Figure 5.4 displays the average signal-to-noise ratio for these recordings, plotted against the gestational ages at which the recordings were performed. In addition, the average peak-to-peak QRS amplitude $(V_{pp,QRS})$ and the average root-mean-square noise amplitude $(V_{rms,noise})$ of these recordings are displayed in figure 5.5.

5.4 Discussion

5.4.1 Maternal ECG estimation

The performance of the maternal ECG estimation algorithm is good and remains more or less constant throughout pregnancy. The average performance over all performed recordings equals 73 %, however the median performance exceeds 85 %. The overall performance is adversely affected by a relatively small number of recordings for which the performance is extremely poor. Visual analysis of these

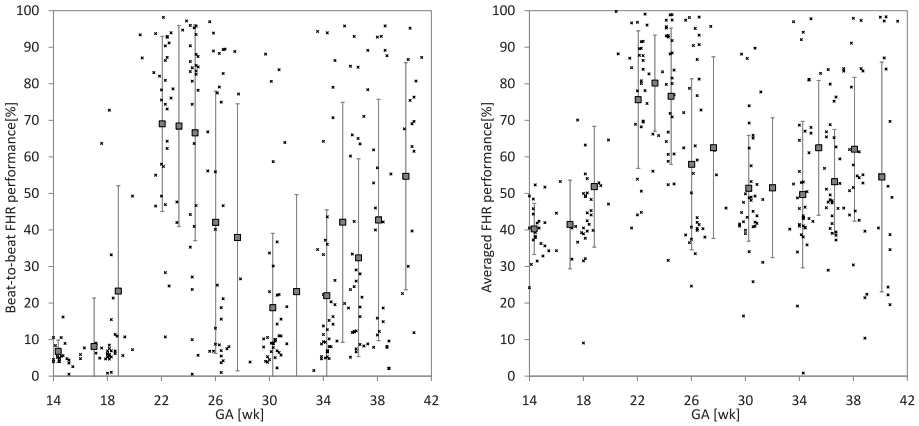

(a) Beat-to-beat fetal heart rate (b) Averaged fetal heart rate

Figure 5.3: *Performance of the algorithms for detection of the beat-to-beat fetal heart rate (a) and the averaged fetal heart rate (b). In the plot, the crosses represent individual abdominal recordings while the squares display the average performance over 20 measurements and their standard deviation.*

recordings learned that in most cases failure was caused by the presence of large noise components in the signal, which usually occurs if the electrical impedance between the measurement electrodes and the patient's skin is too high. This is a practical problem that is characteristic for electrophysiological measurements in general and not specific to abdominal measurements on pregnant women. The electrical impedance can be reduced by adequate skin preparation and careful selection of electrode material. Additionally, the noise components in the signal can be reduced by improving the frontend of the electrophysiological amplifier that is used. This way, the performance of the maternal ECG estimation is expected to further increase.

5.4.2 Fetal heart rate detection

The success of heart rate detection in the retrieved fetal ECG traces fluctuates with the duration of pregnancy. The chance of detecting a fetal heart beat is directly related to the amplitude of the QRS complex that is measured on the maternal abdomen. This amplitude depends on the size of fetal heart muscle and on the conduction from the fetal heart to the abdominal skin surface. Before 20 weeks of gestational age for most recordings, the beat-to-beat fetal heart rate can only be detected in less than 10 % of the recordings. In the same period, the

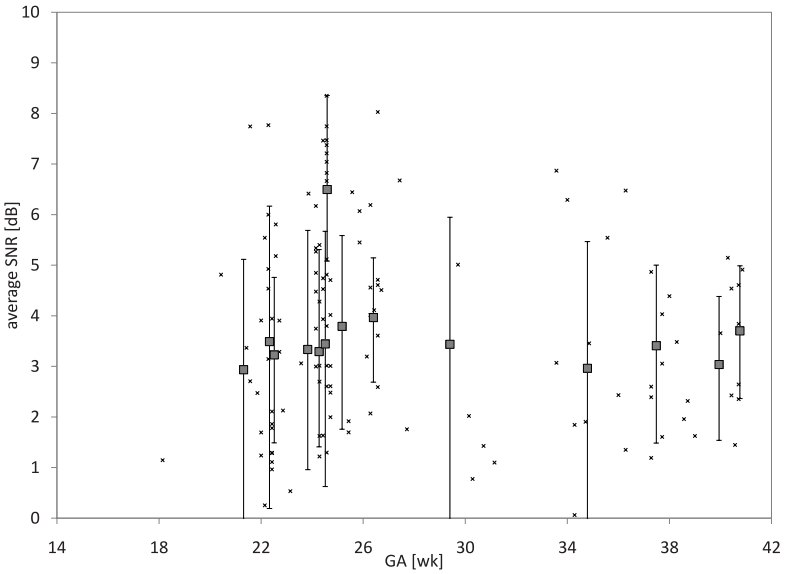

Figure 5.4: *average signal-to-noise ratio calculated for each of the recordings in which the beat-to-beat fetal heart rate performance exceeded 40 %. In the plot, the crosses represent individual abdominal recordings while the squares display the average performance over 10 measurements and their standard deviation.*

averaged fetal heart rate can be detected in 43 % of the recording. In this period of pregnancy, the fetal heart is slightly larger than a centimeter, and the amplitude of the QRS complex that is measured at the abdomen is only a few microvolt, which is too small to be easily detected.

With the growth of the fetal heart, the performance of both fetal heart rate detection techniques significantly increases after 20 weeks of gestational age. Between 20 and 25 weeks of gestational age, both heart rate detection techniques perform at their best, with average success rates of 69 % for the beat-to-beat algorithm and 78 % for the averaged heart rate detection algorithm. Between 28 and 35 weeks of gestational age the success rate of the beat-to-beat fetal heart rate detection drops to 23 % and also the success of the averaged heart rate detection is reduced (53 %). This reduced performance is consistent with findings in literature [19], [20], which suggest that the presence of isolating sections of the vernix caseosa reduces the amplitude of the fetal ECG that is measured on the maternal abdomen. This suggestion is supported by figure 5.5, where the average peak-to-peak QRS amplitude $V_{pp,QRS}$ of the heart beats that could be detected is reduced to 13 µV. After 35 weeks of gestation, the success rate of both heart

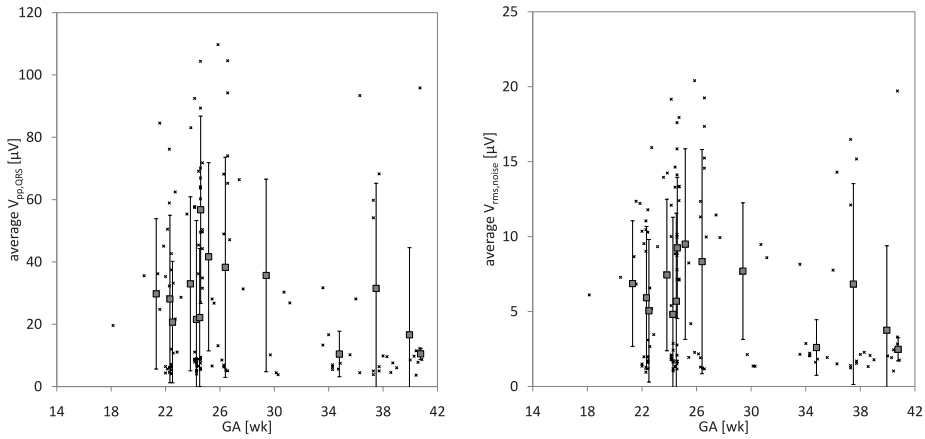

(a) Average $V_{pp,QRS}$ (b) Average $V_{rms,noise}$

Figure 5.5: *Average peak-to-peak amplitude of the QRS complex (a) and average root-mean-square noise amplitude (b) calculated for each of the recordings in which the beat-to-beat fetal heart rate performance exceeded 40 %. In the plot, the crosses represent individual abdominal recordings while the squares display the average performance over 10 measurements and their standard deviation.*

detection methods increasea again to 43 % (beat-to-beat) and 57 % (averaged heart rate), which is consistent with the literature This can be explained by the appearance of gaps in the isolating vernix caseosa [20].

5.4.3 Signal-to-noise ratio

The signal-to-noise ratio of the fetal QRS-complexes that were detected, strongly varies between recordings but the average signal-to-noise ratio remains rather constant throughout pregnancy. From 20 to 28 weeks of gestational age, the average signal-to-noise ratio gradually increases from 3 dB to over 4 dB. Between 28 and 35 weeks of gestational age, the average signal-to-noise ratio drops below 3 dB and after 35 weeks of gestational age rises again to 3.5 dB.

Interestingly, the peak-to-peak amplitude of the QRS complex and the root-mean-square amplitude of the noise in the signal that were used to calculate the signal-to-noise ratio show equal trends. Before 28 weeks of gestation, both $V_{pp,QRS}$ and $V_{rms,noise}$ cover a wide range of amplitudes, but after 28 weeks only low amplitudes are present. Apparently, the level of noise in a recording determines the threshold for the QRS-amplitudes that can be detected by the beat-to-beat fetal heart rate algorithm. Between 28 and 35 weeks of gestational age, only in

recordings with extremely small amounts of noise the QRS-amplitudes exceed this threshold. Between 20 and 25 weeks of gestational age, the QRS amplitude will be relatively large, and therefore also in recordings with larger amounts of noise, fetal heart beats are detected successfully. This is directly reflected in the success rate of the beat-to-beat heart rate detection in these stages of pregnancy.

5.5 Conclusion

Generally, the performance of the maternal ECG estimation algorithm is good. However, for recordings during which the electrical impedance between the measurement electrodes and the skin of the patient is high, the algorithm will fail. Therefore, reduction of noise in the recording will further increase the performance.

Between 20 and 28 weeks and past 35 weeks of gestational age, the success rate of the averaged fetal heart rate detection is clinically acceptable. Abdominal measurement of the fetal ECG would therefore already offer a valuable alternative to Doppler ultrasound cardiotocography in these stages of pregnancy. However, before 20 weeks and between 28 and 35 weeks of gestation, the average success rate is worse than the average signal loss when Doppler ultrasound cardiotocography is used to monitor the fetal heart rate. Therefore, the performance of the prototype fetal monitoring system in these periods needs to be improved, before it can fully replace the current standard for external cardiotocography.

The success rate of the algorithm for beat-to-beat detection of the fetal heart rate is good for gestational ages between 20 and 25 weeks. For this stage of pregnancy, abdominal measurement of the fetal ECG offers a unique opportunity to obtain cardiac information on the fetus that is otherwise unavailable. By using vectorcardiography [21], these recordings offer the potential to obtain standardized diagnostic ECG leads of the fetus, which is extremely valuable for fetal cardiology. For other stages of pregnancy, the quality of the current recordings is insufficient for clinical use.

To exploit the full potential that abdominal measurement of the fetal electrocardiogram offers, significant improvement of the performance of the prototype non-invasive fetal monitor is required. The measurement setup that was used in this study cannot be guaranteed to provide the high quality of electrophysiological recordings that is required. Only by realizing the necessary reduction of in noise in the recordings, a more reliable alternative to existing antepartum fetal monitoring techniques can be obtained and eventually contribute to more reliably assessing fetal wellbeing.

References

[1] J. Pinkerton, "Fetal auscultation–some aspects of its history and evolution," *Ir Med J.*, vol. 69, pp. 363–8, Sep 1976.

[2] M. Cremer, "Über die direkte Ableitung der Aktionströme des menschlichen Herzens vom Oesophagus und über das Elektrokardiogramm des Fötus," *Münch Med Wochenschr.*, vol. 53, pp. 811–3, Apr 1906.

[3] C. Smyth, "Experimental electrocardiography of the foetus," *Lancet*, vol. 1, pp. 1124–6, Jun 1953.

[4] A. Gunn and M. Wood, "The amplification and recording of fœtal heart sounds," *Proc R Soc Med.*, vol. 46, pp. 85–91, Feb 1953.

[5] E. Bishop, "Instrument & method: the Doppler ultrasonic motion sensor," *Obstet Gynecol.*, vol. 28, pp. 712–2, Nov 1966.

[6] H. Banta and S. Thacker, "Assessing the costs and benefits of electronic fetal monitoring," *Obstet Gynecol Surv.*, vol. 34, pp. 627–42, Aug 1979.

[7] G. Dawes, M. Moulden, and C. Redman, "System 8000: computerized antenatal FHR analysis," *J Perinat Med.*, vol. 19, no. 1-2, pp. 47–51, 1991.

[8] D. A. de Campos, J. Bernardes, A. Garrido, J. M. de Sá, and L. Pereira-Leite, "SisPorto 2.0: a program for automated analysis of cardiotocograms," *J Matern Fetal Med.*, vol. 9, pp. 311–8, Sep-Oct 2000.

[9] I. Amer-Wåhlin, C. Hellsten, H. Norén, H. Hagberg, A. Herbst, I. Kjellmer, H. Lija, C. Lindoff, M. Månsson, L. Mårtensson, P. Olofsson, A. Sundström, and K. Marsál, "Cardiotocography only versus cardiotocography plus ST analysis of fetal electrocardiogram for intrapartum fetal monitoring: a Swedish randomised controlled trial," *Lancet*, vol. 358, pp. 534–8, Aug 2001.

[10] S. Cerutti, G. Baselli, S. Civardi, E. Ferrazzi, A. Marconi, A. Pagani, and G. Pardi, "Variability analysis of fetal heart rate signals as obtained from abdominal electrocardiographic recordings," *J Perinat Med.*, vol. 14, no. 6, pp. 445–52, 1986.

[11] A. van Oosterom, "Spatial filtering of the fetal electrocardiogram," *J Perinat Med.*, vol. 14, no. 6, pp. 411–9, 1986.

[12] V. Zarzoso and A. Nandi, "Noninvasive fetal electrocardiogram extraction: blind separation versus adaptive noise cancellation," *IEEE Trans Biomed Eng.*, vol. 48, pp. 12–8, Jan 2001.

[13] L. de Lathauwer, B. de Moor, and J. Vandewalle, "Fetal electrocardiogram extraction by blind source subspace separation," *IEEE Trans Biomed Eng.*, vol. 47, pp. 567–72, May 2000.

[14] M. Ungureanu, J. Bergmans, S. Oei, and R. Strungaru, "Fetal ECG extraction during labor using an adaptive maternal beat subtraction technique," *Biomed Tech (Berl).*, vol. 52, pp. 56–60, Feb 2007.

[15] M. Taylor, M. Smith, M. Thomas, A. Green, F. Cheng, S. Oseku-Afful, L. Wee, N. Fisk, and H. Gardiner, "Non-invasive fetal electrocardiography in singleton and multiple pregnancies," *BJOG*, vol. 110, pp. 668–78, Jul 2003.

[16] R. Vullings, C. Peters, R. Sluijter, M. Mischi, S. Oei, and J. Bergmans, "Dynamic segmentation and linear prediction for maternal ECG removal in antenatal abdominal recordings," *Physiol Meas.*, vol. 30, pp. 291–307, Mar 2009.

[17] C. Peters, J. van Laar, R. Vullings, S. Oei, and P. Wijn, "Beat-to-beat heart rate detection in multi-lead abdominal fetal ECG recordings," *to be published*, pp. 1–12, 2010.

[18] C. Peters, R. Vullings, J. Bergmans, G. Oei, and P. Wijn, "Heart rate detection in low amplitude non-invasive fetal ECG recordings," *Conf Proc IEEE Eng Med Biol Soc.*, vol. 1, pp. 6092–4, 2006.

[19] J. Oldenburg and M. Macklin, "Changes in the conduction of the fetal electrocardiogram to the maternal abdominal surface during gestation," *Am J Obstet Gynecol.*, vol. 129, pp. 425–33, Oct 1977.

[20] T. Oostendorp, A. van Oosterom, and H. Jongsma, "The effect of changes in the conductive medium on the fetal ECG throughout gestation," *Clin Phys Physiol Meas.*, vol. 10, no. Suppl B, pp. 11–20, 1989.

[21] R. Vullings, C. Peters, I. Mossavat, S. Oei, and J. Bergmans, "Bayesian approach to patient-tailored vectorcardiography," *IEEE Trans Biomed Eng.*, vol. 57, pp. 586–95, Mar 2010.

Chapter 6

Beat-to-beat detection of fetal heart rate: Doppler ultrasound cardiotocography compared to direct ECG cardiotocography in time and frequency domain

Abstract

In order to obtain power spectral information of the fetal heart rate in stages of pregnancy earlier than labor, an algorithm has been developed to calculate the fetal heart rate on a beat-to-beat basis from Doppler ultrasound cardiotocographic signals. The algorithm was evaluated by comparing the calculated fetal heart rate with the heart rate determined from direct ECG-signals measured with a scalp electrode. Heart rates were compared both in time and frequency domain. In the time domain the results achieved by both methods correlate well (corr. coef. $= 0.977$ ($p < 0.001$)), in the frequency domain the results correlate even better (corr. coef. $= 0.991$ ($p < 0.001$)). Based on these findings, it can be concluded that the developed algorithm provides a valuable tool for obtaining power spectral information of the fetal heart rate in stages of pregnancy earlier than labor.

6.1 Introduction

A major problem in modern obstetrics with respect to fetal monitoring is the lack of possibilities to extract information from the fetus to assess its condition. The fetal heart rate is one of very few useful fetal signals that can be measured

published as C. Peters, E. ten Broeke, P. Andriessen, B. Vermeulen, R. Berendsen, P. Wijn, and S. Oei, "Beat-to-beat detection of fetal heart rate: Doppler ultrasound cardiotocography compared to direct ECG cardiotocography in time and frequency domain," *Physiol Meas.*, vol. 25, pp. 585-93, Apr 2004.

non-invasively and in many cases in clinical practice the only source of information available. Any improvement in this situation would be greatly appreciated. A possible additional source of information could be the power spectrum of the variation in fetal heart rate. Since the heart rate fluctuates under influence of the parasympathetic and sympathetic nervous systems [1], [2], and since the activity of these systems is a reaction to changes in physiological circumstances, the power spectrum of the variations in fetal heart rate might contain extra information. This method has already been applied successfully for analyzing the fluctuations in heart rate and blood pressure values (e.g. systolic blood pressure) of neonates [3] in the neonatal intensive care unit of our hospital. As the variations in heart rate of the neonates are calculated from ECG signals, the same method can directly be applied on fetal ECG signals acquired with a scalp electrode. Since measuring this signal is only possible during labor, the possibility of assessing heart rate variations from a signal that is non-invasively obtained by external methods would be highly esteemed.

Power spectra of fluctuations in heart rate or blood pressure values only contain meaningful information if the heart rate or blood pressure values can be acquired on a beat-to-beat basis. Determining beat-to-beat fetal heart rates from Doppler ultrasound signals has been a problem ever since the introduction of Doppler ultrasound cardiotocography (CTG) [4], [5]. First-generation monitors calculate fetal heart rates by integrating the acquired Doppler ultrasound signals and applying a level detector [6], which is not a very precise method for determining heart rates. Large improvements were achieved by the introduction of autocorrelation techniques in the second-generation monitors [6]. However, due to the fact that in the autocorrelation process a received Doppler waveform is compared to a number of previous waveforms, the determination of the heart rate still was not on a beat-to-beat basis [5]. More recent monitors are capable of calculating the heart rate even more precisely, but have unfortunately become closed systems. For this reason it has become virtually impossible to access Doppler ultrasound signals from CTG devices as raw data for more advanced analysis. Recent developments in computer technology have increased the calculation power of computers significantly. Therefore, nowadays it should be possible to calculate the fetal heart rate from raw Doppler ultrasound signals on a true beat-to-beat basis. In this paper an algorithm will be presented to calculate the fetal heart rate on a beat-to-beat basis from these signals. Furthermore we will compare both the heart rate as a function of time and the power spectrum of the variations in heart rate with simultaneously measured fetal ECG signals acquired with a scalp electrode from a fetus during labor.

6.2 Material and methods

6.2.1 Doppler ultrasound

Doppler ultrasound signal

In this study a HP 8040A (Agilent, Palo Alto, California), second generation fetal CTG-monitor with a 1.024 MHz probe was used for measuring the Doppler ultrasound signal. From this device the envelope of the original, apart from demodulation and a band-pass filter (100 – 475 Hz) unprocessed, signal was available from an analog output of this monitor. We used this signal because in a separate technical evaluation it could be demonstrated that this signal complies completely with our own calculations of this envelope, based on the same raw data. In newer generations of CTG-monitors these signals are unfortunately not available anymore.

To guarantee sufficient temporal resolution in auto-correlation calculations and in the finally obtained heart rate a sampling frequency of 1 kHz was selected using a NI 6034E data acquisition board. Further signal processing was performed using a personal computer.

Doppler ultrasound algorithm

The calculation of the beat-to-beat heart rate is realized by an algorithm which operates in two steps. In the first step a rough estimation of the points in time at which the heart cycles show up is made. This estimation is achieved by low-pass filtering of the envelope signal with a cut-off frequency of 2 Hz. With this filter the waveforms are transformed into some kind of blunt bumps. By carrying out peak-detection on this 'bumpy' pattern, global estimated locations of the heart cycles in time are obtained.

In the second step of the algorithm, the heart rate is determined beat-to-beat by calculating the auto-correlation in the frequency domain. The time-intervals of the envelope signal which are used in the calculation process are defined by the estimated locations of the heart cycles. In this way it is possible to define intervals in such way that only the waveforms corresponding to two successive heart cycles are involved in the calculation of the auto-correlation. For calculating the heart rate at a time corresponding to a certain heart cycle (n), the location of the preceding heart cycle (n-1) plus a fixed time delay defines the beginning of the interval, and the location of the successive heart cycle (n+1) plus the same time delay defines the end of the interval. In our data it appeared empirically that a fixed time delay of 125 ms resulted in all cases in boundaries of the intervals between two successive heart cycles. In this way each auto-correlation interval contains not more and not less than two heart cycles, which is a constraint to

calculate the heart rate on a beat-to-beat basis. The time delay depends on the method used for filtering in the first part of the algorithm. Figure 6.1 illustrates the intervals used in the calculation of the auto-correlation. Note that the length of the interval is heart rate dependent and equals the estimated time between bump (n-1) and bump (n+1).

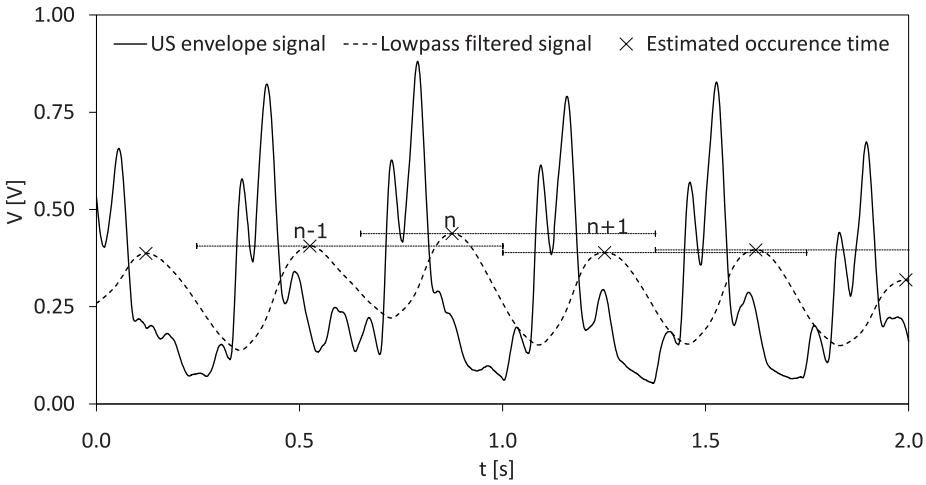

Figure 6.1: *Definition of the intervals used in the calculation of the auto-correlation. The black line represents the US envelope signal that is acquired from the analog output interface of the HP 8040A fetal monitor. The grey line represents the low-pass filtered US envelope signal. Crosses mark the peaks in the low-pass filtered US envelope signal and represent the estimated locations of the heart cycles in time. For each of these estimated locations in time, the interval used for calculating the heart rate is represented by a horizontal dashed line starting 125 ms after the estimated location of the preceding heart cycle and ending 125 ms after the estimated location of the successive heart cycle.*

In the auto-correlation, the local maximum after a certain minimal time offset (in our case 300 ms, no heart rates higher than 200 BPM are allowed) is determined. The location of this local maximum corresponds to the time shift of a waveform (first heart cycle in interval) to the most probable next waveform (second heart cycle in interval). This time shift thus equals the time between the occurrence of two successive heart cycles and therefore is inverse proportional to the heart rate. Similar to the definition of heart rate values in ECG signals, the heart rate value is allotted to the estimated moment in time of the n^{th} heart cycle.

6.2.2 Direct fetal electrocardiogram

The most ideal way to determine the heart rate from an ECG-signal is by measuring the time between the start of the depolarization at the SA-node of two successive heartbeats. In a standard ECG this is expressed by the start of the P-wave. Due to the fact that the measured fetal ECG is by far no standard ECG, it is not always possible to recognize P-waves. For this reason we determined the fetal heart rate by detecting R-waves in the directly measured fetal ECG signal. The location of the peak of the R-wave is determined by means of a polynomial fit, the time between two successive R-peaks is used to calculate the instantaneous fetal heart rate. The use of the R-wave simplifies the calculation of the heart rate, although theoretically the start of the P-wave should be preferred as the definition of the start of the heartbeat. As a result, additional jitter may occur due to variations in P-R interval time. Generally, this jitter is neglected in neonatal and fetal data sets.

6.2.3 Power spectrum

Fourier Transform

To prevent incorrect heart rates from dominating the spectrum, calculated heart rates are inspected and corrected if probably incorrectly determined heart rate values are found. A heart rate value is considered to be probably incorrect if it exceeds a certain range (e.g. 50 – 210 BPM) or strongly deviates from a set of preceding and successive heart rate values. Heart rate values labeled 'probably incorrect' are substituted by values interpolated from correctly determined heart rates.

Spectral information about the heart rates is obtained by calculating the Fourier Transform of data sets of fixed length. We chose the Fourier Transform because it is very straightforward, widely used and makes it easier to compare results obtained in different laboratories than most other frequency domain methods. Additional signal processing is performed to increase the reliability of the frequency domain method. Because the resulting spectral information can depend strongly on this additional signal processing (or on the absence of it) a description of the signal processing steps is given here.

Resampling of the heart rate signal

From the measured fetal ECG or Doppler ultrasound signals, heart rate values can only be determined at times at which a heartbeat occurs. Due to this, measured heart rate values are not equidistantly distributed in time. For calculating the Fourier Transform, the set of determined heart rate values has to be transformed

into an equidistant set of data points. The new, equidistantly distributed data set is obtained by resampling the signal at frequency f_{res}, after using a sample & hold technique and a BoxCar-window convolution. The BoxCar-window is a square wave centered at $t = 0$, having a width of $\frac{2}{f_{res}}$ and a surface equal to 1. To avoid aliasing effects, the frequency of resampling must be higher than the instantaneous heart rate.

Reduction of spectral leakage

Due to the fact that the data set used in the calculation of the spectrum is finite, leakage of power into neighboring frequency bins may occur in the spectrum. To reduce this spectral leakage, the signal is multiplied with a Parzen window function before calculating the Fourier transform. Further the mean of the signal is subtracted to remove the DC-offset from the signal.

Corrections for the applied windows

The application of a Parzen window function reduces the total power of the signal. To correct for this reduction in power, after calculating the Fourier transform every frequency component is divided by the average value of the Parzen window. Note that this correction is frequency independent.

To correct for the application of the BoxCar-window, all frequency components have to be divided by the Fourier transform of the rectangular window.

6.3 Results

6.3.1 Time domain

During labor a direct and indirect cardiotocography was simultaneously recorded from a healthy fetus at a gestational age of 40 weeks.

Figure 6.2(a) shows the heart rates determined from the direct fetal ECG signal by R-peak-detection for a characteristic time interval of 100 s. Figure 6.3(a) shows the heart rates calculated from the simultaneous measured Doppler ultrasound for the same time interval. Note the apparent higher heart rate variability in figure 6.3(a).

In figure 6.4, for the same data-set, the heart rates calculated from the Doppler ultrasound signal are plotted against the heart rates determined from the direct fetal ECG. The figure contains 267 datapoints. A linear model of the form $y = ax$ is fitted to the depicted dataset to describe the relationship between the heart rates calculated by both methods. The best fit is: $y = 1.002x$, R-squared is then 95.43 %. The correlation coefficient is 0.977 ($p < 0.001$).

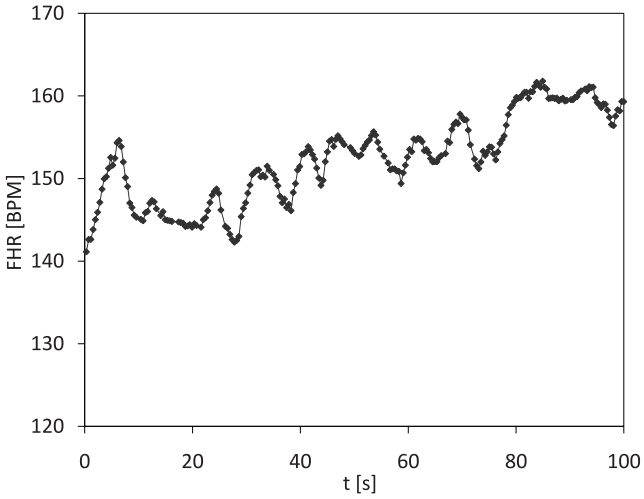

Figure 6.2: *Heart rates determined from the direct fetal ECG signal.*

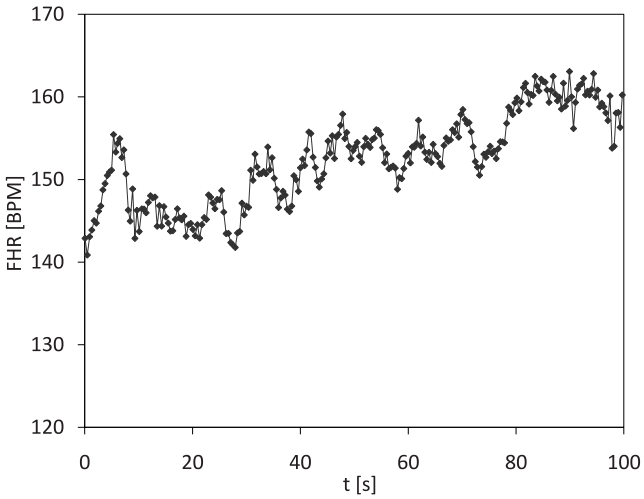

Figure 6.3: *Heart rates calculated from Doppler ultrasound signals by the developed algorithm.*

The agreement of both methods can be assessed by plotting the difference between the results of both methods against the average of both methods (Bland-Altman plot [7]). Figure 6.5 shows the Bland-Altman plot for the data depicted in figures 6.2(a) and 6.3(a). As the differences between both methods do not

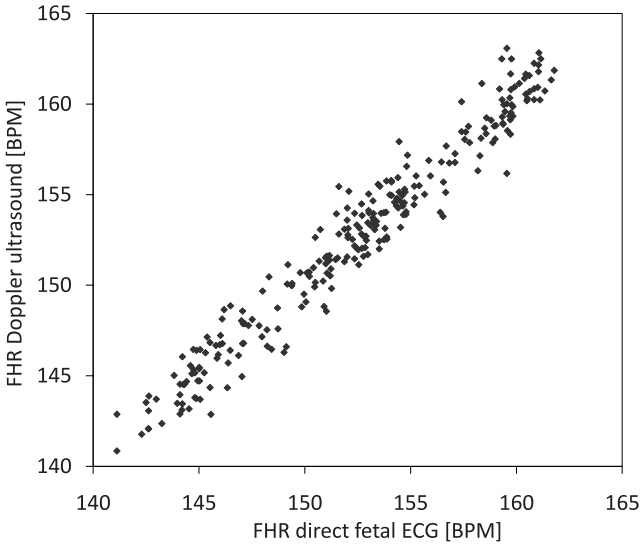

Figure 6.4: *Heart rates calculated by the Doppler ultrasound algorithm plotted against heart rates determined from direct fetal ECG.*

systematically vary with the averages, the standard deviation of the differences can be used to express the agreement between the two methods. The standard deviation calculated from the data depicted in figure 6.5 is 1.18 BPM.

6.3.2 Frequency domain

Frequency analysis of the dataset depicted in figures 6.2(a) and 6.3(a) was performed using the procedure described above. Data were resampled at 4 Hz and for half overlapping intervals of 64 s, 256-points Fast Fourier Transforms were calculated. Figure 6.6 shows the power spectrum of seconds 0 – 96 of the data in figures 2 and 3, calculated by averaging the power spectra of seconds 0 – 64 and 32 – 96. Averaging of the power spectra is performed to reduce the standard error in the spectrum.

In the correction for the box-car resampling procedure, the spectrum is divided by a sinc-function that approaches zero at a frequency of 2 Hz $\left(\frac{f_{res}}{2}\right)$. Therefore the spectrum increases to infinity at this frequency. However, this does not affect the results, because the signal does not contain any components of frequencies around 2 Hz. If a signal does contain higher frequencies, a higher value for the resample frequency f_{res} has to be used.

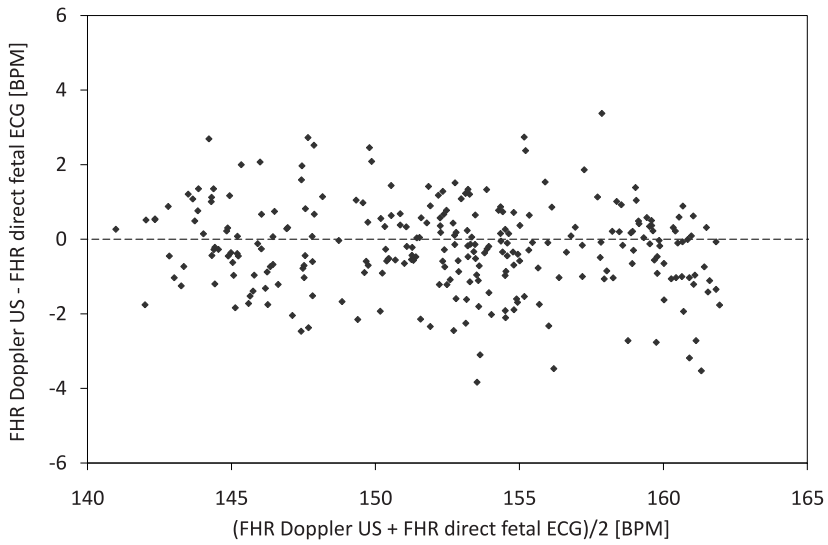

Figure 6.5: *Bland-Altman plot of the heart rates determined by both methods. The difference between the heart rates determined by both methods is plotted against the average of these heart rates.*

In figure 6.7, the contents of the frequency bins of the spectrum obtained by the Doppler ultrasound method are plotted against the contents of the bins of the spectrum obtained by the direct fetal ECG method.

In figure 6.7, the contents of the first frequency bin are disregarded, because these prohibit a correct interpretation of the plot (for the Doppler ultrasound method this bin has a value of 26.52 and for the direct fetal ECG method a value of 27.88). Frequency bins with a content of zero are also excluded. A linear model of the form $y = ax + b$ is fitted to the dataset in figure 6.6 to describe the relationship between the spectra of the heart rates calculated by both methods. The best fit is: $y = 1.068x + 0.031$, R-squared is then 98.24 %. The correlation coefficient is 0.991 ($p < 0.01$).

6.4 Discussion

In the time domain, beat-to-beat heart rate values calculated from Doppler ultrasound signals appear to be consistent with beat-to-beat heart rate values determined from direct fetal ECG signals. The variability of heart rates obtained by the Doppler ultrasound method is higher than the variability of heart rates

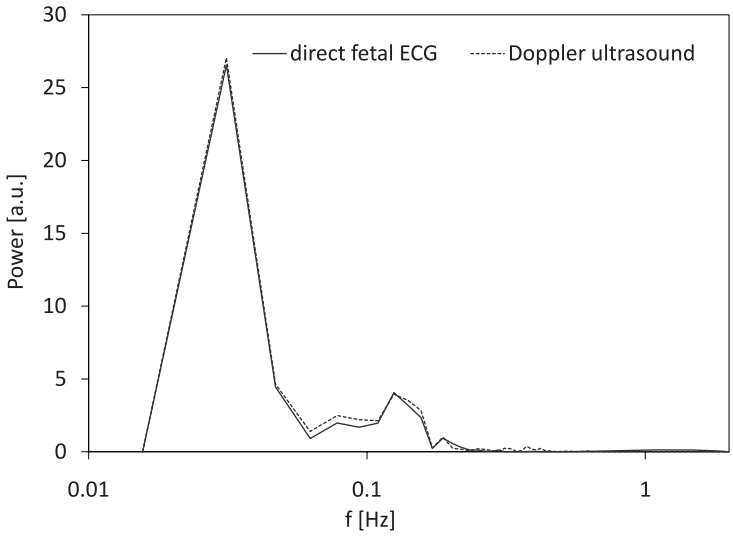

Figure 6.6: *Power spectrum of the heart rates of seconds 0 to 96 for both direct fetal ECG and Doppler ultrasound methods.*

obtained from the ECG signal. For this reason the heart rate values determined by both methods may vary up to a few beats per minute. The trends in the heart rate values however correspond very well. The apparently higher variability of the heart rates calculated by the Doppler ultrasound method is probably caused by the relatively high sensitivity of the ultrasound signal to noise and other disturbances. It should be mentioned, however, that perfect correspondence of the heart rates obtained by both methods can never be expected, simply because the methods are based on two total different physical phenomena (the reflection of ultrasound and the electrical activity of the heart) that can contain similar but never equal information. As the Bland-Altman plot shows no systematical variation, the standard deviation of the differences between the heart rates obtained by both methods can be used as a measure to express the correspondence of both methods. This standard deviation being equal to 1.18 BPM proves that the correspondence of both methods is very high.

The spectra of the heart rates during a period of 96 s obtained by both methods (figure 6.6) correspond very well. The correlation of the heart rates in the frequency domain is even better than the correlation of the heart rates in the time domain. At frequencies where the power contents are very low, the heart rates calculated from Doppler ultrasound signals contain a little more power than the heart rates calculated from direct fetal ECG signals. This can be seen in figure

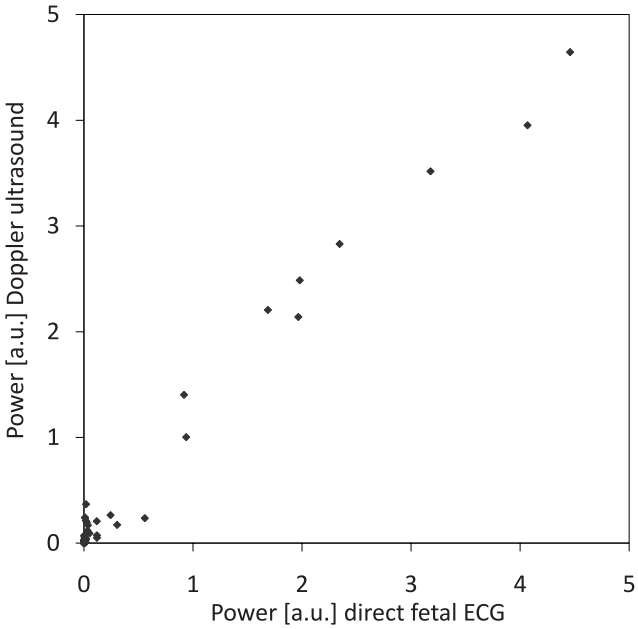

Figure 6.7: *Doppler ultrasound spectrum against direct fetal ECG spectrum (0-96 s).*

6.6, but can also be concluded from the relationship fitted to the data (slope is higher than 1).

6.5 Conclusion

In the time domain, heart rates calculated by the developed ultrasound algorithm on a beat-to-beat basis agree very well with heart rates determined from direct fetal ECG signals. In spite of the higher variability in the heart rates calculated from Doppler ultrasound signals, the power spectra of heart rates obtained from both methods also correspond very well.

Based on these findings, it can be concluded that by developing the ultrasound algorithm a valuable tool is created for obtaining power spectral information of the fetal heart rate in stages of pregnancy earlier than labor. It should be mentioned although, that this tool inevitably suffers from the same drawbacks as the use of ultrasound in general, a relatively high sensitivity to noise and other disturbing factors.

References

[1] S. Akselrod, D. Gordon, F. Ubel, D. Shannon, A. Berger, and R. Cohen, "Power spectrum analysis of heart rate fluctuation: a quantitative probe of beat-to-beat cardiovascular control," *Science*, vol. 213, pp. 220–2, Jul 1981.

[2] R. Eckert and D. Randall, *Animal physiology: mechanisms and adaptations*. W.H. Freeman, 1983.

[3] W. de Jong, *Blood pressure variability in neonates: with a special focus on signal acquisition and signal processing*. PhD thesis, Eindhoven University of Technology, 2000.

[4] T. Fukushima, C. Flores, E. Hon, and E. Davidson, "Limitations of autocorrelation in fetal heart rate monitoring," *Am J Obstet Gynecol.*, vol. 153, pp. 685–92, Nov 1985.

[5] G. Lawson, R. Belcher, G. Dawes, and C. Redman, "A comparison of ultrasound (with autocorrelation) and direct electrocardiogram fetal heart rate detector systems," *Am J Obstet Gynecol.*, vol. 147, pp. 721–2, Nov 1983.

[6] F. Boehm, L. Fields, J. Hutchison, A. Bowen, and W. Vaughn, "The indirectly obtained fetal heart rate: comparison of first- and second-generation electronic fetal monitors," *Am J Obstet Gynecol.*, vol. 155, pp. 10–4, Jul 1986.

[7] J. Bland and D. Altman, "Statistical methods for assessing agreement between two methods of clinical measurement," *Lancet*, vol. 1, pp. 307–10, Feb 1986.

Chapter 7

A continuous wavelet transform based method for time-frequency analysis of artifact corrected heart rate variability data

Abstract

Time-frequency analysis of heart rate variability (HRV) provides relevant clinical information. However, time-frequency analysis is very sensitive to artifacts. Artifacts that are present in heart rate recordings may be corrected, but this reduces the variability in the signal and therefore adversely affects the accuracy of calculated spectral estimates. To overcome this limitation of traditional techniques for time-frequency analysis, a new continuous wavelet transform (CWT) based method was developed in which parts of the scalogram that have been affected by artifact correction are excluded from power calculations. The method was evaluated by simulating artifact correction on heart rate variability data that were originally free of artifacts. Commonly used spectral HRV parameters were calculated by the developed method and by the short-time Fourier transform (STFT), which was used as a reference. Except for the powers in the very low (VLF) and low (LF) frequency band, powers calculated by STFT proved to be extremely sensitive to artifact correction. The CWT-based calculations in the adult (HF_A) and neonatal (HF_N) high frequency bands corresponded well with their theoretical values. The standard deviations of these powers, however, increase with the level of artifact correction which is the result of the non-stationarity of the R-R interval series that were analyzed. The powers calculated in the low frequency band (LF) turned out to be slightly sensitive to artifact correction, but results were acceptable up to 20 % artifact correction. Therefore, the CWT-based method provides a valuable alternative for analysis of heart rate variability data that cannot be guaranteed to be free of artifacts.

submitted for publication

7.1 Introduction

Together with stroke volume and peripheral vascular resistance, the heart rate is one of the main cardiovascular parameters that is regulated by the autonomic nervous system to control the supply of blood to the organs. To fulfill this task, the cardiovascular control centers in the medulla oblongata receive input from various types of sensors in the body. Two very important types of sensor are the pressure sensitive baroreceptors, which are located in the walls of the arteries and in the heart, and the chemoreceptors, which are located in the carotid arteries, the aortic arch and the medulla oblongata. In response to this sensory input, the heart rate is controlled through both neurological and hormonal pathways. Consequently, changes in the heart rate reflect the sensory input to the cardiovascular control centers. Therefore, changes in the heart rate indirectly reflect changes in physiological condition. However, due to the complexity of the cardiovascular regulation, it is difficult to obtain unambiguous information on changes in physiological condition from a recording of the heart rate [1], [2].

To a certain extent, the hormonal and neurological pathways that are used to control the heart rate, operate on different time bases. More in particular, the sympathetic and parasympathetic parts of the autonomic nervous system act on very characteristic time scales. Time-frequency analysis of heart rate variability (HRV) can therefore be used to evaluate sympathetic and parasympathetic nervous activity in regulating the heart rate [3]. Currently, time-frequency analysis of heart rate variability is applied widely in clinical research in various fields of medicine [4], [5]. Successful applications in clinical practice have, however, remained scarce. This is partially due to the complexity of the cardiovascular control mechanisms. Additionally, for accurate results the beat-to-beat heart rate is required, and also data must be preprocessed adequately. Finally, time-frequency analysis is very sensitive to artifacts, and therefore an artifact free heart rate signal is required [6], [7].

In clinical practice, artifact free signals cannot always be guaranteed. An illustrative example is the non-invasive measurement of the fetal ECG from the abdomen of a pregnant woman. Time-frequency analysis of fetal heart rate variability can provide valuable information on fetal condition [8], [9], [10], [11], [12]. However, antepartum the quality of the measured ECG signals can be rather poor, as the electrical source of the signals - the fetal heart - is still very small and only accessible through maternal tissue [13]. Fetal heart rates obtained from the maternal abdomen are therefore often contaminated by artifacts.

The most frequently occurring artifacts in beat-to-beat heart rate signals result from:

(i) incorrect localization of the QRS complex (misdetected heart beat),

(ii) one or multiple undetected QRS complexes (missed heart beats), and

(iii) false detection of a QRS complex (phantom heart beat).

Each of these conditions result in artifacts in the calculated heart rate, which must be detected and corrected before performing time-frequency analysis. Artifact correction normally involves removing phantom heart beats from the recording, replacing misdetected heart beats, and inserting missed heart beats in the recording. Usually, for replacement and insertion, substitute QRS locations are obtained by interpolation. However, artifact correction by means of interpolation will reduce the variability in the signal. Therefore, it is inevitable that artifact correction will adversely affect the accuracy of calculated spectral estimates. This limits the application of traditional techniques for time-frequency analysis to data that are almost entirely free of artifacts.

To overcome this severe limitation, a new method for time-frequency analysis of heart rate variability is introduced. The method that is described in this work, is based on the continuous wavelet transform (CWT) and can be applied for time-frequency analysis of heart rate variability data that contain considerable amounts of artifacts. However, this work does not address the actual detection of these artifacts, which may be a challenge itself. Instead, artifact correction was simulated on heart rate variability data that were originally free of artifacts. This approach allows objective evaluation of the developed method for various levels of artifacts, but implicitly assumes adequate artifact detection. As a reference, the generated data are also analyzed by the short-time Fourier transform.

7.2 Methodology

7.2.1 General approach

Beat-to-beat heart rate data from newborns and fetuses were used to study the effect of artifact correction on time-frequency analysis of heart rate variability. In newborns, the respiration rate is significantly higher than in adults. As the heart rate is modulated by respiration, neonatal heart rate data will contain variability at frequencies of up to 1.5 Hz. Fetal heart rate data will also contain variability at high frequencies, mainly due to respiratory movements. In adult heart rate data, variability is usually absent in this frequency range. Using neonatal and fetal heart rate data therefore provides a unique opportunity to include the effect of artifact correction on high-frequency spectral estimates into the evaluation.

1. *Neonatal data* Neonatal heart rate data were obtained in the neonatal intensive care unit (NICU) of the Máxima Medical Center. Three-lead ECG signals from a General Electric Solar 8000M patient monitor were recorded at a sample rate of 240 Hz. In these ECG signals, QRS-complexes were detected using a quadratic R-fit to reduce sampling errors. This resulted in a data-set containing time stamps for the R-peak in all QRS-complexes that were detected in the recorded signal. Five segments of 192 s that were completely free of artifacts, were selected from this data-set for further analysis. Figure 7.1(a) shows the R-R interval series for one of the five segments.

2. *Fetal data* Fetal heart rate data were obtained in the obstetrics department of the Máxima Medical Center. During delivery, single lead direct fetal scalp ECG signals were recorded from a Neoventa STAN s31 fetal monitor at a sample rate of 500 Hz. A data-set with time stamps for the R-peak in all QRS-complexes that were detected by the fetal monitor was obtained from the digital output of the STAN s31. Five segments of 192 s that were completely free of artifacts, were selected from this data-set for further analysis. Figure 7.1(b) shows the R-R interval series for one of the five segments.

To simulate artifacts, timestamps were deleted at random positions in the fetal and neonatal data segments. Timestamps were deleted until the desired level of artifacts was achieved. Next, R-R intervals were calculated from these data, using linear interpolation to substitute data that were marked as artifact. This way, R-R interval series were created that simulated artifact-corrected heart rate data at 10 different levels of artifacts, varying from 5 to 50 % of the segment length in equal steps. At each level of artifacts, each of the fetal and neonatal data segments was reused to generate 20 different datasets from each original segment. This resulted in a total of 2000 different data segments that were analyzed by the developed CWT-based method and by the short-time Fourier transform.

7.2.2 New CWT-based method

The standard technique for frequency analysis is the Fourier transform. When applied for time-frequency analysis, the Fourier transform is characterized by its constant resolution in time and frequency, which is fixed by the choice of sample rate and window length. Consequently, the time-frequency plane of the spectrogram is tiled in Heisenberg boxes of constant dimensions. For the analysis of heart rate variability in this study, this is a major disadvantage as the presence of artifacts will influence the calculated spectrogram for the entire window length. However, artifacts will mainly affect the higher frequencies in the spectrogram. Therefore, a shorter time resolution in these frequencies would limit the duration

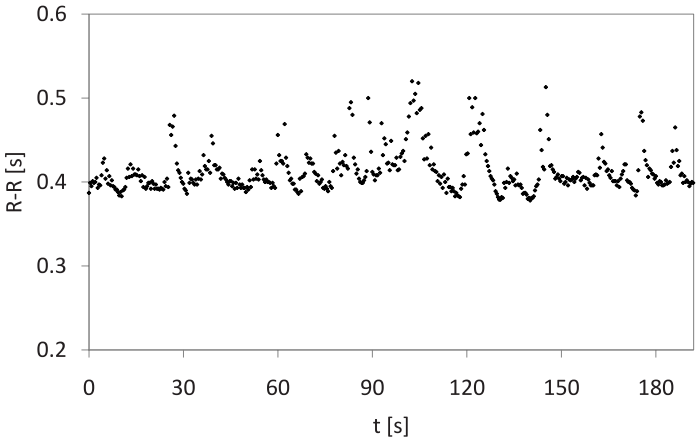

(a) Neonatal heart rate data

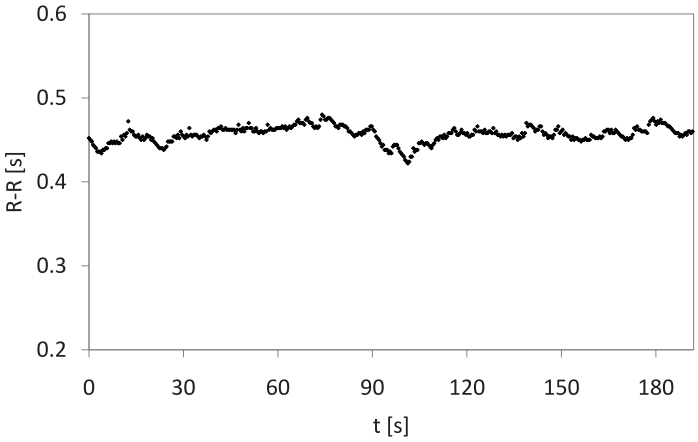

(b) Fetal heart rate data

Figure 7.1:*Examples of artifact-free neonatal (a) and fetal (b) heart rate data.*

of the influence of artifacts and allow for discarding parts of the spectrogram that are affected by artifacts.

A technique that allows for multi-resolution analysis is the wavelet transform, which decomposes the input signal by convolution with scaled and dilated functions of a mother wavelet function [14], [15], [16]. An important natural feature of wavelet transforms is that time and frequency resolution are scalable, with the restriction that the area of the Heisenberg boxes must remain constant. Figure

7.2 shows the tiling of the scalogram for a traditional dyadic wavelet decomposition. The figure also illustrates the duration of the effect that artifacts have for different wavelet scales.

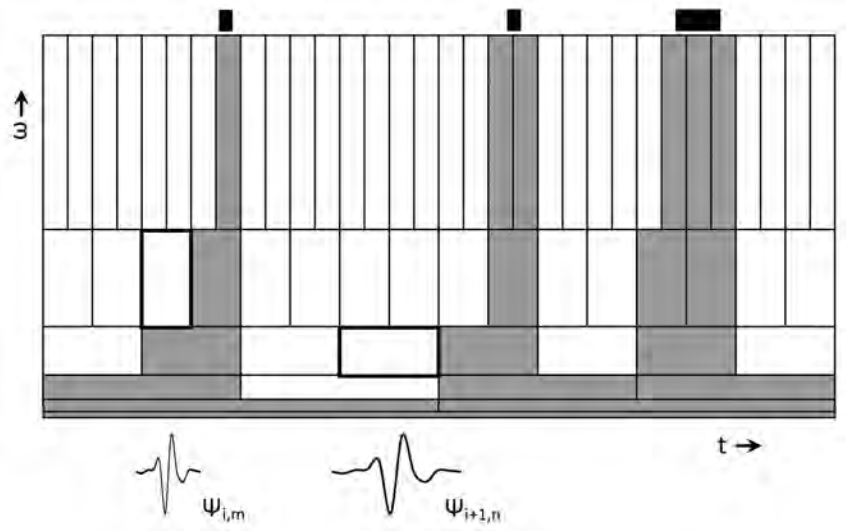

Figure 7.2: *Tiling of the time-frequency plane for a dyadic wavelet decomposition. Artifact locations are indicated above the figure in black, the affected time-frequency tiles are colored grey. The wavelet functions $\psi_{i,m}$ and $\psi_{i+1,n}$ correspond to the bold outlined Heisenberg boxes.*

Because of its scalable time and frequency resolution, the wavelet transform qualifies for analysis of non-stationary signals and therefore has been successfully applied for the analysis of heart rate variability [17], [18], [19]. A dyadic decomposition is however far from ideal for the analysis, as the specific frequency bands of interest [20] will not be matched exactly by dyadic scales. Consequently, the focus of most studies that used the wavelet transform for analysis of heart rate variability has been on matching these frequency bands. Elegant solutions were found in the use of wavelet packets [21] and in integrating the scalogram of the continuous wavelet transform [22].

Table 7.1 contains an overview of the spectral parameters of interest and their corresponding frequency bands. The very low frequency band (VLF) reflects the long-term regulation of the heart rate, including hormonal and thermoregulation. The low frequency band (LF) is associated with both the sympathetic and the parasympathetic branches of the autonomic nervous system, whereas the high frequency band (HF) mainly reflects parasympathetic nervous activity. As vagal

nervous activity is modulated by respiration, the main contribution to the power in the high frequency band is found at the respiration frequency, which lead different definitions for newborns and adults. It is common to express the powers in the low and high frequency bands in normalized units (LFn, HFn) as these parameters may more reliably characterize autonomic cardiovascular control.

Table 7.1: *Overview of spectral parameters of interest.*

Symbol	Description	Frequency band
VLF	power in very low frequency band	$<$ 0.04 Hz
LF	power in low frequency band	0.04 – 0.15 Hz
HF_A	power in high frequency band for adults	0.15 – 0.4 Hz
HF_N	power in high frequency band for newborns	0.4 – 1.5 Hz
TP	total power (outside VLF)	0.04 – 1.5 Hz
LFn	LF power in normalized units	
HF_Nn	HF_N power in normalized units	
LF/HF_N	LF/HF_N ratio	

In our approach, the time resolution of a continuous wavelet transform is exploited to discard parts of the scalogram that are affected by artifacts. A selection of specific scales from a continuous wavelet transform is used to match the frequency bands of interest. Based on the additional requirements of orthogonality and a short support width, the fifth order symlet wavelet was selected for the analysis of heart rate variability. Figure 7.3 displays the mother wavelet function of this wavelet. A least squares calculation was used to select the scales of the CWT that correspond with the frequency bands of interest.

Due to their beat-to-beat character, the R-R interval series are not equidistantly distributed in time. Before performing the CWT, the R-R interval series were transformed into an equidistant set of data. This was achieved by, convolving the R-R interval series with a square function of width 0.5 seconds and energy equal to 1 while applying a sample & hold technique, and then resampling the result at a rate of 4 Hz [23], [24]. The continuous wavelet transform was calculated from scale 0.1 to scale 80, in steps of 0.1. From the calculated wavelet coefficients, the power scalogram was calculated according to:

$$P_{W_f}[n,s] = \frac{1}{C_g}\left|\frac{W_f[n,s]}{s^2}\right|. \tag{7.1}$$

In equation 7.1, $W_f[n,s]$ is the calculated wavelet coefficients, s is the scale and C_g is the admissibility constant of the mother wavelet function. The powers in the frequency bands of interest can be calculated from the power scalogram by

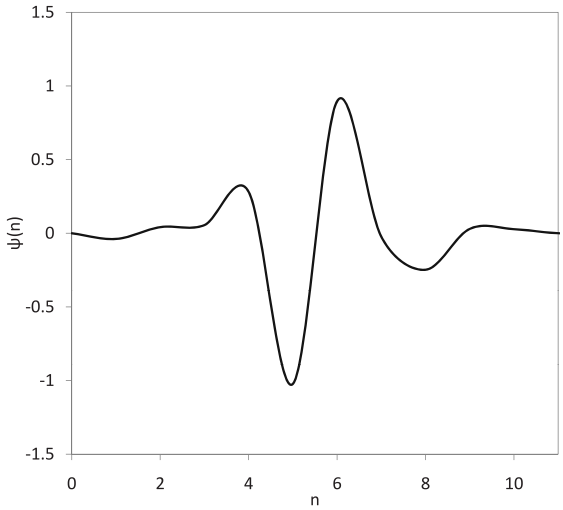

Figure 7.3: *Fifth order symlet mother wavelet function.*

time averaging over the duration of the segment and integrating over scale, as given by:

$$P_{xF} = \sum_{s \in xF} \frac{1}{T} \sum_{n} P_{W_f}[n, s] \Delta t \Delta s. \tag{7.2}$$

To reduce the effect of corrected artifacts, for powers in the high frequency bands the matrix $A[n, s]$ is introduced to eliminate specific parts of the scalogram from the calculation. The power in the high frequency band is then calculated by:

$$P_{HF} = \sum_{s \in HF} \frac{\sum_n \left(A[n, s] \bullet P_{W_f}[n, s] \right)}{\sum_n A[n, s]} \Delta t \Delta s. \tag{7.3}$$

For artifact-free parts of the R-R interval series, the elements of matrix $A[n, s]$ are equal to one. For the neonatal high frequency band (HF_N), $A[n, s]$ is equal to zero around locations of corrected artifacts for one third of the support width of scale s, which was considered an acceptable effective support width. For the adult high frequency band (HF_A), the number elements that are set to zero around artifacts was limited to one third of the support width of the smallest scale in that frequency band, as it is expected that the effect of artifact correction on calculated powers will be smaller for larger scales, and longer effective support widths are undesirable. For the low (LF) and very low (VLF) frequency bands, $A[n, s]$ is equal to one, for all scales for the entire R-R interval series. By point-wise multiplying $A[n, s]$ with the scalogram, parts of the scalogram that are strongly

affected by artifact correction are discarded in the calculation of the powers in the two high frequency bands.

7.2.3 Reference method

As reference method for time-frequency analysis of the generated R-R interval series, the short-time Fourier transform (STFT), or windowed Fourier transform, was used. Identical to the preprocessing for the continuous wavelet transform, the R-R interval series were transformed into an equidistant set of data before processing. The STFT was calculated using a 256 points Parzen window and a window shift of 0.25 seconds. Before application of the Parzen window, the DC offset of the R-R intervals within the window was removed to prevent spectral leakage. The calculated Fourier transforms are squared to obtain the power spectrogram, and corrected for the energy reduction due to the application of the Parzen window and also corrected for the convolution of the input signal with the square function.

7.3 Results

All 2000 segments of fetal and neonatal R-R interval series with various levels of artifact correction were analyzed using both the CWT based method and the STFT. For all calculated spectral estimates, the relative deviation from their theoretical value – the value calculated for the artifact free data segments – was determined. For both methods, figure 7.4 shows the relative deviations in very low frequency power (VLF),low frequency power (LF), and total power (TP) for all analyzed segments. Figure 7.5 shows the relative deviations in adult and neonatal high frequency power (HF_A) and (HF_N). Finally, figure 7.6 shows the relative deviations in the normalized low and neonatal high frequency powers (LFn) and (HF_Nn).

7.4 Discussion

7.4.1 STFT

For the STFT analysis of heart rate variability, the calculated powers in the low frequency (LF) and very low frequency (VLF) range correspond well with their theoretical values for data-sets in which up to 30 % of the R-R interval series has been replaced by interpolated values. The powers in the high frequency ranges for adults (HF_A) and newborns (HF_N) calculated by STFT however are significantly smaller than their theoretical values. This deviation already occurs at relative low levels of artifact correction and increases rapidly as the level of artifact correction

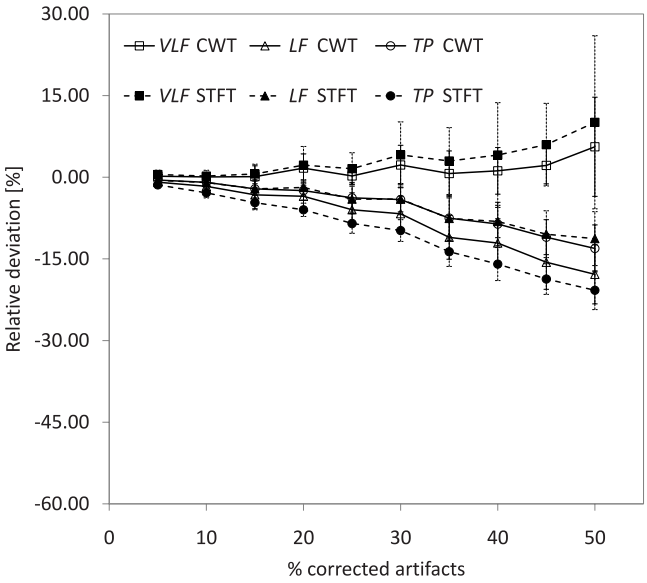

Figure 7.4: *Relative deviations in VLF, LF, and TP and their standard deviations for both the CWT based method and the STFT.*

increases. This is a direct consequence of the reduced variability in these frequency ranges due to the replacement of artifacts by interpolated values. Although the deviations in the adult high frequency band are smaller than in the neonatal high frequency band, in both ranges STFT analysis will not provide reliable parameters when the R-R interval series that are analyzed originally contained artifacts.

Consequently, most other spectral parameters that cover these frequency ranges, such as total power (TP), normalized HF_N power (HF_Nn) and LF/HF_N ratio, can also not be calculated reliably for data sets that originally contained artifacts. However for the analyzed data-sets, the normalized LF power (LFn) could be calculated with acceptable accuracy as long as less than 25 % of the data-set was replaced by interpolated values to correct for artifacts. This can be explained by the relatively very large amount of power that is present in the low frequency range, compared to higher frequencies. For the data-sets that were analyzed this is quite common, however for data-sets in which this is not the case, it is expected that (LFn) powers also will be affected by artifact correction.

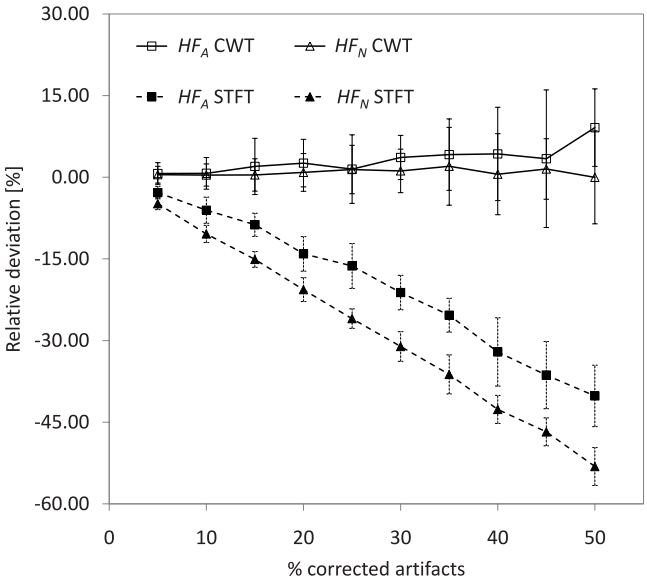

Figure 7.5: *Relative deviations in HF_A, and HF_N and their standard deviations for both the CWT based method and the STFT.*

7.4.2 CWT-based method

Similar to the STFT analysis, the results in the very low frequency domain for the CWT based method, remain unaffected even at very high levels of artifact correction. The calculated powers in the low frequency band on the other hand, show an underestimation of their theoretical value, which grows with the level of artifact correction, but is acceptable for levels of up to 20 %. This effect is due to the trailing edge of the fifth order symlet's frequency response in the high frequency range. The CWT powers in both the adult and the neonatal high frequency band remain within a few percent of their theoretical values even for levels of artifact correction of up to 50 %. The standard deviation of the calculated powers in these frequency bands increases with the level of artifact correction. Most likely, this is the result of the non-stationarity of the R-R interval series that are analyzed. The calculated powers in the high frequency range will therefore fluctuate slightly, dependent on the exact location of artifacts in the original data sets.

Due the relatively large amount of power in the low frequency range, the calculated total powers show almost similar underestimations as the calculated LF powers and therefore the normalized low frequency power is only slightly underestimated. The LF/HF_N ratio is underestimated, which is the direct consequence of

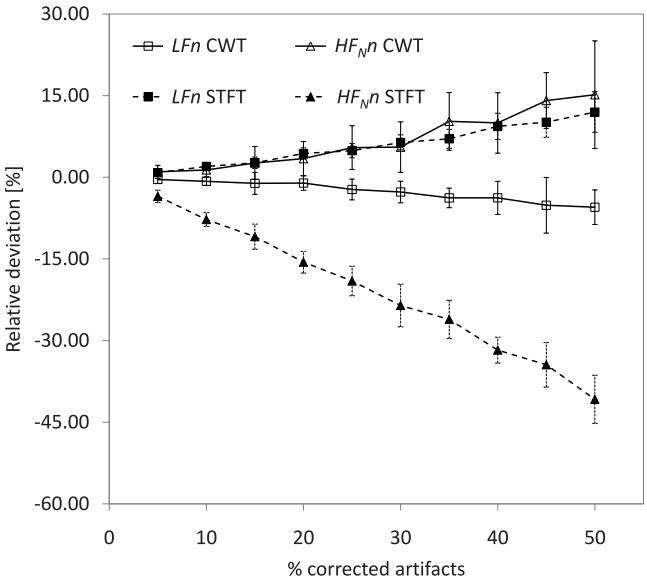

Figure 7.6: *Relative deviations in LFn, and HF_Nn and their standard deviations for both the CWT based method and the STFT.*

the underestimation of the low frequency power. Logically, HF_Nn overestimates its theoretical value. Nevertheless, also for these parameters the correspondence with their theoretical values is acceptable for levels of artifact correction of up to 20 %.

7.5 Conclusion

Time-frequency analysis of heart rate variability by means of the short-time Fourier transform is sensitive to artifact correction. Although low frequency parameters can be calculated accurately when up to 30 % of an R-R interval series is replaced by interpolated values, it is not possible to calculate high frequency parameters reliably if artifacts were originally present in the data-set. STFT analysis is therefore not suitable for time-frequency analysis of heart rate data that are not guaranteed to be free of artifacts.

By developing a continuous wavelet transform based method for time-frequency analysis of heart rate variability, parts of R-R interval series that originally contained artifacts can be discarded in the calculation of high frequency spectral estimates. By using this approach, high frequency spectral parameters can be

calculated reliably even when extremely large parts of data are missing due to artifacts. However, compared to STFT, the calculation of spectral parameters in the low frequency range, is more sensitive to artifacts but acceptable for levels of artifact correction of up to 20 %.

The developed CWT based method offers a valuable alternative for time-frequency analysis of heart rate variability data that contain artifacts, for example, fetal heart rate data from non-invasive recordings of the fetal ECG.

References

[1] C. Notarius and J. Floras, "Limitations of the use of spectral analysis of heart rate variability for the estimation of cardiac sympathetic activity in heart failure," *Europace*, vol. 3, pp. 29–38, Jan 2001.

[2] G. Parati, G. Mancia, M. D. Rienzo, P. Castiglioni, J. Taylor, and P. Studinger, "Point:counterpoint: Cardiovascular variability is/is not an index of autonomic control of circulation," *J Appl Physiol.*, vol. 101, pp. 676–682, Aug 2006.

[3] S. Akselrod, D. Gordon, F. Ubel, D. Shannon, A. Berger, and R. Cohen, "Power spectrum analysis of heart rate fluctuation: a quantitative probe of beat-to-beat cardiovascular control," *Science*, vol. 213, pp. 220–2, Jul 1981.

[4] L. Mainardi, A. Bianchi, and S. Cerutti, "Time-frequency and time-varying analysis for assessing the dynamic responses of cardiovascular control," *Crit Rev Biomed Eng.*, vol. 30, no. 1-3, pp. 175–217, 2002.

[5] U. Acharya, K. Joseph, N. Kannathal, C. M. Lim, and J. Suri, "Heart rate variability: a review," *Med Bio Eng Comput.*, vol. 44, pp. 1031–1051, 2006.

[6] G. Clifford and L. Tarassenko, "Quantifying errors in spectral estimates of HRV due to beat replacement and resampling," *IEEE Trans Biomed Eng.*, vol. 53, pp. 630–8, Apr 2005.

[7] C. Peters, R. Vullings, J. Bergmans, S. Oei, and P. Wijn, "The effect of artifact correction on spectral estimates of heart rate variability," *Conf Proc IEEE Eng Med Biol Soc.*, vol. 2008, pp. 2669–72, 2008.

[8] J. van Laar, M. Porath, C. Peters, and S. Oei, "Spectral analysis of fetal heart rate variability for fetal surveillance: review of the literature," *Acta Obstet Gynecol Scand.*, vol. 87, no. 3, pp. 300–6, 2008.

[9] S. Siira, T. Ojala, T. Vahlberg, J. Jalonen, I. Välimäki, K. Rosén, and E. Ekholm, "Marked fetal acidosis and specific changes in power spectrum analysis of fetal heart rate variability recorded during the last hour of labour," *BJOG*, vol. 112, pp. 418–23, Apr 2005.

[10] T. Rantonen, E. Ekholm, S. Siira, T. Metsälä, R. Leino, U. Ekblad, and I. Välimäki, "Periodic spectral components of fetal heart rate variability reflect the changes in cord arterial base deficit values: a preliminary report," *Early Hum Dev.*, vol. 60, pp. 233–8, Jan 2001.

[11] S. Cerutti, S. Civardi, A. Bianchi, M. Signorini, E. Ferrazzi, and G. Pardi, "Spectral analysis of antepartum heart rate variability," *Clin Phys Physiol Meas.*, vol. 10, no. Suppl B, pp. 27–31, 1989.

[12] J. van Laar, C. Peters, R. Vullings, S. Houterman, J. Bergmans, and S. Oei, "Fetal autonomic response to severe acidaemia during labour," *BJOG*, vol. 117, pp. 429–37, Mar 2010.

[13] M. Lewis, "Review of electromagnetic source investigations of the fetal heart," *Med Eng Phys.*, vol. 25, pp. 801–10, Dec 2003.

[14] S. Mallat, *A wavelet tour of signal processing*. Academic Press, 1998.

[15] P. Addison, *The illustrated wavelet transform handbook*. IOP Publishing, 2002.

[16] A. Akansu and R. Haddad, *Multiresolution signal decomposition*. Academic Press, 2001.

[17] U. Wiklund, M. Akay, and U. Niklasson, "Short-term analysis of heart-rate variability by adapted wavelet transforms," *IEEE Eng Med Biol Mag.*, vol. 16, pp. 113–8, Oct 1997.

[18] Y. Kimura, K. Okamura, T. Watanabe, N. Yaegashi, S. Uehara, and A. Yajima, "Time-frequency analysis of fetal heartbeat fluctuation using wavelet transform," *Am J Physiol*, vol. 275, pp. H1993–9, Dec 1998.

[19] V. Pichot, J. Gaspoz, S. Molliex, A. Antoniadis, T. Busso, F. Roche, F. Costes, L. Quintin, J. Lacour, and J. Barthélémy, "Wavelet transform to quantify heart rate variability and to assess its instantaneous changes," *J Appl Physiol.*, vol. 86, pp. 1081–91, Mar 1999.

[20] Task force of the European society of cardiology and the North American society of pacing electrophysiology, "Heart rate variability: standards of measurement, physiological interpretation, and clinical use," *Circulation*, vol. 93, pp. 1043–65, 1996.

[21] K. Tanaka and A. Hargens, "Wavelet packet transform for r-r interval variability," *Med Eng Phys*, vol. 26, pp. 313–9, May 2004.

[22] M. David, M. Hirsch, E. Toledo, and S. Akselrod, "An estimate of fetal autonomic state by time-frequency analysis of fetal heart rate variability," *J Appl Physiol.*, vol. 102, pp. 1057–64, Mar 2007.

[23] C. Peters, E. ten Broeke, P. Andriessen, B. Vermeulen, R. Berendsen, P. Wijn, and S. Oei, "Beat-to-beat detection of fetal heart rate: Doppler ultrasound cardiotocography compared to direct ECG cardiotocography in time and frequency domain," *Physiol Meas.*, vol. 25, pp. 585–93, Apr 2004.

[24] W. de Jong, *Blood pressure variability in neonates: with a special focus on signal acquisition and signal processing*. PhD thesis, Eindhoven University of Technology, 2000.

Chapter 8

Time-scale analysis of fetal heart rate variability obtained from non-invasive fetal ECG recordings

8.1 Introduction

Since the 1970's the standard method for monitoring fetal condition has been cardiotocography, the simultaneous recording of fetal heart rate and maternal uterine activity. Generally, cardiotocographic recordings are evaluated visually, which includes mainly changes in fetal heart rate and maternal uterine activity that occur on a timescale of multiple minutes. The heart plays an essential role in the transportation of oxygen to the tissues, but is only one of multiple factors that influence oxygen supply. Consequently, the gradual changes in fetal heart rate that cardiotocography examines, provide incomplete information for the evaluation of fetal condition. More specifically, cardiotocography is insufficiently capable of predicting bad fetal outcome [1] and therefore its value in clinical practice is limited.

However, the fetal heart rate is modulated by the autonomic part of the fetal central nervous system on a beat-to-beat basis. Through autonomic cardiovascular control, changes in fetal condition will be indirectly reflected in the beat-to-beat fetal heart rate variability. Therefore, the fetal heart rate contains more potentially useful information than cardiotocography reveals. This additional information can be assessed by means of computerized analysis of fetal heart rate variability. In the past two decades, System 8000 [2] and its successors have already demonstrated that including the short-term variation (STV) into the computerized analysis of the fetal heart rate, increases the predictive value of cardiotocography. Despite their successes, available systems for computerized analysis of the fetal heart rate, merely contribute to the interpretation of cardiotocographic recordings by using mathematical parameters to characterize the fetal heart rate and do not assess true beat-to-beat information.

Parts of the potentially useful information that is contained in the beat-to-beat fetal heart rate, may be revealed by time-frequency analysis. To a certain extent, the hormonal and neurological pathways through which the autonomic nervous system controls the heart rate, operate on different time bases. Time-frequency analysis of heart rate variability can therefore be used to evaluate sympathetic and parasympathetic nervous activity in regulating the heart rate [3]. A low-frequency band (LF) has been defined, which is associated with both the sympathetic the and parasympathetic branches of the autonomic nervous, and a high-frequency band (HF), which mainly reflects modulation by the parasympathetic nervous system [4].

Several studies have applied time-frequency analysis to fetal heart rate recordings during labor and have evaluated the power in the frequency bands associated with sympathetic and parasympathetic nervous activity [5], [6], [7]. These studies have demonstrated changes in the power of fetal heart rate variability in these frequency bands to be correlated with fetal hypoxemia or acidemia, although there are some inconsistencies between the results of these studies [8]. Recent work has demonstrated that the normalized power in the low-frequency band (LF_n) is negatively correlated with fetal scalp blood pH during labor, while the normalized power in the high-frequency band (HF_n) is positively correlated [9]. These promising results suggest that in clinical practice, LF_n and HF_n might be capable of discriminating between normal fetuses and acidotic or acidaemic fetuses.

Ultimately, time-frequency analysis of fetal heart rate variability could be further developed into an early indicator of fetal distress. For this, more insight needs to be gained into cardiovascular control in the fetus and into the value of spectral estimates for monitoring fetal condition. The aim of this study is to obtain insight in how LF_n and HF_n develop with gestational age and to characterize the inter-individual variation of these spectral estimates. The study uses non-invasive abdominal recordings of the fetal electrocardiogram (ECG) to obtain the beat-to-beat fetal heart rate. To calculate LF_n and HF_n, the obtained heart rates were analyzed by means of time-scale analysis using a continuous wavelet transform.

8.2 Methods

8.2.1 Measurements

Within a longitudinal patient study in Máxima Medical Center between January 2007 and January 2009, non-invasive fetal ECG measurements were repeatedly performed on pregnant women during outpatient visits to the maternity ward. A prototype of a non-invasive electrophysiological fetal monitor (NEMO) was used to record the electrical activity on the maternal abdomen. Recordings were performed at approximately 18, 22, 24, 26, 30, 34, 36, 38 and 40 weeks of gestational age.

After approval by the medical ethics committee of the hospital, 40 healthy women, who did not use any medication, with an uncomplicated singleton pregnancy, before 14 weeks of gestation, were asked to participate on their visit to the outpatient department. Exclusion criteria were women under the age of 18 years and multiple pregnancies. Patients were recruited consecutively. All participants were included after informed consent. Pregnancies complicated by hypertension, preeclampsia, fetal growth restriction, diabetes mellitus, fetal congenital malformations or preterm labour, after inclusion were excluded.

8.2.2 Signal processing

The eight input signals were digitized at 1000 Hz with 20 bits precision and processed on a sample-by-sample basis. The signals were bandpass filtered between 1.5 and 70 Hz to remove high-frequency noise and low-frequency electronic drift. Also, a 50 Hz notch filter was used to suppress power-line interference. Maternal QRS-complexes were detected online, which, after acquisition of the complete ECG waveform, triggered the algorithm for removal of the maternal electrocardiogram.

The maternal electrocardiogram was removed from the recording by estimating each individual maternal ECG waveform and subtracting this estimate from the recorded signal. These estimates were created by generating templates from preceding ECG waveforms for each channel of the recording. To generate these templates, the ECG waveform was segmented and corresponding segments of preceding ECG waveforms were aligned and scaled to match the waveform that is estimated. Also, for each segment different weights were attributed to preceding ECG waveforms and segments that were suspected to contain artifacts were excluded in the construction of the template. This way, an accurate estimate of the maternal ECG waveform was obtained and subtracted from the recording, without affecting present fetal ECG complexes [10].

The eight resulting fetal ECG traces were processed to detect the beat-to-beat fetal heart rate. Due to the spatial representation of the fetal vectorcardiogram, small phase differences exist between the fetal ECG components in the different channels. To reduce noise and enhance the QRS complexes in the signals, this inter-channel delay was corrected before further processing. Four non-physiological linear combinations of input channels were calculated and bandpass filtered (12 – 42 Hz) for additional noise reduction. The absolute first derivative of these four filtered signals was calculated and convoluted with a square function that matches the width of the fetal QRS complex (21 ms). The results were squared and summed over the four leads and then further processed to obtain a first estimate of the times at which fetal QRS complexes were present in the recording.

After determining the polarity of the QRS complex in each of the four filtered leads, the exact location of the QRS complexes was detected [11].

8.2.3 Time-scale analysis

Antepartum beat-to-beat fetal heart rate data generally contain a considerable amount of artifacts. Already at very low levels, these artifacts will cause large inaccuracies in the powers that are calculated when using standard methods for time-frequency analysis such as the Fourier transform [12]. To solve this limitation, a method for time-frequency analysis of heart rate variability has been developed that is based on a continuous wavelet transform (CWT) [13].

Contrary to the fixed time-frequency resolution of most methods for time-frequency analysis, wavelets are scalable in the time-frequency plane, or more correctly, the time-scale plane (scale being the inverse of frequency). Time-scale analysis therefore holds the advantage of being able to evaluate changes in the power of a signal at the timescale at which they occur. This offers the opportunity to exclude parts of a signal that contain artifacts from the analysis, without losing too much information. The CWT-based method therefore can be used to analyze antepartum fetal heart rate variability data that contain large amounts of artifacts.

The continuous wavelet transform based method was used to calculate the power LF in the low-frequency band (0.04 – 0.15 Hz), which reflects modulation by both the sympathetic and parasympathetic nervous system, in the high-frequency band (HF, 0.4 – 1.5 Hz for newborns and fetuses), which reflects only modulation by the parasympathetic nervous system, and in the total power (TF, 0.04 – 1.5 Hz), which is used to calculate normalized values of the power in the low (LF_n) and high (HF_n) frequency bands. The powers in these frequency bands were calculated by integrating the corresponding parts of the scalogram.

8.3 Results

The eight-channel recordings that were obtained, contained a mixture of electrophysiological signals in which the fetal electrocardiogram was obscured by the much larger maternal electrocardiogram. The performance of the prototype of a fetal monitor that was used, is directly related to the amplitude of the QRS-complex in the fetal electrocardiogram that is measured on the maternal abdomen. This amplitude gradually changes with gestational age and, consequently, the number of segments that was included for analysis strongly varied between different stages of pregnancy.

A population of 34 patients whose fetal electrocardiogram had been retrieved successfully, was included for further analysis. These recordings were divided in

one minute segments of fetal heart rate data. To evaluate the results of the analysis, it is desired to divide the results into groups of different gestational ages. Ideally, the numbers of segments included in each group should be equal. However, with the strongly varying number of analyzed segments and the multiple weeks intervals between measurements, this was not possible. Also, the duration in weeks of gestational age differed for the groups. More specifically, the group 28 – 36 weeks of gestational age suffers from the difficulties that were experienced in measuring the fetal electrocardiogram when the fetus was covered by the vernix caseosa. Table 8.1 provides an overview of the grouping of the results and the number of segments that were included in each group.

Table 8.1: *Overview of the grouping of the results and the number of segments that were included for analysis.*

Gestational age [weeks]	Number of included segments
20 – 24	277
24 – 26	290
26 – 28	134
28 – 36	148
36 – 40	165
> 40	123

For each group, figure 8.1 shows the average normalized power of the fetal heart rate in the low and high frequency band, LF_n and HF_n. The normalized power in the low-frequency band shows an increase between 20 and 26 weeks of gestational age, which is followed by a gradual decrease throughout the third trimester of pregnancy. The normalized power in the high-frequency range remains relatively constant until 26 weeks of gestational age and slightly increases towards the end of pregnancy.

8.4 Discussion

In the measurements that were performed around 18, 30 and 34 weeks of gestational age, difficulties were experienced in retrieving the fetal electrocardiogram, as the amplitude of the fetal ECG measured on the maternal abdomen was reduced to only a few microvolt. At 18 weeks of gestational age, this is due to the small size of the fetal heart, and at 30 and 34 weeks of gestational age, this is probably due to the presence of isolating sections of the vernix caseosa [14], [15].

For gestational ages between 20 and 24 weeks, the normalized power of the fetal heart rate in the low-frequency range is significantly lower than for gestational

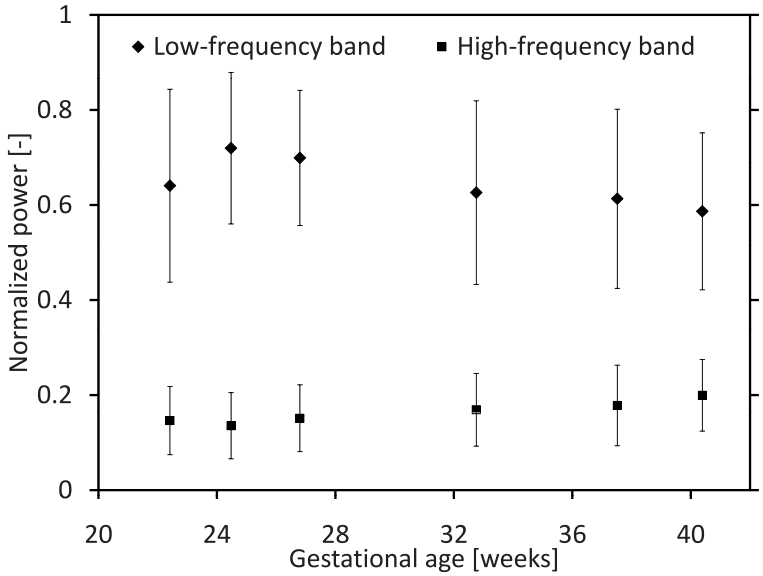

Figure 8.1: *Normalized power in the low and high-frequency band plotted against the gestational age at which the recordings were performed.*

ages of 24 to 28 weeks (t-test, $p < 0.001$). As the normalized power in the high-frequency range remains constant, it is unlikely that changes have occurred in the activity of the parasympathetic nervous system. Therefore, it is assumed that the increase in LF_n is due to changes in the modulation of the fetal heart rate by the sympathetic nervous system. At these gestational ages, sympathetic innervation of the fetal heart is already present and therefore the increase in low-frequency power may reflect the functional development of the sympathetic nervous system.

The slight increase in HF_n towards the end of pregnancy, might indicate increased modulation by the parasympathetic nervous system. These observations are consistent with literature, which reports early maturation of the sympathetic nervous system, followed by maturation of the parasympathetic nervous system [16], [17].

Due to the use of normalized powers, the increase in HF_n that is supposed to be due to increased parasympathetic modulation, is automatically accompanied by a reduction of LF_n. However, the observed increase in HF_n cannot fully account for the gradual decrease in LF_n that occurs. Literature reports that from 30 weeks of gestational age, fetal heart rate patterns are different for periods of rest and periods of activity of the fetus, while differences are absent up to 30 weeks of gestational age [18]. Generally, fetal behavior is considered to reflect the activ-

ity of the fetal central nervous system [19]. As rest is associated with increased parasympathetic activity and decreased sympathetic activity, it is expected that the normalized power of fetal heart rate variability in the low-frequency and high-frequency bands will be influenced by the manifestation of rest/activity cycles in the fetus.

In recent work, spectral analysis of intrapartum fetal heart rate variability has been used to evaluate changes in LF_n and HF_n during active sleep and quiet sleep in near-term and post-term pregnancies [20]. During quiet sleep, LF_n was significantly lower and HF_n was significantly higher for the post-term fetuses, when compared to the near-term fetuses. However, during active sleep, no significant differences were found. These findings may be ascribed to the continuing maturation of the parasympathetic system nervous system.

We hypothesize that with gestation and due to the progressing development of behavioral states, LF_n is increasingly reduced during episodes of quiet sleep. Although we did not discriminate between fetal behavioral states, increased activity of the parasympathetic nervous system together with reduced activity of sympathetic nervous activity during quiet sleep, might explain the gradual decrease in LF_n that is observed. Therefore, we expect that after 30 weeks of gestational age, discriminating between states of quiet and active sleep will demonstrate differences in LF_n between these states. This might also explain the increase in the standard deviation of LF_n at these gestational ages.

8.5 Conclusion

As the results of this study are consistent with existing insights in fetal development, it is plausible that time-scale analysis of antepartum fetal heart rate variability indeed provides information on sympathetic and parasympathetic nervous activity. The increase in normalized power of the fetal heart rate in the low-frequency range at 20-24 weeks of gestational age may reflect the functional development of the sympathetic nervous system. It would be interesting to evaluate LF_n and HF_n earlier in pregnancy, as this may contribute to a more thorough understanding of early human development. However, due to the small amplitude of the fetal electrocardiogram that is measured on the maternal abdomen before 20 weeks of gestational age, this requires significant improvement of the measurement system that was used.

The observed slight increase in HF_n towards the end of pregnancy and the gradual decrease in LF_n, may reflect maturation of the parasympathetic nervous system and manifestation of behavioral states in the fetus. We expect that with gestation LF_n will mainly be reduced during episodes of quiet sleep. Future studies should therefore discriminate between states of quiet and active sleep.

The combination of non-invasive abdominal measurements of the fetal ECG and time-scale analysis using the continuous wavelet transform, provides a promising tool to obtain information on autonomic nervous activity in the fetus. However, future work should consider more advanced spectral estimates of heart rate variability than LF_n and HF_n. Although LF_n and HF_n correlate with fetal scalp blood pH during labor, these parameters represent only a small part of the information that is contained in the scalogram. To further develop the potential of the technique into an early detector of fetal distress, the challenge is to define spectral estimates that may truly characterize fetal autonomic cardiovascular state.

References

[1] K. Nelson, J. Dambrosia, T. Ting, and J. Grether, "Uncertain value of electronic fetal monitoring in predicting cerebral palsy," *N Engl J Med.*, vol. 334, pp. 613–8, Mar 1996.

[2] G. Dawes, M. Moulden, and C. Redman, "System 8000: computerized antenatal FHR analysis," *J Perinat Med.*, vol. 19, no. 1-2, pp. 47–51, 1991.

[3] S. Akselrod, D. Gordon, F. Ubel, D. Shannon, A. Berger, and R. Cohen, "Power spectrum analysis of heart rate fluctuation: a quantitative probe of beat-to-beat cardiovascular control," *Science*, vol. 213, pp. 220–2, Jul 1981.

[4] Task force of the European society of cardiology and the North American society of pacing electrophysiology, "Heart rate variability: standards of measurement, physiological interpretation, and clinical use," *Circulation*, vol. 93, pp. 1043–65, 1996.

[5] S. Siira, T. Ojala, T. Vahlberg, J. Jalonen, I. Välimäki, K. Rosén, and E. Ekholm, "Marked fetal acidosis and specific changes in power spectrum analysis of fetal heart rate variability recorded during the last hour of labour," *BJOG*, vol. 112, pp. 418–23, Apr 2005.

[6] T. Rantonen, E. Ekholm, S. Siira, T. Metsälä, R. Leino, U. Ekblad, and I. Välimäki, "Periodic spectral components of fetal heart rate variability reflect the changes in cord arterial base deficit values: a preliminary report," *Early Hum Dev.*, vol. 60, pp. 233–8, Jan 2001.

[7] S. Cerutti, S. Civardi, A. Bianchi, M. Signorini, E. Ferrazzi, and G. Pardi, "Spectral analysis of antepartum heart rate variability," *Clin Phys Physiol Meas.*, vol. 10, no. Suppl B, pp. 27–31, 1989.

[8] J. van Laar, M. Porath, C. Peters, and S. Oei, "Spectral analysis of fetal heart rate variability for fetal surveillance: review of the literature," *Acta Obstet Gynecol Scand.*, vol. 87, no. 3, pp. 300–6, 2008.

[9] J. van Laar, C. Peters, R. Vullings, S. Houterman, J. Bergmans, and S. Oei, "Fetal autonomic response to severe acidaemia during labour," *BJOG*, vol. 117, pp. 429–37, Mar 2010.

[10] R. Vullings, C. Peters, R. Sluijter, M. Mischi, S. Oei, and J. Bergmans, "Dynamic segmentation and linear prediction for maternal ECG removal in antenatal abdominal recordings," *Physiol Meas.*, vol. 30, pp. 291–307, Mar 2009.

[11] C. Peters, J. van Laar, R. Vullings, S. Oei, and P. Wijn, "Beat-to-beat heart rate detection in multi-lead abdominal fetal ECG recordings," *to be published*, pp. 1–12, 2010.

[12] C. Peters, R. Vullings, J. Bergmans, S. Oei, and P. Wijn, "The effect of artifact correction on spectral estimates of heart rate variability," *Conf Proc IEEE Eng Med Biol Soc.*, vol. 2008, pp. 2669–72, 2008.

[13] C. Peters, R. Vullings, M. Rooijakkers, J. Bergmans, S. Oei, and P. Wijn, "A continuous wavelet transform based method for time-frequency analysis of artifact corrected heart rate variability data," *to be published*, pp. 1–13, 2010.

[14] J. Oldenburg and M. Macklin, "Changes in the conduction of the fetal electrocardiogram to the maternal abdominal surface during gestation," *Am J Obstet Gynecol.*, vol. 129, pp. 425–33, Oct 1977.

[15] T. Oostendorp, A. van Oosterom, and H. Jongsma, "The effect of changes in the conductive medium on the fetal ECG throughout gestation," *Clin Phys Physiol Meas.*, vol. 10, no. Suppl B, pp. 11–20, 1989.

[16] B. Nuwayhid, C. Brinkman, C. Su, J. Bevan, and N. Assali, "Development of autonomic control of fetal circulation," *Am J Physiol.*, vol. 228, pp. 337–44, Feb 1975.

[17] N. Assali, C. Brinkman, J. Woods, A. Dandavino, and B. Nuwayhid, "Development of neurohumoral control of fetal, neonatal, and adult cardiovascular functions," *Am J Obstet Gynecol.*, vol. 129, pp. 748–59, Dec 1977.

[18] M. Pillai and D. James, "The development of fetal heart rate patterns during normal pregnancy," *Obstet Gynecol.*, vol. 76, pp. 812–6, Nov 1990.

[19] J. Nijhuis, H. Prechtl, C. M. Jr., and R. Bots, "Are there behavioural states in the human fetus?," *Early Hum Dev.*, vol. 6, pp. 177–95, Apr 1982.

[20] J. van Laar, C. Peters, R. Vullings, S. Houterman, and S. Oei, "Power spectrum analysis of fetal heart rate variability at near term and post term gestation during active sleep and quiet sleep," *Early Hum Dev.*, vol. 85, pp. 795–8, Dec 2009.

Chapter 9

Concluding remarks and future perspective

9.1 Introduction

From a technological perspective, there has been very little development in fetal monitoring technology in the past 25 years. Although insight in the interpretation of cardiotocographic information has continuously evolved, the technology that is used to measure fetal heart activity and uterine contractions has remained unchanged. Unfortunately, the information that cardiotocography offers, is of limited value in clinical practice [1]. More in particular, in case of a non-reassuring cardiotocographic recording, additional information is required to reliably assess fetal condition. A common method to obtain this information is by determining the pH of a fetal blood sample [2]. However, this procedure is invasive and only provides information on fetal condition at one specific time. Consequently, a large clinical need exists for additional information that may contribute to more reliably evaluating fetal condition. Preferably, this information is obtained non-invasively, and on a continuous basis.

Several methods have been introduced to provide additional information for fetal monitoring, including computerized analysis of the fetal heart rate [3], [4] and analysis of the P-R interval [5], [6] and ST-segment [7] of the fetal ECG waveform. As the developed techniques build on existing measurements, these methods have been easily integrated into routine clinical practice. However, the clinical value of the methods has proven to be rather limited and the need for additional information to evaluate fetal condition has remained. An additional drawback of fetal ECG waveform analysis is that it currently can only be applied during labor, as it requires the attachment of an electrode to the fetal scalp.

A technique that potentially offers valuable additional information for monitoring fetal condition and could be applied also during earlier stages of pregnancy, is analysis of the fetal heart rate variability. The fetal heart rate fluctuates on a beat-to-beat basis under the control of the autonomic part of the central nervous

system. Under normal circumstances, fetal cardiovascular control will respond to changes in fetal condition. As a result, the beat-to-beat variability of the fetal heart rate will indirectly reflect fetal condition. The autonomic nervous system consists of two parts, the sympathetic nervous system and the parasympathetic nervous system, that to a certain extent have opposite effects on the heart rate. Both parts operate on typical, partially different timescales. Time-frequency analysis may therefore be used to quantify the activity of these systems and characterize autonomic cardiovascular control [8]. Spectral estimates of the beat-to-beat fetal heart rate variability have already been studied using fetal ECG recordings that were obtained directly from the fetal scalp, during labor. These studies have shown that changes in the power of fetal heart rate variability within specific frequency bands correlate with fetal hypoxemia or acidemia [9].

To contribute to a more reliable assessment of fetal condition, time-frequency analysis of fetal heart rate variability needs to be further developed to provide valuable clinical information. It is expected that this further development will significantly benefit from antepartum measurement of the beat-to-beat fetal heart rate. Antepartum measurement of the beat-to-beat fetal heart rate offers the opportunity to gain more insight in spectral estimates of fetal heart rate variability and their progression throughout pregnancy. Also, antepartum measurement of the beat-to-beat fetal heart rate potentially allows for early detection of fetal distress, as the method can be applied before rupture of the amniotic membrane.

9.2 Fetal heart rate measurements

9.2.1 Abdominal fetal ECG recordings

The first goal of this thesis was to obtain the beat-to-beat fetal heart rate throughout pregnancy. Currently, the beat-to-beat fetal heart can only be clinically obtained during labor, when the fetal electrocardiogram is measured directly from the fetal scalp. However, the fetal electrocardiogram is also present on the maternal abdomen, although much smaller in amplitude and obscured by the maternal electrocardiogram and, to a lesser extent, muscle activity and noise. Non-invasive measurement of the fetal electrocardiogram from the maternal abdomen therefore was the preferred approach to realize the first goal of this thesis. Additional to the beat-to-beat fetal heart rate, also the waveform of the measured fetal ECG provides clinically relevant information. Other advantages of the measurement method are that it is entirely free of risks, causes very little discomfort and can be used for long-term monitoring.

An online implementation of an already available method to remove the maternal electrocardiogram from abdominal recordings [10], was realized (chapter 2). To obtain the beat-to-beat fetal heart rate directly from the retrieved fe-

tal ECG traces, a robust method was developed to process these traces at relatively low computational power (chapter 3). The method enhances the fetal ECG components in the recording, before detecting QRS-complexes. This way, the beat-to-beat fetal heart rate can be obtained even from recordings with a low signal-to-noise ratio. However, some adjustments to the method are still required, as it was noticed that for some recordings occasionally small shifts (< 10 ms) occur in the detection of the QRS-complex.

In addition, a more theoretical approach was used to develop a method that reconstructs a three-dimensional projection of the fetal vectorcardiogram from the retrieved fetal ECG traces. By fitting an ellipse to the QRS-loop in the vectorcardiogram of several overlayed heartbeats, the spatial correlation between the different measurement channels is used to determine the source signals of the fetal electrocardiogram (chapter 4). The method, however, requires relatively large amounts of computational power and therefore is not suitable for real-time application.

Future development should focus on improving the method from chapter 3, by using the method from chapter 4 to calculate linear combinations of measurement channels. It is expected that this would increase the accuracy of the method, without significantly affecting its computational efficiency.

9.2.2 Technology assessment

To evaluate the suitability of non-invasive fetal ECG measurements for fetal monitoring in clinical practice, the online implementation of the method for maternal ECG removal and the beat-to-beat heart rate detection from chapter 3, were used in a longitudinal patient study. In this study, abdominal fetal ECG measurements were repeatedly performed on pregnant patients during outpatient visits to the maternity ward. Both the success rate of the maternal ECG estimation and the performance of the fetal heart rate detection were evaluated. Also, the signal-to-noise ratios of the retrieved fetal ECG waveforms were calculated.

The performance of the maternal ECG estimation algorithm was good and remained more or less constant throughout pregnancy. Failure of the algorithm occurred when large noise components were present in the recording, which usually is caused by too high electrical impedance between the electrodes and the patient's skin. Fetal heart rates were usually detected from 20 weeks of gestational age and onward. Earlier in pregnancy, for most patients the amplitude of the fetal electrocardiogram was too low to be accurately detected. Between 20 and 25 weeks of gestational age, the quality of the recordings generally was excellent. Not only could the beat-to-beat fetal heart rate be accurately detected, but also the signal-to-noise ratio of the obtained fetal ECG waveforms was very high. For this stage of pregnancy, abdominal measurement of the fetal electrocardiogram

has the unique potential to provide standardized diagnostic ECG leads of the fetus, which might be extremely valuable for fetal cardiology and contribute to a more reliable assessment of fetal condition for treatment decisions around the edge of viability.

Between 28 and 35 weeks the amplitude of the fetal electrocardiogram that is measured on the maternal abdomen, is significantly reduced due to the presence of isolating sections of the vernix caseosa. In this period, the fetal heart rate can only by detected in recordings with very small amounts of noise. After 35 weeks of gestational age, the performance gradually increases again, which can be explained by the occurrence of gaps in the isolating vernix caseosa [11].

Although the quality of the signals recorded after 35 weeks of gestational age cannot be guaranteed to be of sufficient quality to determine the beat-to-beat fetal heart rate, the averaged fetal heart rate generally can be obtained from these recordings. In this stage of pregnancy, abdominal recording of the fetal electrocardiogram therefore could potentially replace Doppler ultrasound cardiotocography. Although the measurement would not provide any additional information, the discomfort to the patient would be less than for Doppler ultrasound cardiotocography and also long term monitoring would be possible. Currently, this basic functionality is already provided by commercially available equipment for abdominal recording of the fetal electrocardiogram.

To exploit the full potential that abdominal measurement of the fetal electrocardiogram offers, the measurement setup that was used should be significantly improved. In particular, the noise in the recorded signals should be reduced to less than 1 μV rms, to accurately measure the fetal electrocardiogram with an amplitude of only a few microvolt. Only then, the measurement method could provide valuable additional information throughout pregnancy and offer a safer and more accurate alternative to replace current cardiotocography.

9.2.3 Doppler ultrasound measurements

Between 28 and 35 weeks of gestational age, abdominal recording of the fetal electrocardiogram fails to provide the beat-to-beat fetal heart rate. Therefore, an alternative measurement method is required to obtain the beat-to-beat fetal heart rate during this period. The developed method to obtain the beat-to-beat fetal heart rate from Doppler ultrasound signals (chapter 6), offers such an alternative. In a direct comparison during labor, the obtained beat-to-beat fetal heart rates showed excellent correlation with the heart rate detected from the simultaneously measured fetal scalp ECG.

For developing this method, Doppler signals were acquired from a cardiotocographic recorder with an analog output interface. To obtain these signals from modern recorders, modification of the recorder is necessary. However, for future

applications, the use of a diagnostic Doppler ultrasound system is recommended. Not only does this simplify the acquisition of the Doppler signal, also will the available visual information allow better positioning of the transducer and thereby ensure adequate measurement quality.

9.3 Time-scale analysis

9.3.1 CWT-based method

The second goal of the thesis was to obtain accurate spectral information on the antepartum fetal heart rate variability. The beat-to-beat fetal heart rate obtained with either abdominal fetal ECG measurements or Doppler ultrasound measurements will generally contain a significant amount of artifacts. Correction of these artifacts will reduce the variability in the signal and therefore affect the spectral estimates, especially in the high-frequency range, that are calculated with traditional techniques for time-frequency analysis such as the short-time Fourier transform.

A continuous wavelet transform based method was developed for time-frequency analysis of fetal heart rate recordings that are contaminated by artifacts (chapter 7). For the calculation of high-frequency spectral estimates, the method discards the parts of the recording that originally contained artifacts. This way, high-frequency spectral estimates can be calculated reliably when up to 50 % of the recording is affected by artifacts. However, for also calculating all spectral estimates in the low-frequency range reliably, not more than 20 % of the recording can be affected by artifacts.

The developed method for time-scale analysis could also be used for calculating more advanced spectral estimates than just the powers in specific frequency bands and their ratios. More specifically, spectral estimates should be defined that characterize physiologically relevant changes in the scalogram of the heart rate variability, as these estimates are more likely to provide clinically relevant information.

9.3.2 Clinical value

Time-frequency analysis of fetal heart rate variability during labor has demonstrated the potential that spectral parameters have for monitoring fetal condition. To further develop this potential into a powerful method for early detection of fetal distress, more insight in these parameters must be gained. The combination of antepartum beat-to-beat fetal heart rate measurements and the developed method for time-scale analysis, provides a unique opportunity for future research to gain this insight.

As preliminary results have been consistent with existing insights in fetal development, it is plausible that time-scale analysis of antepartum fetal heart rate variability indeed provides information on sympathetic and parasympathetic nervous activity (chapter 8). More in particular, it is suggested that the increase in normalized power of the fetal heart rate in the low-frequency range at 20-24 weeks of gestational age, may reflect the functional development of the sympathetic nervous system. Additionally, the observed slight increase in HF_n towards the end of pregnancy and the gradual decrease in LF_n, may reflect maturation of the parasympathetic nervous system and manifestation of behavioral states in the fetus. However, additional research is required to investigate these hypotheses in more detail.

Future work should consider more advanced spectral estimates of heart rate varibility than LF_n and HF_n as these parameters represent only a small part of the information that is contained in the scalogram. To further develop time-scale analysis of fetal heart rate variability into an early detector of fetal distress, the challenge is to define spectral estimates that may truly characterize fetal autonomic cardiovascular state. Highest priority should, however, be given to the realization of necessary technical improvements to the measurement setup, to reduce the noise in the recorded signals.

A mismatch in the development of cardiovascular autonomic regulation has been suggested to be the underlying physiological mechanism for the association between low birth weight and increased risk of cardiovascular disease at adult age [12], [13]. This mismatch in the programming of cardiovascular function in utero, appears to have consequences that stretch far beyond birth and can only be controlled by appropriate intervention if the underlying mechanisms are fully understood. Ultimately, time-scale analysis of antepartum beat-to-beat fetal heart rate variability might also make a modest, but valuable contribution to understanding these mechanisms.

References

[1] H. Banta and S. Thacker, "Assessing the costs and benefits of electronic fetal monitoring," *Obstet Gynecol Surv.*, vol. 34, pp. 627–42, Aug 1979.

[2] R. Beard, "The detection of fetal asphyxia in labor," *Pediatrics*, vol. 53, pp. 157–69, Feb 1974.

[3] G. Dawes, M. Moulden, and C. Redman, "System 8000: computerized antenatal FHR analysis," *J Perinat Med.*, vol. 19, no. 1-2, pp. 47–51, 1991.

[4] D. A. de Campos, J. Bernardes, A. Garrido, J. M. de Sá, and L. Pereira-

Leite, "SisPorto 2.0: a program for automated analysis of cardiotocograms," *J Matern Fetal Med.*, vol. 9, pp. 311–8, Sep-Oct 2000.

[5] M. Mohajer, D. Sahota, N. Reed, A. Chang, E. Symonds, and D. James, "Cumulative changes in the fetal electrocardiogram and biochemical indices of fetal hypoxia," *Eur J Obstet Gynecol Reprod Biol.*, vol. 55, pp. 63–70, May 1994.

[6] N. Reed, M. Mohajer, D. Sahota, D. James, and E. Symonds, "The potential impact of PR interval analysis of the fetal electrocardiogram (FECG) on intrapartum fetal monitoring," *Eur J Obstet Gynecol Reprod Biol.*, vol. 68, pp. 87–92, Sep 1996.

[7] I. Amer-Wåhlin, C. Hellsten, H. Norén, H. Hagberg, A. Herbst, I. Kjellmer, H. Lija, C. Lindoff, M. Månsson, L. Mårtensson, P. Olofsson, A. Sundström, and K. Marsál, "Cardiotocography only versus cardiotocography plus ST analysis of fetal electrocardiogram for intrapartum fetal monitoring: a Swedish randomised controlled trial," *Lancet*, vol. 358, pp. 534–8, Aug 2001.

[8] S. Akselrod, D. Gordon, F. Ubel, D. Shannon, A. Berger, and R. Cohen, "Power spectrum analysis of heart rate fluctuation: a quantitative probe of beat-to-beat cardiovascular control," *Science*, vol. 213, pp. 220–2, Jul 1981.

[9] J. van Laar, M. Porath, C. Peters, and S. Oei, "Spectral analysis of fetal heart rate variability for fetal surveillance: review of the literature," *Acta Obstet Gynecol Scand.*, vol. 87, no. 3, pp. 300–6, 2008.

[10] R. Vullings, C. Peters, R. Sluijter, M. Mischi, S. Oei, and J. Bergmans, "Dynamic segmentation and linear prediction for maternal ECG removal in antenatal abdominal recordings," *Physiol Meas.*, vol. 30, pp. 291–307, Mar 2009.

[11] T. Oostendorp, A. van Oosterom, and H. Jongsma, "The effect of changes in the conductive medium on the fetal ECG throughout gestation," *Clin Phys Physiol Meas.*, vol. 10, no. Suppl B, pp. 11–20, 1989.

[12] D. Phillips and D. Barker, "Association between low birthweight and high resting pulse in adult life: is the sympathetic nervous system involved in programming the insulin resistance syndrome?," *Diabet Med.*, vol. 14, pp. 673–7, Aug 1997.

[13] R. IJzerman, C. Stehouwer, E. de Geus, M. van Weissenbruch, H. D. van de Waal, and D. Boomsma, "Low birth weight is associated with increased sympathetic activity: dependence on genetic factors," *Circulation*, vol. 108, pp. 566–71, Jul 2003.

Acknowledgments

Finally, I am in the privileged position to write the last two pages of my dissertation. This allows me to complete a long period of sometimes hard, but always very pleasant work. However, apart from my own work, this dissertation is also the result of the efforts of many people in my environment. I am very grateful to all who have contributed, directly or indirectly, to the realization of this thesis.

I would like to thank my promotors Prof.dr.ir. P.F.F. Wijn and Prof.dr. S.G. Oei for offering me the opportunity to start this PhD project and for their support during the years. Pieter, thank you for always confiding in me and for occasionally presenting me a mirror. Guid, it was your enthusiasm that started this chain-reaction ten years ago. I am glad that together we have taken the next step to improve perinatal care with our technology.

I am very thankful to my copromotor Dr. P. Andriessen. Peter, although we could only realize a small part of our plans, you really inspired me and I have highly appreciated your input.

I would like to express my gratitude to Prof.dr. H.C.W. Beijerinck. Dear Herman, I have highly appreciated the positive influence you have had on my work. Without your occasional provocations, there would not have been a thesis.

I also would like to express my gratitude to Prof. P.R. Stone. Dear Peter, I enjoyed the short time that I worked with you in Auckland and the discussions we had on fetal monitoring. I am very grateful that you could be part of my PhD committee and hope to do some more work with you in the future.

I would like to thank Prof.dr.ir. J.W.M. Bergmans for his support and advice. Dear Jan, your SPS-group has felt like a second home to me.

Prof.dr.ir. R.M. Verdaasdonk is gratefully acknowledged for his participation in my PhD committee.

This work would not have been possible without my colleague PhD-researchers in the fetal monitoring project at Máxima Medical Center and Eindhoven University of Technology: Chiara, Judith and Rik. I treasure nice memories of the conferences we have visited in New York, Florence, Vancouver and Berlin. Chiara, without your success, Nemo would still be "nobody"! Judith, despite our differences we make a great team. Good luck with the completion of your thesis. Rik, when we work together, there is something special in the air. I am happy that we have joined forces to realize our dream and thank Bas for the courage of accepting that

challenge with us! I also would like to thank our co-researchers in the project, in particular Massimo and the students that participated: Anne, Ilham, Floor, Michiel, and Maartje.

It is a pleasure to thank my former colleagues at Máxima Medical Center: Carola, Jannie, Job, Ward, Martijn, Barbara, and last but not least, Rian. In addition, I would like to thank my former colleagues at Amphia Hospital for the nice time working there: I am sorry that I left you early!

I am thankful to my colleagues at Jeroen Bosch Hospital, especially in the Medical Technology and Nuclear Medicine departments. I am very thankful to our Medical Physics unit for creating a stimulating work environment and in particular to Ad and Noud for providing me the opportunity to complete my PhD work.

I thank my family and friends for their patience and support and thank my parents for giving me such a good start!

Dear Timo, since you came into our life, every day has been a joy! Your presence really helped me getting through the last two years of research. From now on, daddy will have more time to play and catch up with you!

Dearest Farrah, I can not imagine how I could have completed this work without you and your unconditional love and support through the years. Words can not express my gratitude to you, but hopefully life will every day!

Curriculum Vitae

Chris Peters was born on June 13, 1977 in Sittard, the Netherlands. After finishing Gymnasium in 1995 at Serviam Lyceum in Sittard, he studied Applied Physics at Eindhoven University of Technology in Eindhoven, the Netherlands. In 2001 he graduated within the Medical Physics group on fetal monitoring. From 2001 to 2003 he worked as consultant at M+P Raadgevende Ingenieurs in Vught, the Netherlands, and in 2003 he started his residency in medical physics in Máxima Medical Center in Veldhoven, the Netherlands. In 2006 he completed the PDEng design program Design and Technology of Instrumentation at Eindhoven University of Technology and started a PhD project of which the results are presented in this dissertation. Since 2007 he has been officially registered as medical physicist. From 2007 to 2009 he was employed at Amphia Hospital in Breda, the Netherlands as medical physicist and specialist manager of the Medical Technology department. Since 2010 he is employed at Jeroen Bosch Hospital in 's-Hertogenbosch, the Netherlands as medical physicist. In 2010 he co-founded Nemo Healthcare, a spin-off company of Eindhoven University of Technology, winner of the Brainport Health Innovation Award 2010, and finalist for the Herman Wijffels Innovation Award 2010.

Reliable evaluation of fetal condition and early detection of fetal distress is one of the largest challenges in modern obstetrics. Safely protected within the maternal womb, the fetus is rather inaccessible for physiological measurements. One of few physiological phenomena that can be measured antenatal, is fetal heart activity. Small beat-to-beat fluctuations in the fetal heart rate reflect modulation by the fetal autonomic nervous system. Analysis of this beat-to-beat heart rate variability might provide valuable information for assessing fetal well-being. Unfortunately, existing fetal monitoring technology can only obtain the beat-to-beat fetal heart rate during labor, by applying an electrode directly to the fetal scalp. This dissertation explores the possibility of obtaining the beat-to-beat fetal heart rate throughout pregnancy by non-invasive measurements. In addition, a method is presented for time-scale analysis of antepartum fetal heart rate variability, and applied to fetal heart rate recordings obtained by abdominal measurement of the fetal electrocardiogram during clinical practice.